UNIVERSITEIT VAN PRETORIA
UNIVERSITY OF PRETORIA
YUNIBESITHI YA PRETORIA

Assessment of the Baseline Meteorological and Air Quality Conditions over Uubvlei, Oranjemund, Namibia

by

Anzel Swart

Submitted in fulfilment of the requirements

for the degree

MASTER OF SCIENCE

in the

Faculty of Natural and Agricultural Sciences

University of Pretoria

September 2016

UNIVERSITEIT VAN PRETORIA
UNIVERSITY OF PRETORIA
YUNIBESITHI YA PRETORIA

DECLARATION

I, Anzel Swart, declare that the dissertation, which I hereby submit for the degree Master of Science at the University of Pretoria, is my own work and has not previously been submitted by me for a degree at this or any other tertiary institution.

25/09/2016

SIGNATURE DATE

UNIVERSITEIT VAN PRETORIA
UNIVERSITY OF PRETORIA
YUNIBESITHI YA PRETORIA
UNIVERSITEIT VAN PRETORIA
UNIVERSITY OF PRETORIA
YUNIBESITHI YA PRETORIA

Assessment of the Baseline Meteorological and Air Quality Conditions over Uubvlei, Oranjemund, Namibia

Anzel Swart

Supervisor: Prof George Djolov (UP)

Co-Supervisor: Dr Joel Botai (SAWS)

Department: Geography, Geo-Informatics and Meteorology

Faculty: Natural and Agricultural Science

University: University of Pretoria

Degree: Master of Science

SUMMARY

The 800 MW Kudu power project in south-west Namibia is a Combined Cycle Gas Turbine (CCGT) that will use natural gas from the Kudu gas field located in the Atlantic Ocean, 170 km off-shore. The Kudu Project aims to respond to the increased power demand in the southern African region and to limit Namibia's importation of energy from South Africa. The proposed site for the CCGT power plant is located at Uubvlei (25 km north of Oranjemund town and less than a kilometre from the coast). The proximity of the ocean to the proposed site means that ocean influence will play a significant role in the meteorological factors that affect pollution dispersion in the atmosphere. It is, therefore, necessary to study its effect by quantifying the occurrence of sea breeze circulation and fog in the region. It is also essential to study the formation and structure of the Thermal Internal Boundary Layer (TIBL) at this location, for it will affect the air quality in the region by creating fumigation conditions. An analysis of the meteorological and air-pollution climatology of the region is of importance in assessing the baseline conditions present over the region. The Air Dispersion Potential (ADP) of the study region was calculated based on an integral index that combines the parameters responsible for the dispersion of pollutants in the atmosphere.

UNIVERSITEIT VAN PRETORIA
UNIVERSITY OF PRETORIA
YUNIBESITHI YA PRETORIA

The meteorology and air-pollution climatology of the region are studied. These results are based on 20 years of meteorological data from the Alexander Bay weather station as well as on modelled data for a grid over the study region. The focus is predominantly on the parameters that have an influence on pollution dispersion. These include the wind speed and direction, stability conditions, mixing height, temperature, relative humidity, and precipitation.

The ADP index, as proposed in the dissertation, gave an indication as to whether conditions were unfavourable, moderate or favourable for the dispersion of pollutants. It was found that, overall, the biggest contributor to favourable dispersion of air-pollution in the region is the Monin-Obukhov Length. Wind speed mostly contributes moderately to ADP, while mixing height is predominantly unfavourable.

The occurrence of sea breeze circulation, foggy days, as well as the structure of the TIBL are discussed. Making use of the relevant meteorological data, it was found that sea breeze circulation occurs predominantly in the summer months. Fog conditions at the proposed site also occur mostly during the summer months, with the highest number of foggy hours being in the months of January, March and November. Fog is also expected to occur mostly between 21:00 and 09:00 at this site. All algorithms for the calculation of fog and breeze conditions, TIBL height, and ADP has been realized on MATLAB platform and can be used as a forecasting tool during the operation of the proposed CCGT power station.

Taking into account the complicated coastal meteorology at the proposed site, the location is less than ideal and will present many challenges for pollutant dispersion and structural upkeep. The influence of mesoscale meteorological phenomena such as sea breezes and the TIBL, the frequent events of fog and the poor overall mixing heights in the region will all contribute unfavourably to the dispersal of pollutants emitted from the CCGT power station. Re-circulation and fumigation of pollutants will cause high ground-level pollutant concentrations in the region. A location further inland will experience better conditions for pollutant dispersion, less episodes of fog and will not experience the same corrosive effects as a coastal site. Placing the power station approximately 40 km inland could lessen or totally eliminate the effects of the unfavourable mesoscale meteorological phenomena (sea breezes and TIBL) and consequently also the processes of re-circulation and fumigation of pollutants.

UNIVERSITEIT VAN PRETORIA
UNIVERSITY OF PRETORIA
YUNIBESITHI YA PRETORIA

ACKNOWLEDGEMENTS

- I would like to express my gratitude to my supervisor, Prof. George Djolov for his continuous support and genuine interest in this dissertation. Thank you for the hours of assistance and your invaluable contribution to this research project.
- Dr. Joel Botai for co-supervising this dissertation.
- The South African Weather Service (SAWS) for providing 20 years of observational data from the Alexander Bay weather station.
- Dr. Gerhard Fourie for supplying modelled meteorological data.

UNIVERSITEIT VAN PRETORIA
UNIVERSITY OF PRETORIA
YUNIBESITHI YA PRETORIA

TABLE OF CONTENTS

UNIVERSITEIT VAN PRETORIA
UNIVERSITY OF PRETORIA
YUNIBESITHI YA PRETORIA

UNIVERSITEIT VAN PRETORIA
UNIVERSITY OF PRETORIA
YUNIBESITHI YA PRETORIA

UNIVERSITEIT VAN PRETORIA
UNIVERSITY OF PRETORIA
YUNIBESITHI YA PRETORIA

LIST OF ACRONYMS

ADP	Air Dispersion Potential
Ar	Argon
Br	Bromide
Ca^{++}	Calcium
CCGT	Combined Cycle Gas Turbine
CH_4	Methane
Cl^-	Chlorine
CO_2	Carbon Dioxide
DPT	Dew Point Temperature
E	East
EPA	Environmental Protection Agency
F^-	Fluoride
GDP	Gross Domestic Product
H	Hydrogen
HCO_3^-	Bicarbonate
He	Helium
$H_2BO_3^-$	Borale
H_2S	Hydrogen Sulphide
H_2SO_4	Sulphuric Acid
IBL	Internal Boundary Layer
IFC	International Finance Corporation
ITCZ	Inter-Tropical Convergence Zone
K^+	Potassium
KCl	Potassium Chloride
Kr	Crypton
MATLAB	Matrix Laboratory
MMM	Mesoscale and Microscale Meteorology
MW	Megawatts
N	North
Na^+	Sodium
$NaCl$	Sodium Chloride
Nampower	Namibia Power
Ne	Neon

UNIVERSITEIT VAN PRETORIA
UNIVERSITY OF PRETORIA
YUNIBESITHI YA PRETORIA

NO_x	Oxides of Nitrogen
NO_2	Nitrogen Dioxide
N_2	Nitrogen
N_2O	Nitrous Oxide
O_2	Oxygen
O_3	Ozone
Pb	Lead
PBL	Planetary Boundary Layer
PM	Particulate Matter
RH	Relative Humidity
SA NAAQS	South African National Ambient Air Quality Standards
SAWS	South African Weather Service
Sr^{++}	Strontium
S	South
S	Sulphur
SSA	Sea Salt Aerosols
SO_x	Oxides of Suplhur
SO_2	Suplhur Dioxide
SO_4^{-2}	Sulphate
SST	Sea Surface Temperature
T	Temperature
TAPM	The Air-Pollution Model
TIBL	Thermal Internal Boundary Layer
W	West
WB	World Bank
WHO	World Health Organisation
Xe	Xenon

UNIVERSITEIT VAN PRETORIA
UNIVERSITY OF PRETORIA
YUNIBESITHI YA PRETORIA

LIST OF FIGURES

UNIVERSITEIT VAN PRETORIA
UNIVERSITY OF PRETORIA
YUNIBESITHI YA PRETORIA

UNIVERSITEIT VAN PRETORIA
UNIVERSITY OF PRETORIA
YUNIBESITHI YA PRETORIA

LIST OF TABLES

UNIVERSITEIT VAN PRETORIA
UNIVERSITY OF PRETORIA
YUNIBESITHI YA PRETORIA

CHAPTER 1: INTRODUCTION, PROBLEM STATEMENT, AIMS AND OBJECTIVES

1.1 Introduction

The task to monitor and evaluate the air quality and changes in environmental conditions that may be caused by the proposed Kudu CCGT power station was undertaken by The Business Enterprises at University of Pretoria (Pty) Ltd. The evaluation of the proposed Kudu CCGT power station is essential because of the global and local need for energy as well as the new policies for cleaner energy production.

Meteorological science is becoming an important tool in economic development projects, agricultural practices, environmental protection, air-pollution dispersion, solar and wind power developments, urban planning, forensic investigations, insurance, weather and climate predictions, health exposure studies and many more. In particular, the energy sector, which plays a major role in the development of any country and in the eradication of poverty, demands meteorological information in two major areas. The first being the use of theoretical, observational and modelling results for assessing the background climatic and air quality conditions needed for planning and design in many fields of human activities. The second area of application of meteorological science is the evaluation of the impact on human health and environmental conditions due to the construction of industrial facilities, roads, residential developments as well as energy-production facilities.

NamPower (Namibia Power), the only electricity utility in Namibia, has a production capacity of 384 MW. Peak load in Namibia is 480 MW; the shortage in electricity is dealt with by importation from nearby countries such as South Africa. In 2004, Namibia imported more than half of its energy from South Africa and a rising demand in Namibia was likely to lead to a shortfall in supply from 2007 (Pallet, 2009). Electricity demand will soon exceed the electricity supply in Southern Africa. It is, therefore, essential to limit Namibia's import of energy from neighboring countries. This need has led to the proposal of the Kudu power project near Oranjemund.

Figure 1.1 shows the water and electricity distribution networks along the Namibian coastline. The Namibian coast and the study region are supplied with electricity through the national electricity grid. The study region, along with the rest of Namibia, faces serious electricity supply challenges (Robertson et al., 2012).

UNIVERSITEIT VAN PRETORIA
UNIVERSITY OF PRETORIA
YUNIBESITHI YA PRETORIA

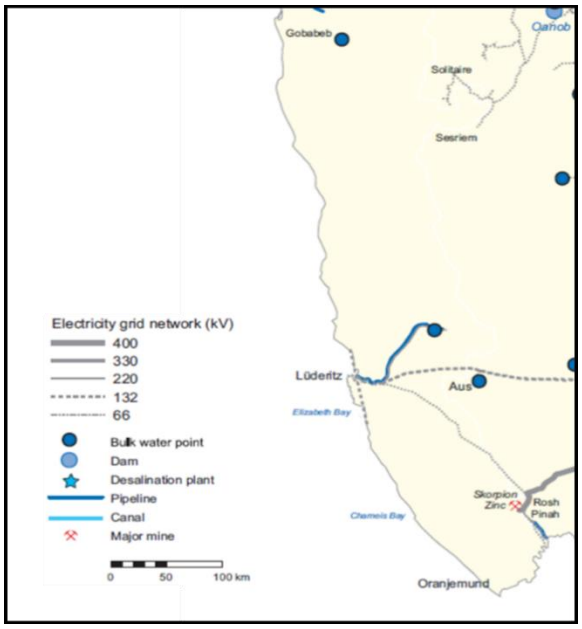

Figure 1.1: Water and electricity distribution networks along and into the coastal region of southern Namibia (Robertson et al., 2012).

The growth of the mining sector and the desalination of sea-water along the Namibian coast will further increase the demand for electricity (Robertson et al., 2012). The Namibian government is undertaking a vast project, which will secure a relatively clean source of power for Namibia. The successful completion of the Kudu Gas Project will provide Namibia with sufficient generating capacity, independence of power import from South Africa, and the opportunity to export energy.

According to NamPower, there are currently four power stations in Namibia. Table 1.1 describes each power station and its generating capacity.

Table 1.1: Type, capacity and purpose of Namibian power stations (NamPower, 2015).

Name	Type	Capacity	Purpose
Ruacana Power Station	Hydroelectric	330 MW	Core of Namibian power supply
Van Eck Power Station	Coal-fired	120 MW	Contributes to power supply
Paratus Power Station	Diesel	16 MW	Standby
ANIXAS Power Station	Diesel	22.5 MW	Emergencies

Growth in the Gross Domestic Product (GDP) of a country is proportional to the amount of electricity sold and used in that country. Therefore, to keep up with the demand for electricity (resulting from economic growth) in Namibia, there needs to be an increase in electricity production (Van Zyl et al., 2011). Van Zyl et al. (2011) has calculated that, for every N$ 1 spent in Namibia during the construction phase of the CCGT power station, Namibia's economy will expand by N$ 2.60. Namibia's GDP will grow by approximately 1% each year that the CCGT

UNIVERSITEIT VAN PRETORIA
UNIVERSITY OF PRETORIA
YUNIBESITHI YA PRETORIA

power station is being constructed. This contribution to economic growth can be attributed mostly to the job opportunities that will be created during the construction phase and operation of the power station.

The Kudu Power Project was identified as one of the preferred options to address this shortfall in electricity and meet the growth in demand (Pallet, 2009). The advantages of this project for Namibia will be the provision of secure and adequate generation capacity, the diversification of Namibia's energy mix, and the reduction of their dependence on the importation of electricity. Upon the completion of the CCGT power station, Namibia will be a net exporter of electricity.

1.1.1 Combined Cycle Gas Turbine (CCGT) power station

Different options for alternative energy sources in Namibia were considered, including hydropower, biomass, wind power, solar power, nuclear power, and natural gas (SAIEA, 2006). The Kudu Power Project is a Combined Cycle Gas Turbine (CCGT) that will use natural gas reserves located at the Kudu gas field to generate electricity. The gas is estimated to be sufficient to drive an 800 MW power station for at least 20 years (Pallet, 2009). The Kudu gas field was discovered in 1979 by Chevron and Partners and is located approximately 170 km offshore the proposed site. The power station will be constructed and operated by NamPower (Pty) Ltd and its partners (Namcor, 2014).

Combined Cycle Gas Turbine (CCGT) power stations combine a gas-powered turbine with a steam turbine in order to use the fuel it consumes more efficiently. CCGT power stations are considered to be among the world's safest fossil-fired stations when considering the environment and climate (Siemens, 2015). CCGT technology (Figure 1.2) replaces the conventional coal-fired power stations in areas where natural gas is available. The proposed power station will consist of two shaft CCGT units. Each of these units is made up of a gas turbine, a waste heat recovery boiler and a steam boiler (CSIR, 2005b).

UNIVERSITEIT VAN PRETORIA
UNIVERSITY OF PRETORIA
YUNIBESITHI YA PRETORIA

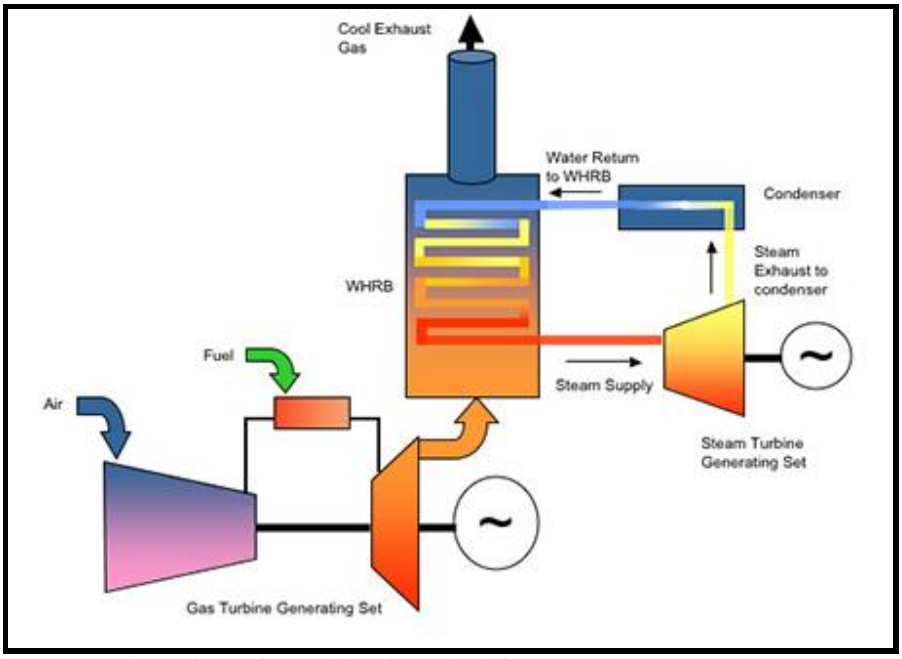

Figure 1.2: The Gas Turbine-based Combined Cycle (Siemens, 2015).

The technology that will be used for the proposed CCGT power station is one of the most efficient non-renewable electricity-generation methods; it is cost-effective and can be built and put into operation within 3 years (SAIEA, 2006). This type of power station has lower cooling water requirements than a conventional thermal station (Pallet, 2009), lower carbon emissions than other power-generation options such as coal and diesel, and could possibly generate carbon credit revenue for Namibia (KuduPower, 2014). Air pollutants from the CCGT power-generation process include Oxides of Nitrogen (NO_x), Particulate Matter (PM), Sulphur Dioxide (SO_2) as well as greenhouse gases like Carbon Dioxide (CO_2) (CSIR, 2005b). Only a minor amount of black smoke will be produced per unit of energy consumed and the emissions of PM will be of negligible amounts during operation. The main emissions from the proposed CCGT power station will be NO_x. These NO_x emissions will be 81% per unit of power generated less than for a coal-burning station and emissions of CO_2 will be more than 50% less (CSIR, 2005b).

Table 1.2 summarizes the sources and possible effects of the emissions from the proposed Kudu CCGT power station on human health and the environment.

UNIVERSITEIT VAN PRETORIA
UNIVERSITY OF PRETORIA
YUNIBESITHI YA PRETORIA

Table 1.2: Sources and possible effects of NO_x, PM and SO_2 (CSIR, 2005b).

Pollutant	Sources	Sources from Kudu power plant	Possible environmental effects	Possible effects on human health
NO_x	Bacterial and volcanic action, lightning, burning fuel in motor vehicles, electric power plants, use of explosives, etc.	Stack emissions from gas and fuel oil cycles.	Acidic deposition (wet and dry) can also cause acidification and accelerated corrosion.	Inhalable, headaches, nausea, coughing, dyspnoea, decrements in lung function, airway resistance, and irreversible inflammation of lungs.
PM	Fuel combustion from motor vehicles, power generation, industrial facilities, fires, etc.	Dust generated during construction and combustion of fuel oil when gas is unavailable.	Haze, can travel far and be deposited on ground/water, erosion, staining of structures.	Inhalable, asthma, bronchitis, inflammatory responses, respiratory disease, and respiratory mortality.
SO_2	Volcanoes, oceans, biological decay, forest fires, fossil fuel combustion, metal smelting, coal burning, etc.	Combustion of fuel when gas is unavailable.	Acidic deposition (wet and dry), acidification of lakes and streams, accelerated corrosion, impaired visibility, contributes to climate change.	Inhalable, reduction in lung function, increase in airway resistance, wheezing, shortness of breath.

1.1.2 Regulations

The need to comply with regulatory norms is crucial in the case of the proposed CCGT power station. This is not only to secure the health of the population and preserve environmental conditions, but also to ensure the acceptance of the project by the World Bank (WB). The ambient air-quality guidelines for international organizations accepted by the WB Group are reported in The Environmental, Health and Safety Guidelines of the International Finance Corporation (IFC, 2007).

At present, there are no Namibian air quality standards or dust control regulations. South African National Ambient Air Quality Standards (SA NAAQS) and National dust control regulations are discussed below together with internationally recognized guidelines from the World Health Organisation (WHO).

UNIVERSITEIT VAN PRETORIA
UNIVERSITY OF PRETORIA
YUNIBESITHI YA PRETORIA

1.1.2.1 Ambient air-quality standards

Ambient air-quality standards are enforced nationally and internationally in order to safeguard human health and protect the environment. The pollutant concentration thresholds presented in Tables 1.3 and 1.4 are based on scientific evidence related to the effect of these pollutants on human health (Lazaridis, 2010). Table 1.3 shows the acceptable regulatory amounts of different pollutants for South Africa, while Table 1.4 contains the acceptable amounts of pollutants as defined by the WHO. For the majority of the pollutants, the acceptable concentration levels for South Africa are higher than is acceptable for the WHO.

Table 1.3: SA NAAQS for pollutants over different averaging periods (DEAT, 2004a & DEAT, 2012).

Pollutant	10-minute average	1-hour average	8-hour average	24-hour average	Annual average
$PM_{2.5}$				40 µg/m^3	20 µg/m^3
PM_{10}				75 µg/m^3	40 µg/m^3
SO_2	500 µg/m^3	350 µg/m^3		125 µg/m^3	50 µg/m^3
NO_2		200 µg/m^3			40 µg/m^3
CO_2					
O_3			120 µg/m^3		

Table 1.4: WHO ARG for pollutants over different averaging periods (WHO, 2005).

Pollutant	10-minute average	1-hour average	8-hour average	24-hour average	Annual average
$PM_{2.5}$				25 µg/m^3	10 µg/m^3
PM_{10}				50 µg/m^3	20 µg/m^3
SO_2	500 µg/m^3			20 µg/m^3	
NO_2		200 µg/m^3			40 µg/m^3
CO_2					
O_3			100 µg/m^3		

1.1.2.2 Trace metals

Trace metal species can be emitted into the atmosphere naturally or in an anthropogenic manner and are categorized as either $PM_{2.5}$ or PM_{10}. One of the sources of naturally emitted trace metals is the ocean. These metal species are the cause of possible health-related and environmental problems. Trace-metal concentrations are known to peak in the dry months and decrease in the wet season because of wash-out of the atmosphere due to precipitation (Van Zyl et al., 2014). There are a possible 27 different trace-metal species present in the atmosphere.

UNIVERSITEIT VAN PRETORIA
UNIVERSITY OF PRETORIA
YUNIBESITHI YA PRETORIA

According to the SA NAAQS, there is only one trace metal with concentration limits. Lead (Pb) has to have a concentration below 0.5 µg/m^3 for an averaging period of 1 year (DEAT, 2004a).

1.1.2.3 Dust-control regulations

Dust is used to describe any material that is made up of particles smaller than 1 mm and large enough to settle into a sampling container from ambient air by their own weight. Consequently, dust fall means the deposition of dust, and is usually measured as a 30-day average (DEAT, 2004b). The regulations pertaining to dust-fall rates in South Africa are less than 600 $mg/m^2/day$ in residential areas and between 600 and 1200 $mg/m^2/day$ in non-residential areas.

1.2 Problem statement

The establishment of a power station with the capacity of Kudu requires compliance with the World Bank (WB) and other regulations. The proximity of the ocean to the proposed site means that ocean influence will play a significant role in the meteorological factors influencing atmospheric pollution dispersion. The frequency of occurrence of meteorological conditions, which are unfavourable for the dispersion and distribution of pollutants, are of interest. It is, therefore, necessary to study the effects of these relevant meteorological phenomena by quantifying the occurrence of sea breeze circulation and fog occurrence in the region. It is also essential to study the formation and structure of the Thermal Internal Boundary Layer (TIBL) at this location, for it will have an effect on air quality in the region by creating fumigation conditions. An analysis of the meteorological and air-pollution climatology of the region is of importance in assessing the baseline conditions present over the region. The Air Dispersion Potential (ADP) in the vicinity of the power station could also be of interest to the day-to-day and long-term operation of the power station. These are tasks that require the application of appropriate methodology and the analysis of data, which are in the domain of meteorological science.

Projects such as the Kudu CCGT power station should be properly evaluated before construction, commissioning and operational phases. An assessment tool is required to be applied to any energy product in order to secure evaluation of environmental conditions and to minimize possible negative effects on human beings and the environment. The result of the study also has relevance to South Africa, because the proposed location of the power station is very close to the border. Emissions from the power station could possibly have an influence on human beings and the environment in South Africa.

UNIVERSITEIT VAN PRETORIA
UNIVERSITY OF PRETORIA
YUNIBESITHI YA PRETORIA

1.3 Aims and objectives

The aim of the project is to establish the baseline meteorological and air-quality conditions in the study region prior to the design process and construction of the CCGT power station.

Objective 1

Study the effect that the proximity of the ocean has on the study region by quantifying the occurrence of fog conditions, the occurrence of sea breeze circulation, the height of the TIBL, and the characteristics of the relevant meteorological parameters; wind, mixing height, stability and humidity.

Objective 2

Analyse the air-pollution characteristics of the study region on the basis of an ADP index.

UNIVERSITEIT VAN PRETORIA
UNIVERSITY OF PRETORIA
YUNIBESITHI YA PRETORIA

CHAPTER 2: COASTAL METEOROLOGY

The term ‘dispersion’ describes the diffusion and advection of pollutants in the atmosphere (Stokie, 2011). The meteorology and topography of an area, together with the technological and physical emission characteristics of an emission source, are the most important factors in determining the way in which pollutants will disperse in the atmosphere.

The proximity of the study region to the ocean means that the South Atlantic Ocean has a significant influence on both the meteorology and the way in which pollutants disperse in the region. In this Chapter, the composition of the atmosphere and the influence of different site-specific meteorological phenomena on pollution dispersion will be discussed. The chemical influence of some pollutants on the CCGT power station is also described.

The influence of the ocean on the study region includes the formation of land and sea breezes, the formation of the TIBL, sea fog, salt spray, and Hydrogen Sulphide eruptions. These factors influence the way in which pollution from the CCGT power station will disperse and be transported. This, in turn, affects the environment, human health and the power station itself.

2.1 Atmospheric composition

All pollution on earth is emitted into the atmosphere. Pollutants are transported, dispersed and transformed by the atmosphere and its dynamics (Lazaridis, 2010). The lower parts of the earth’s atmosphere contain a combination of gas and aerosols.

The atmosphere is well mixed and, consequently, the composition of ‘dry air’ in the atmosphere remains mostly constant. Table 2.1 contains the 12 most abundant chemical constituents of the lower atmosphere and the ratio of each.

UNIVERSITEIT VAN PRETORIA
UNIVERSITY OF PRETORIA
YUNIBESITHI YA PRETORIA

Table 2.1: Chemical constituents of 'dry air' and their volumes (Lazaridis, 2010).

Name and Symbol	Volume (%)
Nitrogen (N_2)	78.08
Oxygen (O_2)	20.95
Argon (Ar)	0.93
Carbon Dioxide (CO_2)	0.03
Neon (Ne)	18.18×10^{-4}
Helium (He)	5.24×10^{-4}
Methane (CH_4)	$\sim 2.2 \times 10^{-4}$
Crypton (Kr)	1.14×10^{-4}
Nitrous Oxide (N_2O)	0.5×10^{-4}
Hydrogen (H)	$\sim 0.5 \times 10^{-4}$
Xenon (Xe)	0.087×10^{-4}

Water vapour in the atmosphere is variable and can range from 0% to 4% volume ratio. Water vapour in the atmosphere is of significance, because its condensation could cause cloud formation, and it acts as a source of thermal energy.

Atmospheric aerosols refer to suspended particles in both solid and liquid form. Aerosols can be natural or anthropogenic in nature. Dry deposition (gravitational settling of aerosols) and wet deposition (removal of aerosols during precipitation) are the two main methods whereby aerosols are removed from the atmosphere (Lazaridis, 2010).

2.2 Meteorology and air-pollution

The meteorological factors that determine the fate of pollutants in the atmosphere can be illustrated by using, without loss of generality, the Gaussian approach of diffusion and transport processes in the atmosphere. Gaussian distribution is one way to describe the dispersion of pollutants in the atmosphere, as it considers the technological factors (height and diameter of the stack) and physical emission properties (emission rate and temperature of the emissions) of the emission source and the meteorological factors influencing pollutant concentration at a point. The Gaussian equation gives a good indication of the factors influencing dispersion in the atmosphere and their effect on concentration of pollutants.

2.2.1 Gaussian distribution

In the Gaussian equation (Equation 2.1), C is the concentration of pollution at the location x, y, z (Cimorelli et al., 2004). Concentration is measured in micrograms per cubic meter ($\mu g/m^3$). Q is the rate at which emissions exit the source and is measured in grams per second (g/s). U is the average wind speed measured at the top of the stack in meters per

UNIVERSITEIT VAN PRETORIA
UNIVERSITY OF PRETORIA
YUNIBESITHI YA PRETORIA

second (m/s). σ_y is the standard deviation of concentration distribution in the horizontal, and σ_z is in the vertical, both parameters are stability dependant and measured in metres (m).

$$C(x,y,z) = \frac{Q}{2\pi\sigma_y^2\sigma_z U}\exp\left(\frac{-y^2}{2\sigma_y^2}\right)\left(\exp\left(\frac{-(z-h)^2}{2\sigma_z^2}\right)+\exp\left(\frac{-(z+h)^2}{2\sigma_z^2}\right)\right) \qquad (2.1)$$

H represents the combination of the physical height of the stack and the rise of the plume as it exits the stack (measured in metres); x is the distance downwind from the stack; y is the crosswind distance from the plume centreline, and z is the vertical distance from the surface of the earth. x, y, z are all measured in metres (m) (Stokie, 2011).

The concentration of a pollutant at a point in the atmosphere (x, y, z) is directly proportional to the technological specifications and physical emission properties of the stack. This means that, when pollutants are emitted from the source at a higher rate, the concentration of the pollutants will also be higher. According to Equation 2.1, concentration is inversely proportional to meteorological factors such as wind speed. This means that lower pollutant concentrations will be measured when higher wind speeds are present at the height of the stack and, reversely, lower wind speed favours higher pollutant concentrations. The standard deviations σ_y and σ_z reflect the influence of the turbulence and stability conditions of the diffusion process.

2.2.2 Meteorological factors influencing pollutant concentration

The dynamics in the atmosphere has a direct effect on the concentration and distribution of pollutants. Thermodynamic and dynamic processes cause meteorological phenomena in the atmosphere. These processes occur as a result of the way in which the atmosphere circulates, and are caused by temperature differences in the various regions of the atmosphere and the rotation of the earth (Lazaridis, 2010). There are many meteorological factors that might affect the way in which a pollutant will disperse in the atmosphere. These factors include solar radiation, air-temperature distribution, turbulence, wind speed and direction, precipitation, as well as atmospheric stability and mixing height.

2.2.2.1 Solar radiation and air temperature

The sun is the most important source of heat energy for the earth. Cloud cover, latitude and altitude all have an effect on solar radiation reaching the earth (Faiz, 1990). The formation of secondary pollutants such as Ozone (O_3) is highly dependent on solar radiation.

Atmospheric temperature is an important meteorological factor influencing pollution dispersion (Godish, 1997). Vertical air movements depend on the atmospheric lapse rate (change in atmospheric temperature with height). The change in temperature with height leads

UNIVERSITEIT VAN PRETORIA
UNIVERSITY OF PRETORIA
YUNIBESITHI YA PRETORIA

to vertical mixing of pollutants. Pollutants are transported upward by rapid mixing and are then transported further by wind.

Solar radiation reaching the earth surface contributes to the atmospheric stability in a region (Faiz, 1990). Cloud cover is one of the factors that obstruct solar radiation reaching the surface of the earth, consequently reducing turbulent processes. The atmosphere will be more stable and pollutants will not disperse as freely as they would in an unstable atmosphere (Godish, 1997).

2.2.2.2 Temperature inversions

A temperature inversion forms when air temperature increases, instead of decreases, with height in some sections of the atmosphere. Cooling of the lower layer of the atmosphere, adiabatic warming of sinking air as well as the horizontal transport of warm or cold air could all lead to the formation of a temperature inversion (Lazaridis, 2010).

Inside the temperature inversion, vertical air movement is inhibited, because there exists a state of stable equilibrium (Lazaridis, 2010). The layer of atmosphere above the surface of the earth and below the inversion layer (mixing layer) is unstable. Vertical mixing exists in this layer up to the height where the stable inversion layer begins. This is also known as the mixing height.

A temperature inversion layer acts as a ‘cap’ and traps gaseous pollutants in the layers beneath it. A higher mixing height allows for large volumes of pollutants and air to mix. If the inversion layer moves downward towards the earth surface, the mixing height lowers, and less mixing of pollutants will take place. Gaseous pollutants will be stuck in a thin layer of air, which could lead to concentrations exceeding limits and cause health risks.

Gaseous pollutants from a low source (located within the inversion layer) will be trapped inside the inversion (Figure 2.1). A higher source (located above the inversion layer) will release its gaseous pollutants above the inversion layer where it will be able to disperse as normal.

UNIVERSITEIT VAN PRETORIA
UNIVERSITY OF PRETORIA
YUNIBESITHI YA PRETORIA

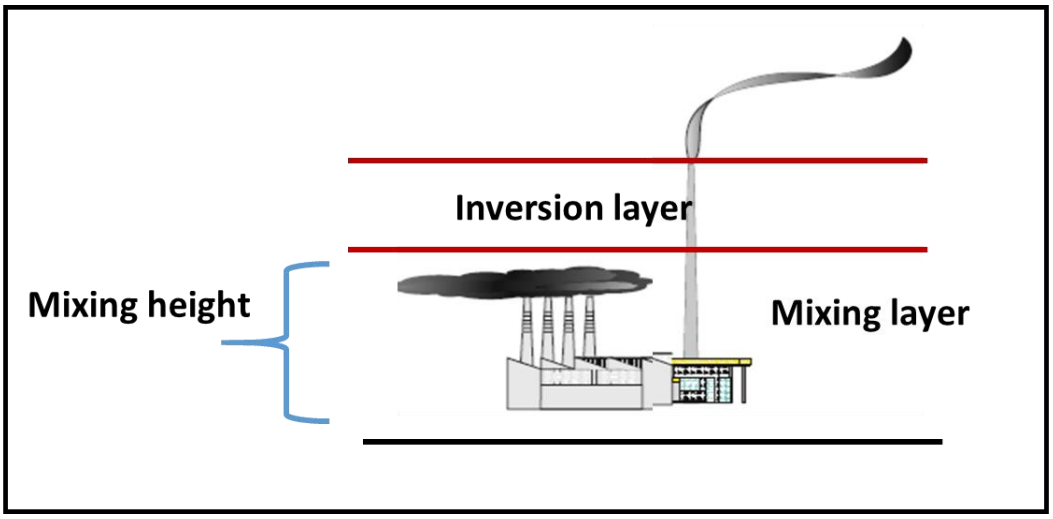

Figure 2.1: Low vs high source (Adapted from Lazaridis, 2010).

2.2.2.3 Wind speed and direction

Horizontal winds have a significant effect on pollution processes in the atmosphere. Increasing wind speed means an increase in the volume of air being transported in a period of time (Liu and Lipták, 2000). As described by the Gaussian equation, there exists an inverse proportionality between pollutant concentration and wind speed at a point.

Prevailing wind direction in a region will influence where the pollutant will be transported. Consequently, the same down-wind region can constantly be affected by high concentrations of pollution. If wind direction is more variable, pollution will be dispersed over a larger area and concentrations influencing a single region will not be as high (Liu and Lipták, 2000).

The dominant wind direction at the study region, with a 30% annual frequency of occurrence, is southerly. These southerly breezes prevail for most of the year and cause widespread sand movement and scouring (SAIEA, 2006). West and south-westerly on-shore winds also occur in the region. During the winter, offshore berg winds develop.

In Summer, Namibia experiences the highest wind speeds. These winds occur throughout the afternoons and evenings. Airflow from the sea speeds up in the late afternoon because of the pressure gradient that forms, due to temperature differences between the cool ocean and the warmer land. Berg winds tend to cause high temperatures at the Namibian coast throughout the winter. Because of this phenomenon, maximum average temperatures at coastal regions are higher during winter than during summer. Coastal temperatures might be mild, but berg winds moving over the escarpment and out to sea have caused some of the highest temperatures in Namibia to be recorded at coastal stations (Robertson et al., 2012).

UNIVERSITEIT VAN PRETORIA
UNIVERSITY OF PRETORIA
YUNIBESITHI YA PRETORIA

The South Atlantic anticyclone influences the wind direction experienced at the coast. Wind leaves its anticyclonic high-pressure centre in an easterly direction towards the Namibian coastline. Coriolis force causes the direction of wind to deflect towards the north – this is the reason for the dominant southerly wind at the coast (Robertson et al., 2012). During winter, when the Botswana anticyclone is located over southern Africa, strong easterly berg winds blow from the interior of the country to the sea. These north-easterly winds lead to dry, dusty, and very hot conditions (CSIR, 2005b).

2.2.2.4 Precipitation

Precipitation such as rain is considered a natural cleansing agent when referring to atmospheric pollution, because of the way it removes pollutant particles from the air. Rain and humidity in the atmosphere may have adverse effects on some pollutants. Oxides of Nitrogen (NOx) and Sulphur (SOx) react with precipitation to form acids or acidic depositions. These newly formed substances can corrode metal, destroy buildings and cause damage water and land ecosystems (Faiz, 1990).

a. Rainfall

The study region receives very little rainfall and is considered to be arid (CSIR, 2005b). The average annual rainfall at this coastal location is 49 mm. The study region and the southern areas of Namibia are located in a winter rainfall region, but this part of the coast does receive rainfall during all seasons (Robertson et al., 2012). Some years there may be very little rainfall while, in other instances, the annual average rainfall total can be reached because of one large rainfall event. As noted in Figure 2.2, the annual rainfall in the study region is variable.

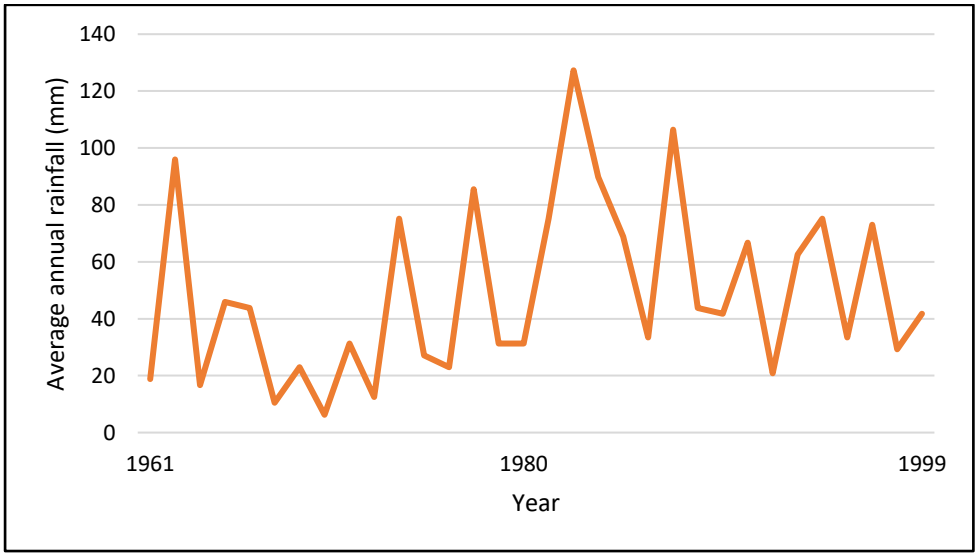

Figure 2.2: Average annual rainfall at Oranjemund, Namibia (Adapted from Robertson et al., 2012).

UNIVERSITEIT VAN PRETORIA
UNIVERSITY OF PRETORIA
YUNIBESITHI YA PRETORIA

Figure 2.3 shows that rainfall in the study region is present throughout the year, with a definite increase during the winter months. Normally, rainfall at the coast is rare, but, as noted in Figure 2.3, in May 2011, areas on the Namibian coastline experienced more rain in a few days than is usually experienced over the course of an entire year. The annual average rainfall figures for this part of the coast are normally higher than for other coastal regions in Namibia (Robertson et al., 2012).

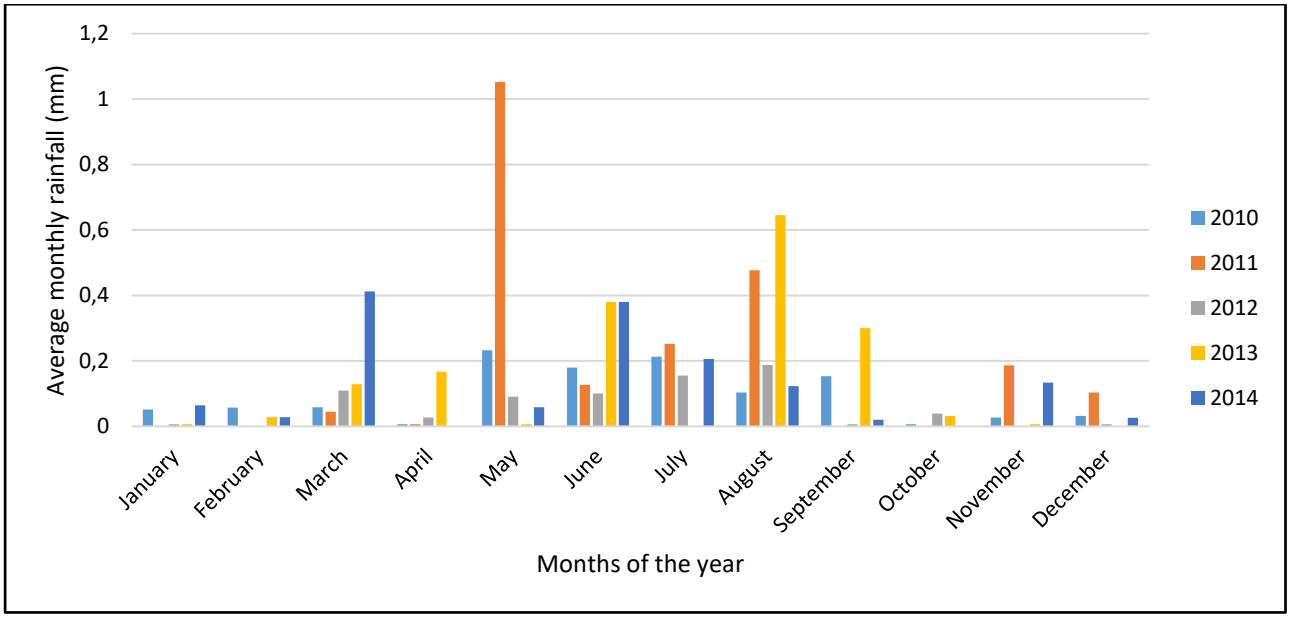

Figure 2.3: Monthly average rainfall from 2010 to 2014 at Alexander Bay.

b. Fog

Fog is the most distinctive feature of the coastal climate of Namibia. Precipitation on the coastal areas of Namibia consists mostly of fog. Fog is more frequent along the coast than inland and yields five times more water than rain or drizzle in the central Namib (Robertson et al., 2012). Fog normally occurs in the mornings and the evenings, and usually starts to disperse as the sun warms the earth. As fog dissipates, visibility along the coast improves. On average, Oranjemund is affected by fog on more than 100 days annually. These fog conditions usually form when cold moist air from the ocean meets hot dry air from the desert (SAIEA, 2006). Fog is regarded as a weather hazard, as it reduces visibility and contributes to weathering and mineral breakdown (CSIR, 2005a).

The most important type of fog that occurs near the coast is advective. Advection fog forms when warmer air blows over a cold land or water surface; it gives off heat to the colder underlying surface. This process will cool the air to dew point and advection fog will form.

UNIVERSITEIT VAN PRETORIA
UNIVERSITY OF PRETORIA
YUNIBESITHI YA PRETORIA

Over land, if the wind speed is higher than 10 m/s, the air will be mixed through a relatively deep layer because of larger frictional effect. Thus, low stratus or stratocumulus clouds, rather than fog, will form. Over the sea, however, because there is less frictional effect than over land, advection fog will form even when wind speeds are 15 m/s (Hsu, 1988).

At the Namibian coast, fog may be transported up to 15 km inland by the south-westerly winds (Robertson et al., 2012). Fog on higher levels of the atmosphere can be transported up to 60 km inland and can cause precipitation for up to 33% of days per year. When studying a region near the ocean, sea fog is most likely present. Sea fog forms when salt from the ocean is used as condensation nuclei and could cause fog formation when humidity is as low as 70% (Sandburg,1916).

According to Olivier (2002), fog at Alexander Bay has occurred between a minimum of 49 days and a maximum of 145 days annually from 1954 to 1986. The average for annual fog-day occurrence is 83.9 at Alexander Bay. This is based on fog-day frequency statistics for the 32-year period. Figure 2.4 shows the yearly occurrence of foggy days.

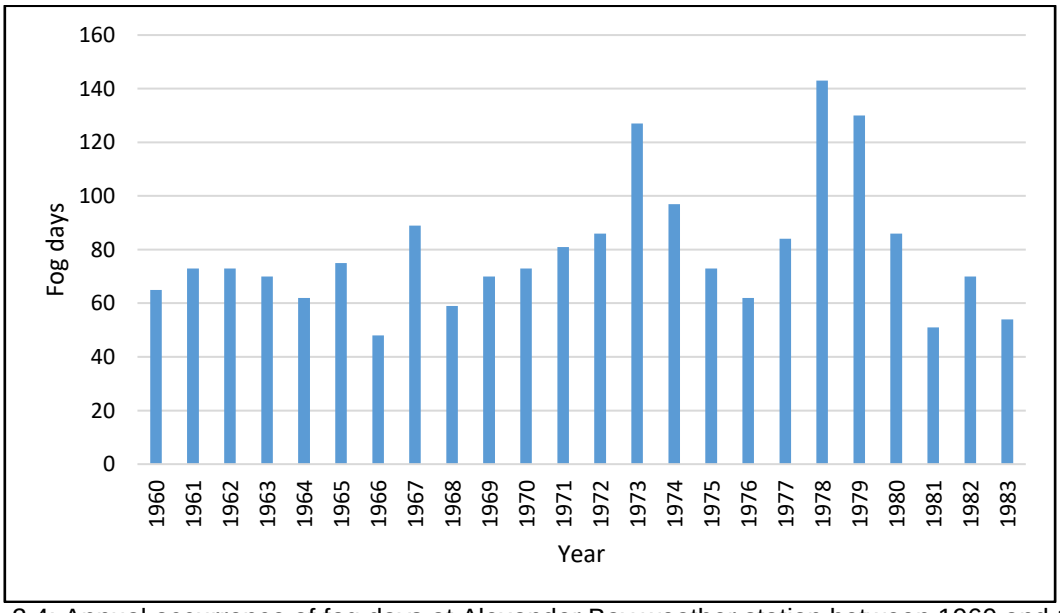

Figure 2.4: Annual occurrence of fog days at Alexander Bay weather station between 1960 and 1983 (Adapted from Olivier, 2002).

Along the coast, fog mostly forms during the night when temperatures are lower. Fog occurrence peaks between 24:00 and 08:00, with the majority of foggy episodes occurring between 05:00 and 07:00. Although coastal fog usually dissipates by 09:00, due to the moist layers of air warmed by the sun, it is not uncommon for fog to last throughout the day (Olivier, 2002).

UNIVERSITEIT VAN PRETORIA
UNIVERSITY OF PRETORIA
YUNIBESITHI YA PRETORIA

c. Relative humidity

Relative humidity is defined as the percentage of water vapour present in the air compared to the maximum amount of water vapour needed for the air (at a certain pressure and temperature) to be saturated (Ahrens, 1994). This ratio is measured as a percentage. A relative humidity measurement of 50% means that the air at a certain pressure and temperature contains half of its water vapour capacity, whereas a relative humidity of 100% means that the air is saturated.

2.2.2.5 Atmospheric stability

The tendency of the atmosphere to increase or suppress vertical movement affects the concentration of pollutants. A stable atmosphere will cause higher pollutant concentrations and inhibit dispersion, whereas in an unstable atmosphere, pollutant concentration will be less and dispersion will increase (Faiz, 1990).

In Figure 2.5 (a), looping of pollution takes place because the lapse rate is super adiabatic and wind speeds are low. Substantial dispersion of pollution takes place when conditions for looping are dominant. Coning of pollution is illustrated in Figure 2.5(b), and takes place when lapse rate is neutral, meaning that the atmosphere is slightly stable to slightly unstable. Coning of pollutants will be most prevalent on cloudy or windy days and at night. Relatively symmetrical dispersion of pollution takes place under coning conditions. A fanning plume (Figure 2.5 (c)) is usually present under stable atmospheric conditions. Vertical motions are inhibited by the stable atmospheric conditions; this means that the plume disperses mostly horizontally (Godish, 1997).

UNIVERSITEIT VAN PRETORIA
UNIVERSITY OF PRETORIA
YUNIBESITHI YA PRETORIA

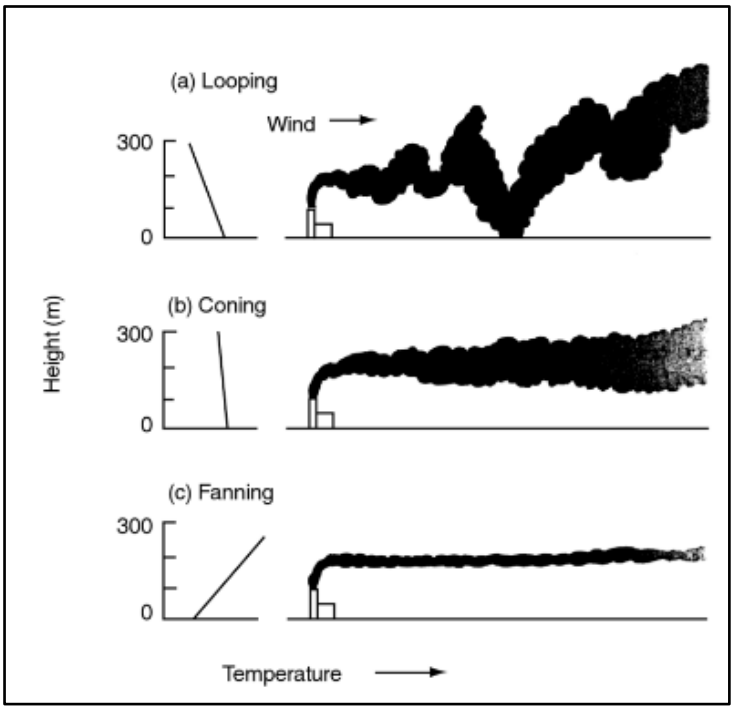

Figure 2.5: Plumes of pollution dispersing under different conditions of atmospheric stability (Godish, 1997).

Monin-Obukhov Length (Equation 4.1) is a stability parameter with the dimension of length (L) and assumes vertical fluxes in the surface layer to be constant. Monin-Obukhov Length is used to describe atmospheric stability. In this equation, κ is the Von Kármán constant and is equal to 0.4. As stated by A.M. Obukhov (1971) in the Journal of Boundary Layer Meteorology, the parameters gravity acceleration (g), temperature at the surface of the earth (T_0), friction velocity (υ), kinematic heat flux (q), specific heat (c_p), and density of the air (ρ) all influence and describe turbulence above the roughness sub-layer in the atmosphere (Foken, 2006).

$$L = -\frac{\upsilon_*^3}{\kappa\left(\frac{g}{T_0}\right)\left(\frac{q}{c_p\rho}\right)} \qquad (4.1)$$

Monin-Obukhov Length is one of the parameters produced by TAPM on a grid over the study region. Monin-Obukhov Lengths range from -1000 metres to 1000 metres, and are used to classify the atmosphere as stable or unstable (Table 4.1). Any lengths larger than 1000 metres or smaller than -1000 metres are classified as neutral.

UNIVERSITEIT VAN PRETORIA
UNIVERSITY OF PRETORIA
YUNIBESITHI YA PRETORIA

Table 2.2: Monin-Obukhov Length stability regimes.

Stability regime	Monin-Obukhov Length (L) in metres (m)
Extremely unstable	-100 to 0
Unstable to slightly unstable	-1000 to -100.1
Neutral	Values bigger than 1000 or smaller than -1000
Slightly stable to stable	1000 to 10.1
Extremely stable	10 to 0

2.2.2.6 Mixing height

Mixing height is measured in metres and can be defined as the height of the area above the surface of the earth where turbulent airflow is present. Mixing height is a key parameter when characterizing the air-pollution climate of a region. Any pollutants or particles released or entrained into this layer will be transported and dispersed vertically (Austin et al., 2002). Convective heating and turbulence due to friction from the earth's surface are the main reasons for dispersion and transport in the mixing layer.

2.3 Meteorology of the region

The weather along the coast of Namibia and in the study region is generally windy, cool and wet. According to Robertson et al. (2012), the unique weather in this region can be attributed to a few important factors. First, two high-pressure systems situated in close proximity to Namibia and, secondly, the cold upwelling of the Benguela sea current. Atmospheric circulation and the Benguela sea current influence precipitation, wind direction, wind speed as well as temperatures at the study area.

2.3.1 Atmospheric circulation

Namibia is classified as a mostly arid country; this can be partly attributed to the atmospheric circulation associated with its location. This unique pattern of circulation exists because of two high-pressure systems situated in close proximity to Namibia as well as the Inter-Tropical Convergence Zone (ITCZ).

The persistent and powerful high-pressure cell located offshore the Namibian coast is called the South Atlantic Anticyclone (Figure 2.6). The circulation around this high-pressure system transports cold air from the south and the south-west and moves it along the Namibian coastline. The cool air reaching the coastline is the reason for the characteristic windy, cool and dry conditions at the Namibian coast (Robertson et al., 2012).

UNIVERSITEIT VAN PRETORIA
UNIVERSITY OF PRETORIA
YUNIBESITHI YA PRETORIA

The second high-pressure cell is the Botswana Anticyclone, situated east of Namibia over the interior of southern Africa. The circulation around this pressure system moves dry air over the region and blocks moist air from the ITCZ from reaching Namibia (Goudie and Viles, 2015). The location of the Botswana Anticyclone during the winter causes significant air pressure variances between the interior and the coast. Consequently, strong easterly Berg winds develop. These warm and dry winds can reach speeds of 50 to 60 km/h and can move massive plumes of desert sand from the interior to the coast and out to sea.

The locations of the two high-pressure systems vary with the seasons. The systems shift southwards during the summer and northwards in winter. The ITCZ also shifts seasonally; it is located south of the equator in the summer and moves northwards in winter. The southwards shift of the ITCZ allows warm, moist air, with the potential to cause rain, to move over Namibia (Robertson et al., 2012). Figure 2.6 shows the relative positions of the two high-pressure systems and the ITCZ in summer (February) and in winter (May).

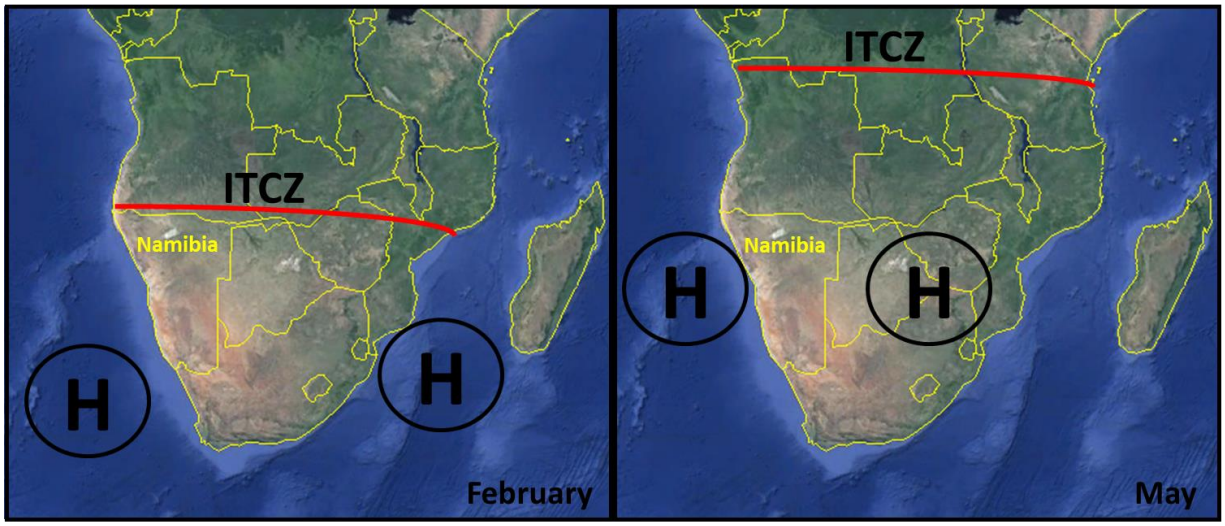

Figure 2.6: Positions of the two anticyclonic high-pressure systems and the ITCZ in May and February (Adapted from Robertson et al., 2012).

2.3.2 Benguela sea current

The cold Benguela sea current (Figure 2.7), which flows parallel to the coast of Namibia in a northerly direction, strongly influences the climate of the study region. The cold ocean temperatures modify air temperatures at the study region because of its proximity to the coast. Temperatures increase abruptly moving inland (CSIR, 2005b). The proposed site is located in the desert, but it still experiences frequent foggy and cool conditions, due to its location in close proximity to the cold Benguela sea current.

UNIVERSITEIT VAN PRETORIA
UNIVERSITY OF PRETORIA
YUNIBESITHI YA PRETORIA

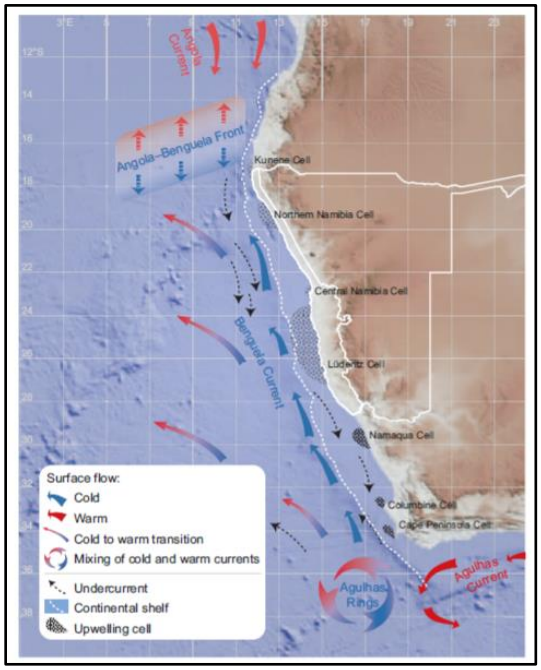

Figure 2.7: The north-flowing Benguela sea current (blue), the south-flowing Angola sea current (red) and the systems associated therewith (Robertson et al., 2012).

a. Benguela current upwelling

Upwelling of deep, cool water along the Namibian coast is caused by the Benguela sea current. The strongest upwelling cells are located where the inner-continental shelf is narrow and winds are strong. This upwelling causes deep, nutrient-rich water to move to the sea surface where planktonic plants use the nutrients; these plants then serve as a food source for fish and other animals (Robertson et al., 2012). The consequence of this upwelling is Hydrogen Sulphide eruptions along the Namibian coast.

b. The Benguela Nino event

The Benguela Nino event can be defined as warm Sea Surface Temperatures (SSTs) occurring off the Angolan and Namibian coasts. Benguela Nino is caused by wind stress changes in the western equatorial Atlantic Ocean and can cause SST to reach temperatures of up to 5°C higher that what is normal for a specific season. These events occur every few years and significantly affect variability of rainfall in south-western Africa (Rouault, 2015).

2.4 Land- and sea breeze circulation

Land- and sea breeze circulations are typical thermally driven mesoscale phenomena with a time span ranging between hours and days. The energy for initiating and maintaining the breeze circulation is due to differential solar heating caused by the different heat capacities and albedo of land and water. Land masses have a low heat capacity and are a poor thermal

UNIVERSITEIT VAN PRETORIA
UNIVERSITY OF PRETORIA
YUNIBESITHI YA PRETORIA

conductor, whereas the sea has a higher heat capacity and is a better conductor of heat. Heating or cooling of a column of air above a land or water mass leads to differences in pressure. A pressure gradient will cause air masses to move and form a mesoscale circulation (Ackerman, 1995).

During the day, land masses warm quickly and, consequently, the air above them heats and rises. The upward movement of air masses causes a high-pressure region to form over the land mass. A horizontal pressure gradient now exists; this means that the pressure over land is higher than the pressure over the sea. This difference in pressure between the two masses creates a thermal circulation, causing a wind to start blowing from the land out to the ocean (Ackerman, 1995). A low pressure forms at the surface over the land mass and a high pressure forms over the ocean; this again causes a horizontal pressure gradient to form between the two masses. At the surface, the air is moving from the ocean towards the land. To replace the surface air volumes, air sinks from above (Ackerman, 1995). This is called a sea breeze circulation (Figure 2.8).

As the day progresses, the differences in temperature between land and sea get larger and the circulation strengthens. As the circulation gets stronger, the wind speed increases and reaches a maximum in the middle to late afternoon (Ackerman, 1995). A sea breeze may be experienced up to 15 km inland and up to a height of 500 m. A sea breeze can have velocities of up to 10 m/s (Lazaridis, 2010).

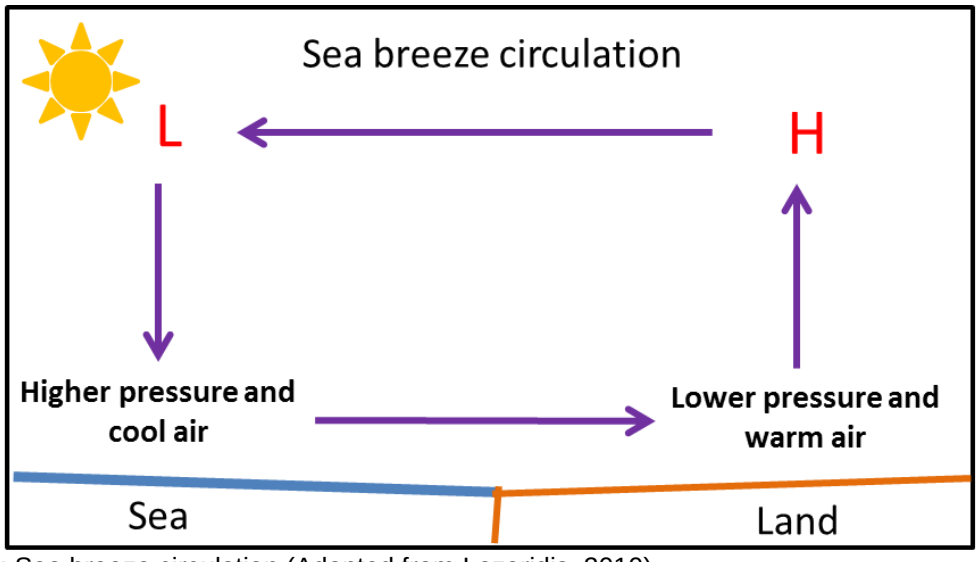

Figure 2.8: Sea breeze circulation (Adapted from Lazaridis, 2010).

In the evening, land masses cool faster than the ocean and the circulation is reversed, causing the development of a land breeze (Figure 2.9). The wind at the surface now blows from the land to the ocean. A land breeze may be present up to a height of 100 m. The velocities and

UNIVERSITEIT VAN PRETORIA
UNIVERSITY OF PRETORIA
YUNIBESITHI YA PRETORIA

height of a land breeze are much less than a sea breeze, because the temperature differential is not as intense as during the day (Lazaridis, 2010).

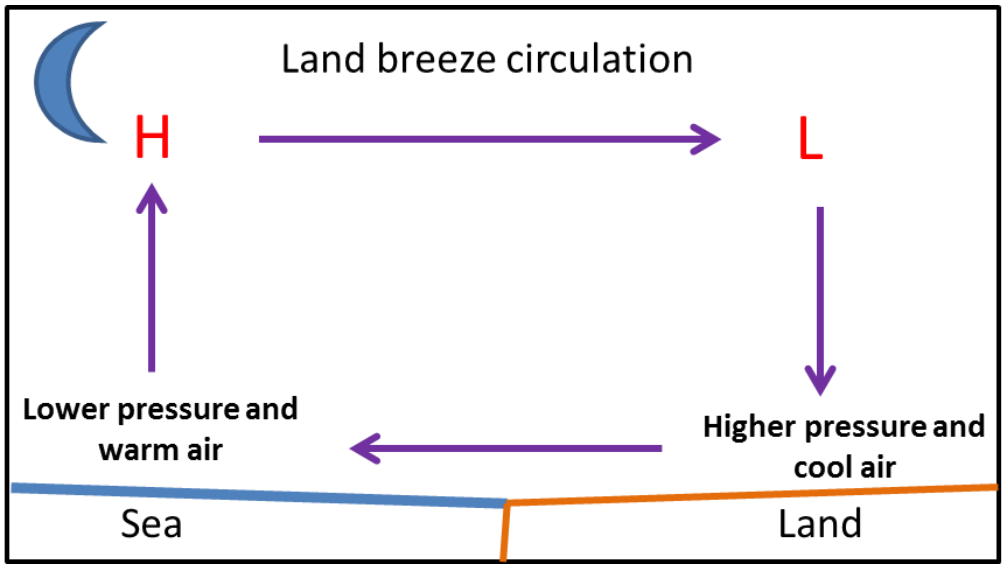

Figure 2.9: Land breeze circulation (Adapted from Lazaridis, 2010).

2.4.1 Climatology of land and sea breezes

Sea breezes are present on 3 out of 4 days along tropical coasts. The high temperatures, high solar radiation, and weak prevailing winds are some of the reasons why the sea breeze is so common at the low latitudes. The climatic significance of sea breezes normally decreases with latitude. In temperate regions, sea breezes generally occur during late spring and summer when the atmospheric environment is favourable to the development of the thermal sea-land circulation system (Heidom, 1998).

Land breezes occur less frequently than sea breezes. Along steep coastlines or coasts of volcanic islands, however, it may be the prevailing breeze circulation with speeds in excess of 9 m/s. Land breezes occur in the temperate regions during winter, particularly when the current that flows along the coastline is warm (Heidom, 1998).

2.5 The Planetary Boundary Layer

The Planetary Boundary Layer (PBL) can be described as the region of the atmosphere located directly above the surface of the earth. The PBL is influenced by the surface of the earth and responds to surface forcing (frictional drag, evaporation, transpiration, heat transfer and terrain induced flow alteration) with a timescale of no more than an hour (Stull, 1988). The vast majority of pollutants are emitted into this layer of the atmosphere, and turbulence in the layer has a major influence on pollution diffusion and accumulation (Thomas, 2008).

UNIVERSITEIT VAN PRETORIA
UNIVERSITY OF PRETORIA
YUNIBESITHI YA PRETORIA

The Kudu CCGT power station location was chosen because of its proximity to the Kudu gas field and the ocean. The location of the Kudu CCGT power station means that ocean and land interactions are important when considering the structure of the PBL in the study region.

2.5.1 The Internal Boundary Layer

An Internal Boundary Layer (IBL) in the atmosphere develops when horizontally moving air passes across a change in some meteorologically relevant property of the earth's surface. A discontinuity in terms of surface roughness, temperature, humidity, or a change in turbulent surface flux of heat or moisture could cause the formation of an IBL (Garratt, 1989).

The coastal area of the earth, which separates two surfaces, presents a combination of few or all discontinuity of roughness length (the ocean roughness, in most instances, being smaller than the land) and temperature difference. This is due to the large difference in the heat capacity and albedo properties between the ocean and the land, which leads to a marked alteration in humidity and turbulent fluxes of heat and momentum. Therefore, the coastal area development of IBL is mostly due to a combination of meteorological and surface discontinuities. Turbulence and flow characteristics of the boundary layer, which are determined by the nature of the upwind surface, have an effect on the way in which pollution will disperse (Benson, 2005).

When air, whose wind profile is in equilibrium with an underlying surface, passes through a relevant discontinuity, it has to adjust to the new surface or the changed conditions (Elliot, 1958). The fact that the surface of the earth is not homogeneous means that changes in surface roughness are always present. Airflow over these surfaces will adjust to the changing surface characteristics. The IBL forms as a result of these changes (Benson, 2005).

The IBL grows in depth downwind and its height can be calculated as a function of distance from the discontinuity. The effect of thermal stability on IBL height is found to be small; it will raise the height of the IBL in lapse conditions and lower it when an inversion is present (Elliot, 1958).

2.5.2 The Thermal Internal Boundary Layer

The IBL developing concurrently with sea breeze circulation is often denoted as a Thermal Internal Boundary Layer (TIBL). These circulations have a special relevance, since they affect the transport and diffusion of pollutants in coastal regions. The typical depth of a TIBL is several hundreds of meters and it can extend up to 10 km inland before an equilibrium is reached.

UNIVERSITEIT VAN PRETORIA
UNIVERSITY OF PRETORIA
YUNIBESITHI YA PRETORIA

The TIBL forms near the earth's surface when stable and cool marine air moves from the ocean and meets with an unstable region that formed over the hot land surface. The marine air is now situated above the land mass and conducts heat from the surface, leading to convective currents forming within the mass of marine air. These convective currents transport air vertically upward from the land surface and grow in height as the air moves further inland (Miller et al., 2003).

The TIBL causes many air-pollution problems in cities near the coast, due to the stable marine air above the TIBL acting as a 'cap' and reducing the mixing depth of the atmosphere. The stable marine air prevents mixing between the region underneath and above the TIBL. Pollutants are often trapped close to the surface in a shallow layer, which quickly leads to unhealthy concentration levels of pollutants.

The most typical phenomenon illustrating the importance of TIBL is fumigation (Figure 2.10). Industrial plumes when emitted from a stack located near the shoreline are emitted into the stable marine air above the PBL. The pollution plume travels in this layer with little diffusion and later intersects the top of the turbulent layer; due to downward entrainment, the pollutants are 'trapped' within the TIBL (Misra, 1980). Pollutants from plumes are mixed to the surface, where they then meet the convective conditions associated with the TIBL (Miller et al., 2003). The fumigation process causes mixing of the plume to the ground, which frequently results in high ground level concentration of pollution that may last for hours.

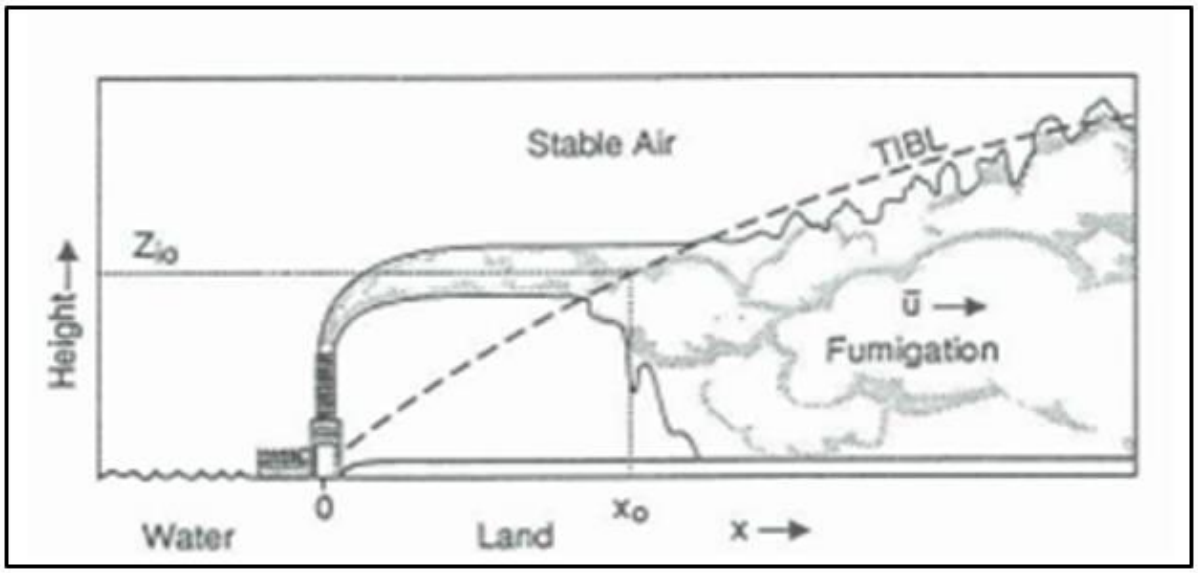

Figure 2.10: Illustration of the shoreline fumigation phenomenon (Luhar, 1995).

Updrafts associated with the convective turbulence in the TIBL transports plumes of pollution hundreds of meters vertically upwards. These plumes can be divided into many branches.

UNIVERSITEIT VAN PRETORIA
UNIVERSITY OF PRETORIA
YUNIBESITHI YA PRETORIA

Some branches will move towards the ocean and be transported kilometres offshore. These branches of pollution can also be circulated landward because of the sea breeze circulation (Miller et al., 2003). Concentration of pollutants within the sea breeze circulation will increase as the day progresses because of the process of shoreline fumigation. New emissions are added to older pollutants already present in the circulation.

Along the coast, topographical structures and meteorological features often cause the development and circulation of wind in the lower levels of the atmosphere. Industries (e.g. power stations), which are often located near the coast, release high levels of pollutants into these mesoscale circulations. It is essential to investigate the downwind behaviour of these circulations. Understanding the way in which the pollutants behave contributes to the control of health risks associated with high concentrations of pollutants (Miller et al., 2003).

2.6 Salt spray from the ocean

The ocean is the main supplier of salt aerosol in the atmosphere. Salt spray is expected to create very high chloride contents in the sand and atmosphere around the study region. It is, therefore, important to have a good understanding of the causes and consequences of this phenomenon.

Salt spray refers to increased amounts of Sodium (Na^+) and Chloride (Cl^-) ions in the environment, and involves the transport of salt from the ocean to the land in the form of spray. Wave size, wind speed, and wind direction have an effect on the salt spray occurrence and formation. Salt spray influences living organisms and structures located near the coast. Salt crystals in the environment also act as condensation nuclei that may cause damage to structures such as the CCGT Kudu power station by abrasion during wind-storms (Maun, 2009).

The formation of salt spray starts with a large number of small foam bubbles that are usually associated with waves that have high amplitudes and turbulence. These small bubbles will only exist at wind velocities larger than 5 m/s^{-1}. Large bubbles will form as soon as the wind exceeds 5 m/s^{-1}. Large bubbles burst and produce very small droplets, each bubble producing approximately 5 droplets. The seawater droplets are now ejected into the air to heights of 0.5-15.0 cm.

While the seawater droplets are in the airstream, their inland transportation is dependent on the velocity of the onshore wind. If relative humidity, wind speed and the size of the droplet are not favourable, it will evaporate while being transported. If the water evaporates, droplet-weight is reduced and a salt crystal forms. This reduction in the size of

UNIVERSITEIT VAN PRETORIA
UNIVERSITY OF PRETORIA
YUNIBESITHI YA PRETORIA

the droplet will cause the rate of settlement of salt crystals to decrease. Salt spray are carried inland under lower humidity conditions. Fallout of salt crystal nuclei happens when nuclei can no longer be transported in the airstream.

The intensity of salt spray episodes and salt deposition is low at wind speeds lower than 6 m/s^{-1} and increases suddenly as wind velocities increase to 7.5 m/s^{-1} and higher. Salt-spray deposition decreases as the distance from the mean tide line increases. On coasts with strong winds, salt spray travels long distances inland.

Sea salt aerosols (SSA) originate from sea spray. These aerosols play a significant role in the interaction between air and sea, meteorology, cloud physics, climate, oceanography and the chemistry of the atmosphere. SSAs could have adverse effects on economic and technological factors as well as on human health. These aerosols are an important component of cloud condensation nuclei and influence the formation and specific properties of fog and rain (Lewis and Schwartz, 2004).

SSA have an effect on the atmospheric cycles of Chlorine, Halogens and Nitrogen; they decrease visibility and inhibit the spread of electromagnetic radiation in the atmosphere by scattering light. SSA influence the clear-sky radiation balance over oceans through changes in albedo. This has an impact on the radiation budget of the earth. SSA also play a role in coastal ecology, corrosion and fouling of sensors, and weathering of stone and marble (Lewis and Schwartz, 2004).

The degree of precipitation and evaporation, river flow into oceans and the degree of mixing of ocean waters control the salinity of seawater. The majority of dissolved elements in seawater are comprised of eleven major elements (Table 2.2).

UNIVERSITEIT VAN PRETORIA
UNIVERSITY OF PRETORIA
YUNIBESITHI YA PRETORIA

Table 2.3: Average concentrations of the main ions in seawater (% by weight) (Adapted from Brown et al., 1989).

Ion	Parts per thousand by weight
Chloride (Cl^-)	18.980
Sulphate (SO_4^{2-})	2.649
Bicarbonate (HCO_3^-)	0.140
Bromide (Br^-)	0.065
Borate ($H_2BO_3^-$)	0.026
Fluoride (F^-)	0.001
Sodium (Na^+)	10.556
Magnesium (Mg^{++})	1.272
Calcium (Ca^{++})	0.400
Potassium (K^+)	0.380
Strontium (Sr^{++})	0.013

The concentration of Chlorides is very high, due to gas released from volcanoes and the weathering of rocks. Most of the other elements present in seawater come from the weathering of earth's crust; this means that seawater contains higher concentration of salts which dissolve easily in water (Maun, 2009).

2.7 Chemistry of pollutants

Air pollutants are classified as primary or secondary. Pollutants emitted directly from a source such as a power station are called primary, whereas secondary pollutants are those formed by physical or chemical processes in the atmosphere (Faiz, 1990). Pollutants of concern to this research project are those that pose a potential threat to the operation of the CCGT power station as well as the combustion products of the CCGT power station.

Natural gas, composed predominantly of Methane (CH_4), will be used to power the GGCT power station. The percentage of Methane in natural gas usually varies between 60% and 95%, the remaining volume is made up of Ethane, Propane, Butane and Hexane in decreasing percentages. The composition of the natural gas will affect the heating value and combustion products of the gas (Skrotzki, 1956).

UNIVERSITEIT VAN PRETORIA
UNIVERSITY OF PRETORIA
YUNIBESITHI YA PRETORIA

2.8 Hydrogen Sulphide eruptions

The population of Namibia's desert coastline is intermittently affected by Hydrogen Sulphide eruptions that manifest as a 'rotten egg smell' originating from the Atlantic Ocean. These eruptions are caused by decaying plants on the sea floor. The Hydrogen Sulphide gas that results from these eruptions is highly toxic to the fish and other marine animals that feed off the phytoplankton.

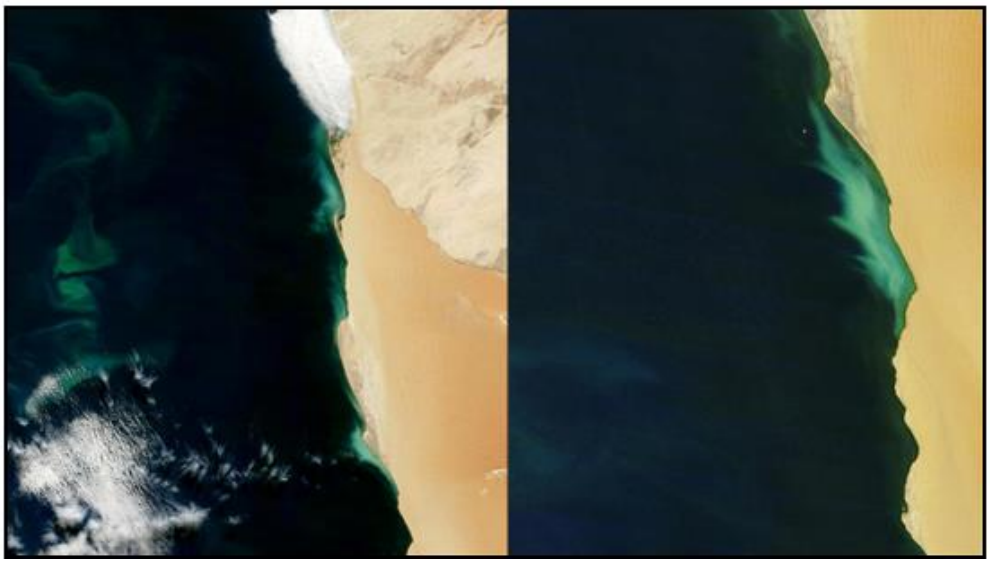

Figure 2.11: Hydrogen Sulphide eruption along the Namibian coast on 12 May 2004 (left) and on 10 April 2004 (right) (Nasa.gov, 2016).

Strong ocean currents transport nutrient-rich water from the depths of the ocean to the surface of the south-east Atlantic Ocean. Phytoplankton, among other sea life, use the nutrient-rich water to live. Phytoplankton only live for a few days and sink to the floor of the ocean when they die. The decay process of the phytoplankton utilizes all the underwater oxygen; consequently, anaerobic bacteria have to complete the decomposition process. The anaerobic bacteria produce Hydrogen Sulphide gas as a by-product that then starts to build up on the ocean floor. The Hydrogen gas eventually erupts from the ocean floor and reaches the surface where Hydrogen molecules combine with Oxygen from the atmosphere to form water. This reaction leaves behind solid white Sulphur in the ocean (Figure 2.11).

The presence of Hydrogen Sulphide near the proposed CCGT power station is of great concern. Not only is Hydrogen Sulphide gas very toxic; it is also corrosive. With the source of gas for the CCGT power station being located some kilometres offshore, there will be the need for pipelines in the ocean to connect the station to the source gas. It will be crucial that materials resistant to corrosion be used in this environment. Contact with Hydrogen Sulphide

UNIVERSITEIT VAN PRETORIA
UNIVERSITY OF PRETORIA
YUNIBESITHI YA PRETORIA

will cause structures made from materials such as concrete and metals to weaken (EPA, 1991).

2.9 Corrosion

Corrosion is the natural process that occurs when a material (such as iron or steel) combines with Oxygen and water to form rust (Davis, 2000). Corrosion poses a threat to the structure of the CCGT power station, because it enhances the deterioration of building material.

In the study region, corrosion is largely related to the production of Hydrogen Sulphide (H_2S) and SSA. Atlantic sea fog contains weak Sulphuric Acid (H_2SO_4) and is considered to be the biggest contributor to corrosion of metals and concrete in the region. Sodium Chloride ($NaCl$) and Potassium Chloride (KCl) are also of concern, as the proposed CCGT power station will be located approximately 1 km from the coastline. These two salts can react with Sulphur (S) to produce corrosive agents that can result in corrosion of power station blades (Wilkes, 2007). To combat this effect, corrosion-resistant materials such as metal alloys, concretes resistant to corrosions, plastics and metallic coatings can be used (EPA, 1991).

2.10 Conclusion

CCGT technology can successfully function in many types of climates and environments, because the inlets to the turbines are fitted with filtration systems. Air-filtration systems remove airborne particles and some contaminants from the intake air so as to minimize the harm that might be done to the CCGT power station. These systems are designed according to the location of the station and the air quality of the region (Wilkes, 2007).

It is clear from the above that the proximity of the study region to the coast holds many meteorological challenges when considering pollutants and pollution dispersion. Understanding the factors leading to the relevant meteorological phenomena and quantifying the frequency of occurrence can assist with the decision-making processes when the CCGT power station is being designed and when it is in operation. Using threshold values in order to forecast meteorological phenomena (sea breezes, foggy days, etc.) will also be of use when the station is operational.

UNIVERSITEIT VAN PRETORIA
UNIVERSITY OF PRETORIA
YUNIBESITHI YA PRETORIA

CHAPTER 3: DATA AND METHODOLOGY

3.1 Study region

The study region is Oranjemund, a small diamond-mining town on the south-western coast of Namibia. Uubvlei, located 20 km north-east of Oranjemund has been selected as the proposed site for the CCGT power station. It was identified as the optimum location for a power station rather than more distant towns from the gas field such as Luderitz and Keetmanshoop (Figure 3.1). The CCGT power station will be located approximately 1 km from the coastline.

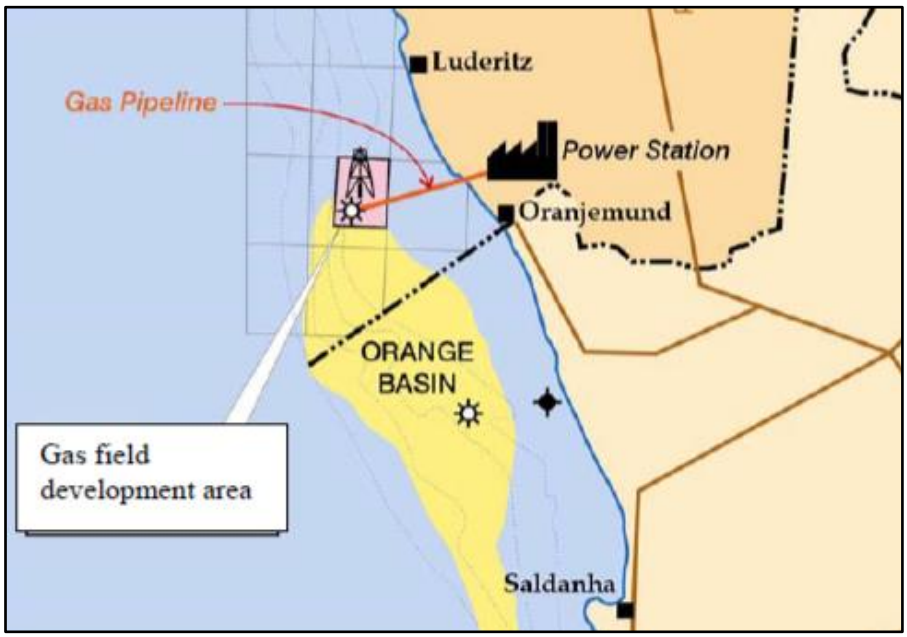

Figure 3.1: The Kudu gas field located offshore the south-west coast of Namibia in the Orange basin (Namcor, 2014).

One of the shortcomings of the proposed site is that it is located far from the main power demand areas in Namibia, except for Skorpion Zinc and the Namdeb Diamond Corporation (SAIEA, 2006). The site consists of mined-out land; this means that all construction activities will be conducted on already disturbed land (Pallet, 2009).

Oranjemund and Luderitz are located in the Karas region of Namibia and have populations of 9 837 and 13 859, respectively (NSA, 2011). Alexander Bay is located in the Richtersveld region of South Africa and has a population of 1 739 (Statssa, 2011). These are the only populated areas close to Uubvlei that might be affected by the commissioning of the proposed power station (Figure 3.2).

UNIVERSITEIT VAN PRETORIA
UNIVERSITY OF PRETORIA
YUNIBESITHI YA PRETORIA

Figure 3.2: The locations of Luderitz (green), Uubvlei (blue), Oranjemund in Namibia and Alexander Bay, South Africa (red) (Google Earth Pro, 2015b).

The Namibian coast is unique because of the day-to-day weather it experiences. Temperatures within 50 km of the Namibian coast are moderate and generally do not exceed 20°C. This can be attributed to cool onshore winds, frequent foggy conditions, and the occurrence of low cloud (Robertson et al., 2012). Foggy skies, low temperatures, strong onshore winds caused by breeze circulation, the formation of the TIBL, and salt spray are all characteristic features of the study region.

3.2 Data

The data used was gathered from different sources. First, 20 years of observed surface weather data from the South African Weather Service (SAWS) was utilized in order to climatologically characterize the weather in the study region. Secondly, data from an air-pollution model was used to calculate the Air Dispersion Potential (ADP) and supplied the relevant information on shoreline breeze circulation, fog processes, and the TIBL in the study region.

3.2.1 Meteorological data

The meteorology of an area plays a role in determining the diluting effects of the atmosphere (Kanevce and Kanevce, 2006). The dispersion of pollutants in the atmosphere is caused by turbulent eddy movement and advection due to the motion of air masses by the wind (Stokie, 2011). This means that wind speed, atmospheric stability and turbulent processes are the

UNIVERSITEIT VAN PRETORIA
UNIVERSITY OF PRETORIA
YUNIBESITHI YA PRETORIA

most important meteorological factors influencing dispersion in the atmosphere. Other important meteorological factors to consider include: wind direction, temperature, and relative humidity.

3.2.1.1 Modelled meteorological data

The Air Pollution Model (TAPM) is an air-pollution model comprising of a meteorological and an air-pollution component. The meteorological component of TAPM was used to produce the hourly meteorological parameters at points on a grid over the study region (Hurley et al., 2005a and Hurley et al., 2005b). These parameters are used to describe the potential of air dispersion at points over the study region.

The meteorological section of TAPM is a primitive equation, three-dimensional model. It contains a terrain-following vertical coordinate system and includes parameterizations for the micro-physical processes associated with cloud and precipitation, turbulence, fluxes, and soil processes (Hurley, 2008). The model equations disregard time zones and the curvature of the earth; it uses a uniform distance grid across the domain.

The study region is covered by 81 points, which are approximately 20 km apart (Figure 3.3). TAPM was used to model all necessary meteorological information for each point on this grid. This information includes wind speed, wind direction, temperature, relative humidity, mixing height, and Monin-Obukhov Length.

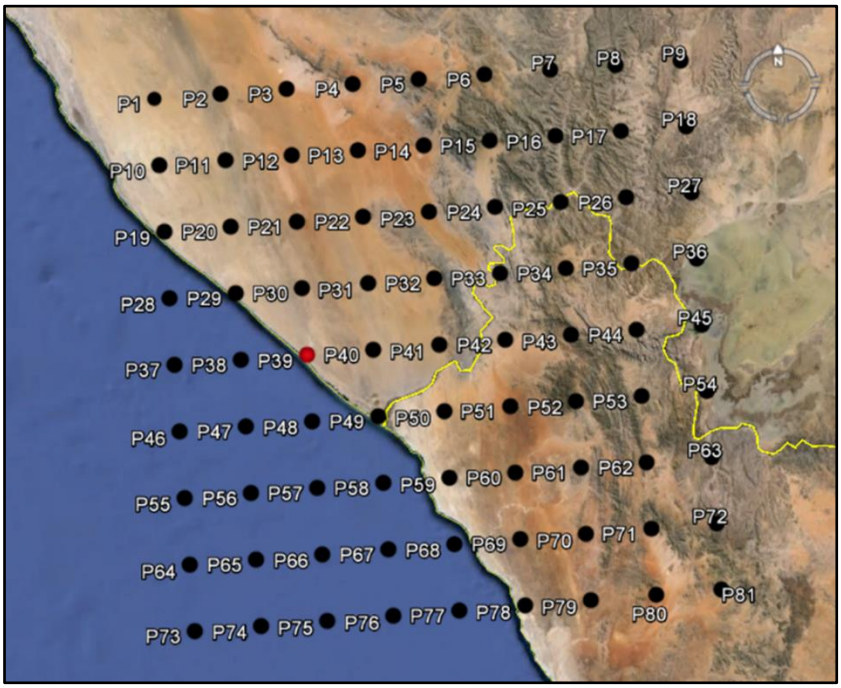

Figure 3.3: 9x9 grid for producing TAPM data over the study region. The red circle represents the origin at Uubvlei (Point 39), whereas each black circle represents points on the grid (Google Earth Pro, 2016a).

UNIVERSITEIT VAN PRETORIA
UNIVERSITY OF PRETORIA
YUNIBESITHI YA PRETORIA

3.2.1.2 South African Weather Service (SAWS) data

Twenty years of hourly weather data (January 1995 to December 2014) pertaining to the climate for the study region was utilized. The data was made available by the South African Weather Service (SAWS). The Alexander Bay weather station was used, because it is located only 35 km south-east of the proposed site at Uubvlei and the data is readily available. Meteorological data from Alexander Bay weather station was used because of the proximity of Alexander Bay to the study region and the fact that the nearest Namibian Meteorological Service station is located at Luderitz (CSIR, 2005a).

3.3 Methodology

The methods used to obtain the results documented in this dissertation are discussed in the following sections.

3.3.1 Air-pollution climate of the region

A combination of TAPM meteorological data and 20 years' observed meteorological data was used to compile results on the air-pollution climate of the region. The meteorological parameters investigated include wind speed and direction, Monin-Obukhov Length, mixing heights, temperature, and relative humidity.

3.3.2 Air Dispersion Potential (ADP)

The atmosphere is the medium in which emitted pollutants from various natural and man-made sources are transported by the winds and diffused by numerous processes. The ever-present atmospheric boundary layer turbulence is a major role player in the diffusion process. The air-pollution phenomenon is further determined and complicated by the interaction of pollutants with the underlying surface, land, vegetation, water bodies, and precipitation events, all of which are associated with different physical and chemical processes.

Atmospheric science plays a major role in determining the daily weather and long-term climatological conditions that are relevant to the levels of air-pollution concentrations in the atmosphere. The information on the type of pollutant, emission rate of a pollutant source, observed concentrations, and air-pollution modelling results are major tools for making policy and planning decisions, developing and updating air-quality regulations and management plans at national, provincial, district and local levels, as well as determining the effects of pollutants on human population and the environment.

UNIVERSITEIT VAN PRETORIA
UNIVERSITY OF PRETORIA
YUNIBESITHI YA PRETORIA

The characterization of the ability of the atmosphere to adequately dilute and disperse any admixture is often referred to as Air-Pollution Potential (Holzworth, 1967) or, in this paper, as Air Dispersion Potential (ADP). The PBL processes that contribute to the dispersal potential of any area are turbulent eddy movement and advection, due to the motion of air masses by the wind (Stokie, 2011). Therefore, the PBL parameters chosen to represent the ADP in this paper are the horizontal wind velocity, the PBL height, and the atmospheric stability.

In this research paper, Air Dispersion Potential (ADP) is implemented. ADP, as proposed in this dissertation, is a novel, comprehensive and contemporary representation of the characteristics of air-pollution. ADP is a joint probability distribution that considers the combined effect of all relevant dynamic, thermodynamic and turbulence processes which determine the conditions of air pollutant dispersion in the atmosphere.

The ADP index uses the input information required to run a contemporary air-pollution model which includes the dynamic factors: wind velocity ($|\vec{V}|$) (preferably at several levels in the atmosphere), appropriate atmospheric stability information (Monin-Obukhov Length (L)), height of the PBL (H) and/or inversion height ($H_{inversion}$), and turbulence parameters.

The ADP index is based on the conditional probability distribution of these parameters, which allows for constructing the relevant probability tree. This means that the probability of the comprehensive ADP index is the multiple of probabilities for wind speed P($|\vec{V}|$), height of the PBL $P(H)$, and stability $P(L)$. Therefore, the probability tree for individual realization of ADP will be:

$$P(ADP)=P(|\vec{V}|)P(H)P(L) \qquad (3.1)$$

Equation 3.1 is used to calculate the individual ADP values as determined by the weather forecast model (for example TAPM gives output for every hour). The individual ADP values are then used to determine hourly and long-term averages. Equation 3.1 reveals its atmospheric physics correctness by applying a dimensional analysis. The dimension of the ADP is $m.s^{-3}$ multiplied by the stability factor $P(L)$. Therefore, ADP index gives how many cubic metres per second (ventilation rate) are passing through a certain point and what the conditions are for the pollutants to diffuse.

Further, the intervals for the wind speed, PBL height, and stability are quantified by proxy for favourable, moderate and unfavourable. The ADP index will have value describing the combined effect of the meteorological variables, which determine the ADP for a certain

UNIVERSITEIT VAN PRETORIA
UNIVERSITY OF PRETORIA
YUNIBESITHI YA PRETORIA

region. The coefficients for the favourable, moderate and unfavourable (Table 3.1) ADP index are chosen in such a way that the ADP value can be in the range of 100 to 25 (value 100 gives absolutely favourable air-dispersion conditions, 50 moderate, while a value of 25 is very unfavourable).

Table 3.1: Parameters and limits used in ADP calculation.

	Unfavourable	**Moderate**	**Favourable**
Wind speed	0-2 m/s	2-5 m/s	>5 m/s
Mixing height	0-400 m	400-1000 m	>1000 m
Monin-Obukhov Length	0 to 200 m	>1000 m	0 to -200 m

The individual values of ADP can be used to obtain average daily, monthly, seasonal, and annual statistics. These values can also be used to create the joint distribution of wind direction and ADP.

3.3.3 Occurrence of sea breeze circulation

The frequency of occurrence of coastline circulations at the study region is of importance, as it will influence the way in which pollutants disperse. Not only the direction and speed of the wind, but also the accompanying phenomena (fumigation, salt spray, etc.) plays a role. Crucial to the development of sea breeze circulation (or any similar type of circulation) is a sufficient temperature difference between water and the land surface. In the case of sea breeze development, the temperature of the land surface must be at least 3°C warmer than the adjacent water (MetEd, 2016). The potential for sea breeze development also increases when there is an onshore wind component present.

A MATLAB program has been developed to determine periods that are favourable for sea breeze occurrence. The script calculates the temperature conditions relevant for the breeze process over a region that is adjacent to the ocean, using all data for all points over the region. Classification for a sea breeze entails that it must be during day-time (between 08:00 and 16:00), temperature difference between land and ocean must be larger than 3°C, and there must be an onshore wind component present (between 180° and 270°).

UNIVERSITEIT VAN PRETORIA
UNIVERSITY OF PRETORIA
YUNIBESITHI YA PRETORIA

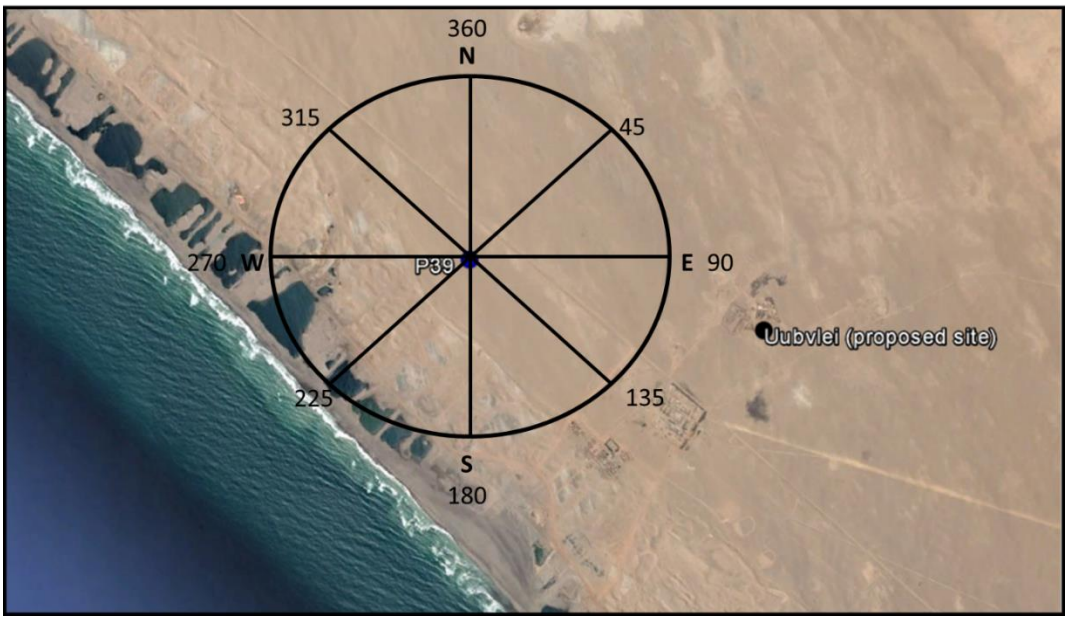

Figure 3.4: Study site with wind directions.

As seen in Figure 3.4, the entire north-easterly quadrant of the wind rose (90° to 360°) can be classified as a region from which a land breeze would blow. In addition, winds originating in the entire south-westerly quadrant (180° to 270°) can be viewed as sea breezes with the proposed site as reference.

3.3.4 Occurrence of coastal fog

Coastal fog occurs frequently in the study region. Coastal fog and low-level clouds are the visible aggregate of condensation droplets that are suspended in the atmosphere, close to the earth's surface (Hsu, 1988). The cold Benguela current together with the upwelling of even cooler water results in normal Sea Surface Temperatures (SST) ranging from 13°C to 18°C, causing the coastal air to cool. Because of this cooling, coastal air is now too cold to rise sufficiently to form rain clouds and fog forms instead (Robertson et al., 2012).

When studying the volume of moisture in air, relative humidity (RH) and dew point temperature (DPT) are two very useful parameters. Clouds or fog develop in the atmosphere when dew point and air temperatures (T) are equal or close to each other. Consequently, RH is equal to 100%.

The ground fog condition near the ocean shore can be determined by using the DPT distributions over the study region. There exists an equation derived by Lawrence (2005) to calculate DPT using only RH and T. The coefficients for Equation 3.1 have the following values: $A1$=17.62, $B1$=243.04, and $C1$=610.94:

UNIVERSITEIT VAN PRETORIA
UNIVERSITY OF PRETORIA
YUNIBESITHI YA PRETORIA

$$DPT = \frac{B1*(ln(RH/100)+((A1*T)/(B1+T)))}{(A1-ln(RH/100)-((A1*T)/(B1+T)))} \qquad (3.1)$$

Fog usually occurs when surface temperatures are within 2.5°C of the dew point temperatures and when RH is close to 100% (AMS Glossary, 2012). The algorithm used for determining fog conditions in this project calculates the DPT and the difference between air temperature and DPT. The difference is tested against the observational value which confirms fog and is around 1°C. The absolutely certain conditions for fog are when this difference is zero and, therefore, the relative humidity is 100%.

In this dissertation, the occurrence of 'foggy days' at the site is calculated using modelled hourly meteorological data for the period of one year. An hour is classified as 'foggy' when the difference between temperature and calculated dew point temperature is small (less than or equal to 1°C).

3.3.5 Thermal Internal Boundary Layer height

The convectively dominated TIBL forms when the stable airflow from the ocean reaches the land and interacts with upward heat fluxes caused by temperature variances between the land and the air. The height of the TIBL increases with distance from the shoreline and is important in air-pollution modelling.

The intensive study of the dynamic and thermodynamic characteristics of TIBL started as early as 1940 and still continues. A review of relevant works and major developments can be found in Garratt (1990), Stunder and Sethuraman (1985), Savelyev and Taylor (2005), Walmsley (1989), and Miller et al. (2003).

The research in finding an appropriate TIBL height formula or description can be grouped in three major categories: a) empirical formulae, b) formulae based on physical principles, and c) numerical models.

The major shortcoming of all empirical formulae is that they are applicable at best for the area where the observational data is collected. In most cases, the approximation formulae used does not have the necessary asymptotes, especially for the equilibrium height. They are not robust and need readjustment for use in different environmental conditions, due to their sensitivity to uncertainties in input parameters. The studies in the group b) have more general applicability, since they are based on the first principles and, despite the use of simplifying assumptions, retain the right asymptotes at short distances from the shoreline. However, they might need use of data from the site of application to choose constants best applicable for

UNIVERSITEIT VAN PRETORIA
UNIVERSITY OF PRETORIA
YUNIBESITHI YA PRETORIA

obtaining the most correct results. The numerical models, in general, are based on the first principles and allow for inclusion of a parameterization scheme for the processes that cannot be solved at present by means of a numerical scheme. They are very complex and can seldom be used for forecasting applications, being a domain of research for processes relevant for the TIBL dynamics and thermodynamics.

In the present study, the use of a formula based on physical principles and appropriately adjusted to the conditions of the study area will be required. General physical consideration requires the height equation to comply with the pertinent conservation laws (in the case under consideration, law of energy conservation), and to have the right asymptotes at short and long distances from the shoreline. The law of conservation of energy is the main equation used in all studies on the topic.

Figure 3.5 illustrates the structure of the TIBL and the application of the first law of thermodynamics. It can be noted that the stably stratified flow from the ocean is modified by the convective turbulence over the land.

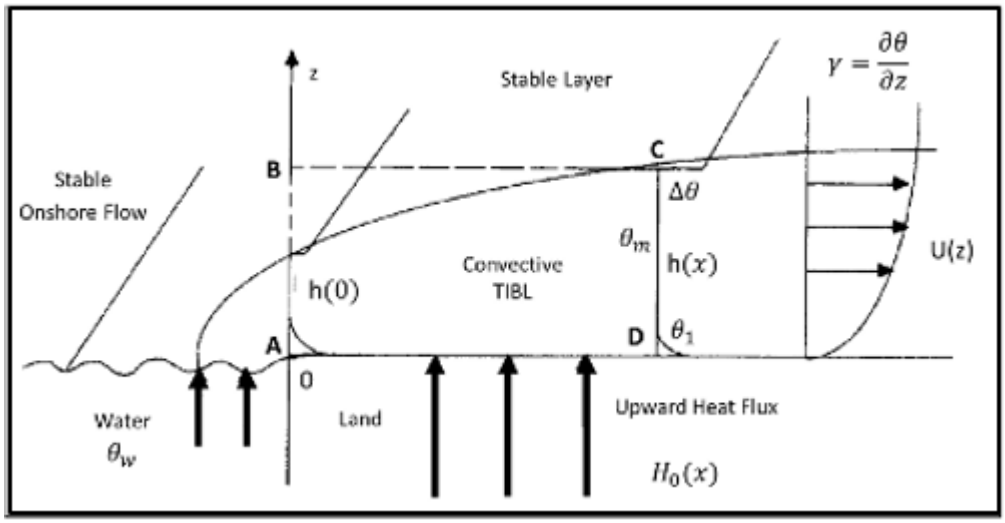

Figure 3.5: Schematic diagram of an IBL and application of the first law of thermodynamics (Adapted from Venkatram, 1986).

Applying the energy conservation balance to the volume ABCD (Figure 3.5) as the energy flux inflow through the boundaries is equal to energy outflow:

$$\rho_a c_p \left[\int_0^{h(x)} u(x,z)\,\theta(x,z)dz - \int_0^{h(x)} u(0,z)\theta\,(0,z)dz\right] = \int_0^x H_0(x)dx \qquad (3.2)$$

where ρ_a is the air density, c_p the specific heat at constant pressure, $u(x,z)$ the horizontal velocity, $\theta(x,z)$ the potential temperature, and $H_0(x)$ the upward heat flux.

UNIVERSITEIT VAN PRETORIA
UNIVERSITY OF PRETORIA
YUNIBESITHI YA PRETORIA

Without loss of generality assuming that $u(z) = const = u_m$ and the entrainment assumption that $\Delta\theta = F\gamma h(0)$ ($F = const$ determined experimentally), the final form of Equation 3.2 for the height of TIBL is:

$$h^2(x) = h^2(0) + \frac{2}{\gamma(1-2F)u_m}\int_0^x Q_0(x)dx \tag{3.3}$$

where $Q_0(x) = H_0/\rho_a c_p$ is the kinematic heat flux.

The physical meaning of Equation 3.3 is that the functional form of the $h(x)$ is determined by the distribution of heat flux with x. If Equation 3.3 is integrated in the simplest case of $Q_0 = const$, it reduces to:

$$h^2(x) = h^2(0) + \frac{2}{\gamma(1-2F)u_m}Q_0 x \tag{3.4}$$

The only asymptote confirmed by experimental evidence and clear physical assumption in deriving Equation 3.4 is:

$$h \sim Ax^{1/2} \tag{3.5}$$

Equation 3.4 contains a major shortcoming in that it does not secure finite value of h at long distances. The same deficiency is contained in many contemporary papers (see, for example, Batchvarova and Gryning (1990, 1994) and Gryning (2005)).

Observational data indicate that, for small x, the TIBL height behaves like $h(x) \sim x^{1/2}$ and $h(x) \sim h_e$ (equilibrium height) at large x. Then an empirical formulation based on the energy balance premise for $h(x)$ is proposed by Venkatram (1986):

$$h^2(x) = h^2(0) + (h_e^2 - h^2(0))\left(1 - e^{-x/L}\right) \tag{3.6}$$

In Equation 3.6, L is the relaxation distance at which the flow from the ocean is adjusted to the turbulent heat flux present over land. Formally, using the exponential function series decomposition for small and large x/L ratios, assuming that $L = \beta h_e$ and $\beta = const$, we have:

$$\begin{aligned} h(x) &\sim x^{1/2} \quad for\ small\ distances \\ h(x) &= h_e \quad for\ large\ distances \end{aligned} \tag{3.7}$$

UNIVERSITEIT VAN PRETORIA
UNIVERSITY OF PRETORIA
YUNIBESITHI YA PRETORIA

Equation 3.7 shows that the proposed formula (Equation 3.6) has the anticipated asymptotes and is very appealing to be generalized for non-steady conditions.

In the case of non-stationary conditions, the function $h^2(x)$ is proposed in this study to become $h^2(t,x)$ with L being a function of time $L(t)$. The next step is to define a method for calculating the relaxation distance $L(t)$. If the realistic assumption that the relaxation distance over which the air flow as well the equilibrium height adjust to the heat flux over the land is used, i.e. $L(t) \sim h_e(t) \sim Q_0(t) \cong \beta h_e(t)$ (β is empirical constant), Equation 3.8 will still retain the required asymptotes as in Equation 3.6. The equation for the calculation of h_e as a function of time using model data or observational data for the time variation of the vertical heat flux is:

$$h_e{}^2(x) = h_e{}^2(0) + \frac{2}{\gamma(1-2F)} \int_0^{t_e} Q_e(t)dt \qquad (3.8)$$

3.4 Conclusion

Using a combination of modelled and observed meteorological data, the air-pollution climate of the study region was characterized based on wind, stability conditions, mixing heights, temperature, and relative humidity. Tools for the prediction of ADP, the occurrence of sea breeze circulation, the occurrence of fog and the height of the TIBL are developed using relevant meteorological parameters obtained by means of any weather-forecast model.

UNIVERSITEIT VAN PRETORIA
UNIVERSITY OF PRETORIA
YUNIBESITHI YA PRETORIA

CHAPTER 4: RESULTS

4.1 Air-pollution climatology

Meteorology provides information of many variables that are relevant to the transport and diffusion of pollutants in the atmosphere. This section presents results based on the previously mentioned methods. It focuses not only on wind climate, but also on other factors which have an influence on determining the air-pollution climate of an area. These variables include wind speed, stability, mixing height, temperature, and relative humidity.

4.1.1 Wind climate

Wind speed and direction data for 20 years from the South African Weather Service (SAWS) weather station at Alexander Bay is used in Figures 4.1 and 4.2. Alexander Bay weather station was chosen, because it is the closest SAWS weather station to the proposed site in Namibia. The average annual wind speed at Alexander Bay according to observations is $4.3\ m/s$. Wind speeds at this weather station can reach speeds of over $20\ m/s$ on occasion.

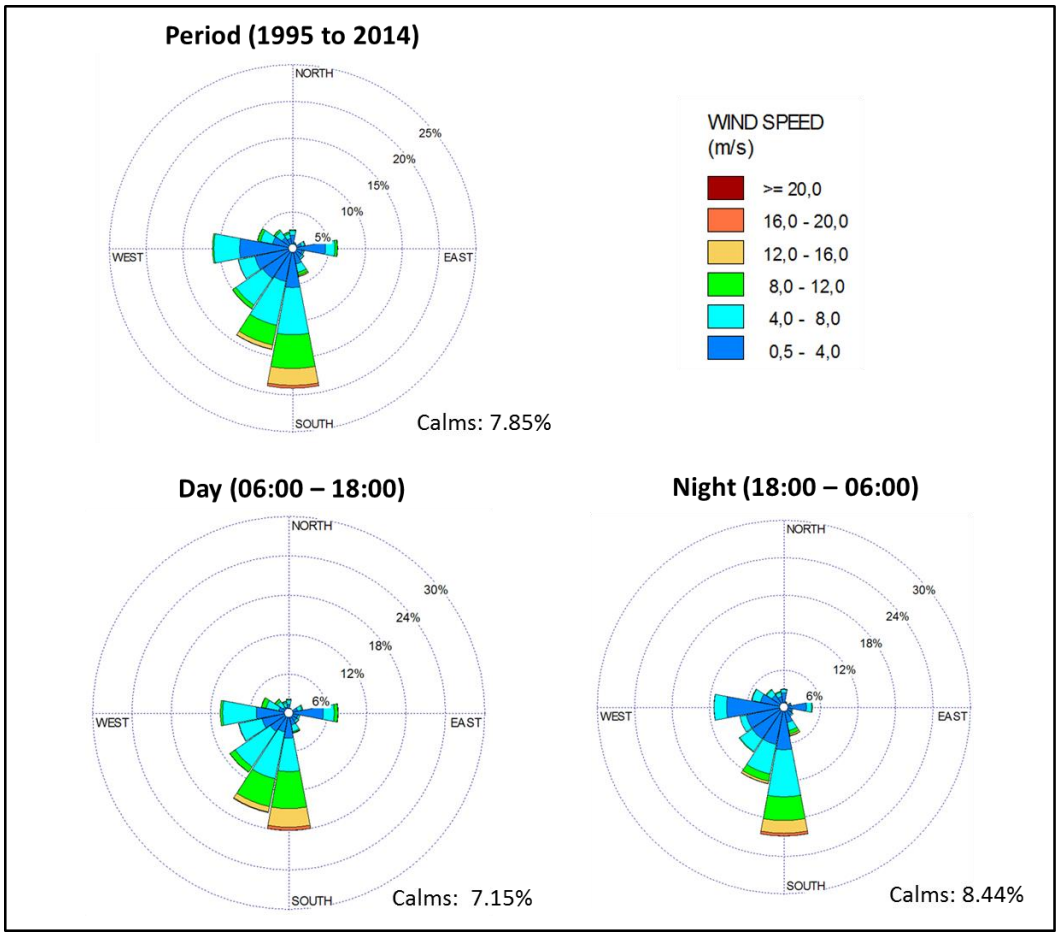

Figure 4.1: Yearly, day and night wind roses for Alexander Bay weather station over a 20-year period.

UNIVERSITEIT VAN PRETORIA
UNIVERSITY OF PRETORIA
YUNIBESITHI YA PRETORIA

In Figure 4.1, the dominant wind direction at the Alexander Bay weather station over the 20-year period is southerly, with most winds originating in the south-westerly quadrant of the wind rose. There also exists a relatively frequent easterly wind component at the site.

During the day, wind directions from the entire south-west quadrant of the wind rose are high in frequency, with southerly, westerly and easterly winds being the most dominant. At night, distribution of wind speeds and directions are similar to the daytime, with a few minor differences in the frequency of occurrence of the dominant wind directions.

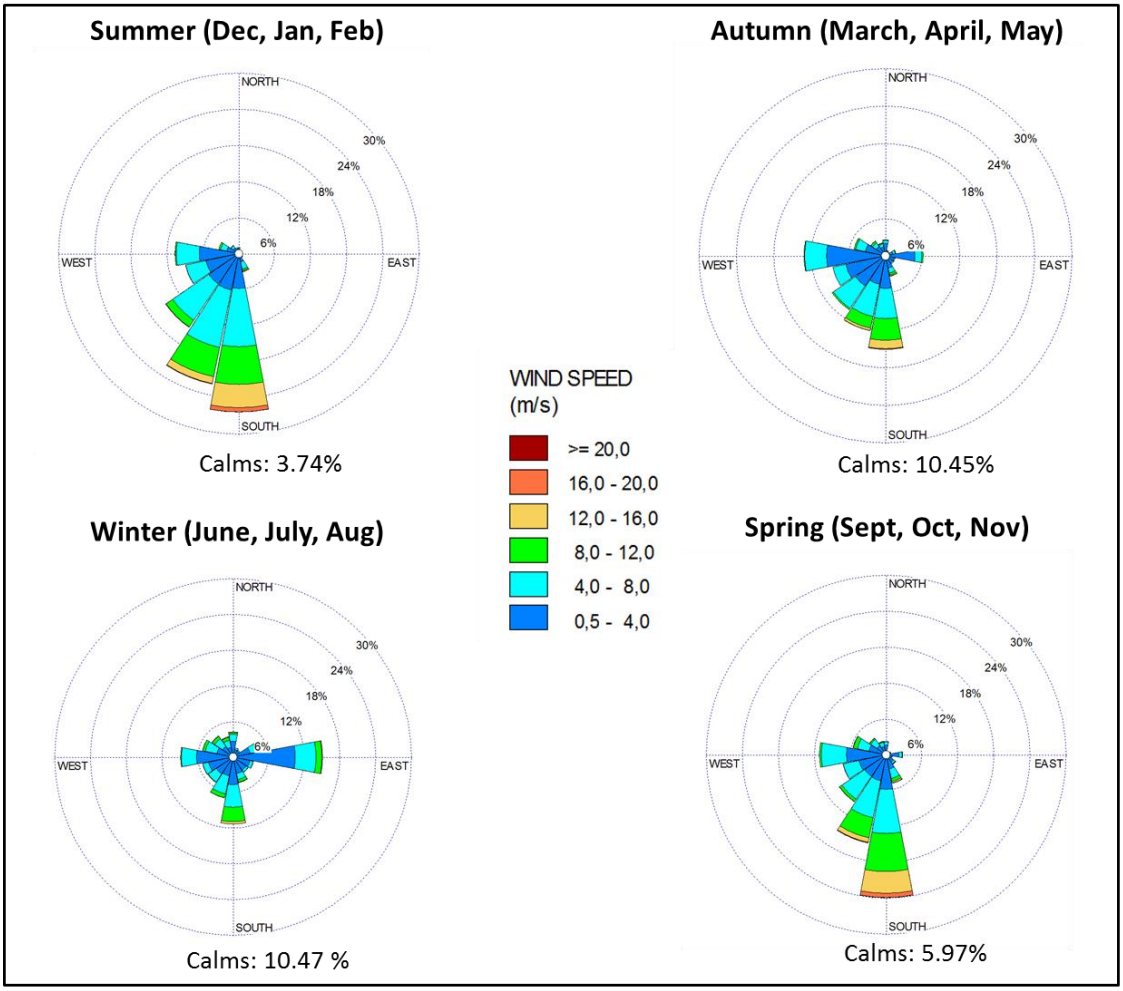

Figure 4.2: Seasonal wind roses for Alexander Bay weather station over a 20-year period.

During summer (Figure 4.2), southerly winds prevail, with the majority of these blowing from the south-west quadrant; the wind speed is mainly between 4 and 8 m/s. Spring shows a similar pattern to summer, but there is an additional easterly wind component with wind speeds varying mostly between 0.5 and 8 m/s. Summer and spring wind roses show a very similar distribution of wind direction and speed; both summer and spring experience relatively strong southerly winds that frequently vary from 8 to 16 m/s. During winter, winds blow from all directions with southerly and easterly winds dominating, and with the dominant wind speed

UNIVERSITEIT VAN PRETORIA
UNIVERSITY OF PRETORIA
YUNIBESITHI YA PRETORIA

being from 0.5 to 4 m/s. Easterly wind occurs approximately 15% of the time during winter. Autumn months are dominated by southerly wind and wind coming mostly from the south-westerly quadrant of the wind rose. Wind speeds during autumn mainly vary between 0.5 and 8 m/s.

Since February 2009, a new mast (10 metres in height) was installed at ground level at the Alexander Bay weather station. Prior to 2009, the mast was located on top of a tower that was approximately 30 metres high, with an additional 3-metre mast on top of the building. The national standard for the height of a wind mast is between 9 and 11 metres. This change in the height of the wind mast has had a noticeable effect on the wind speeds and directions observed at the Alexander Bay weather station.

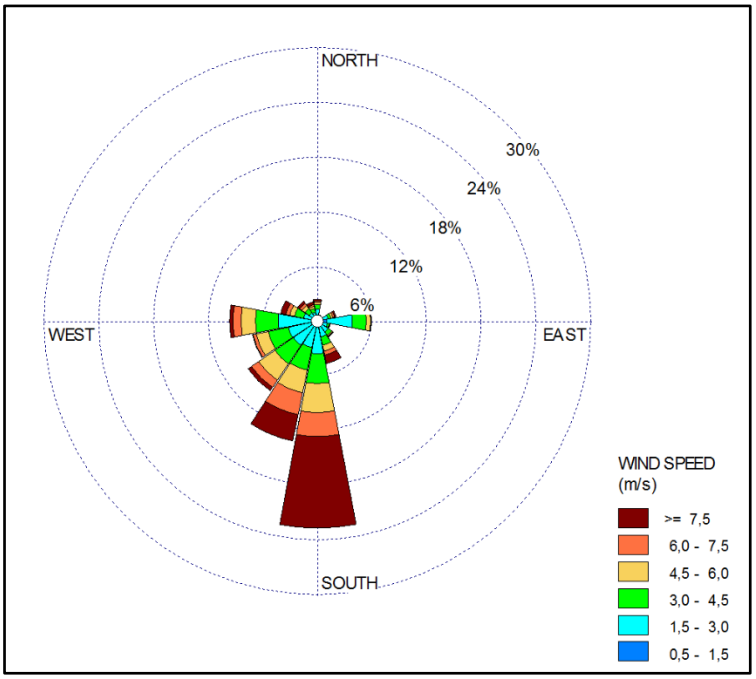

Figure 4.3: Wind rose for Alexander Bay using SAWS hourly wind speed and direction data from January 1995 to January 2009 (wind mast at a height of 33 metres).

Figure 4.3 shows a wind rose for a period of hourly wind speed and direction data where the wind mast was located at a height of 33 metres. A southerly wind dominates at this height and occurs 23% of the time, whereas the south south-westerly wind (which dominates in Figure 4.4) only occurs about 12% of the time.

UNIVERSITEIT VAN PRETORIA
UNIVERSITY OF PRETORIA
YUNIBESITHI YA PRETORIA

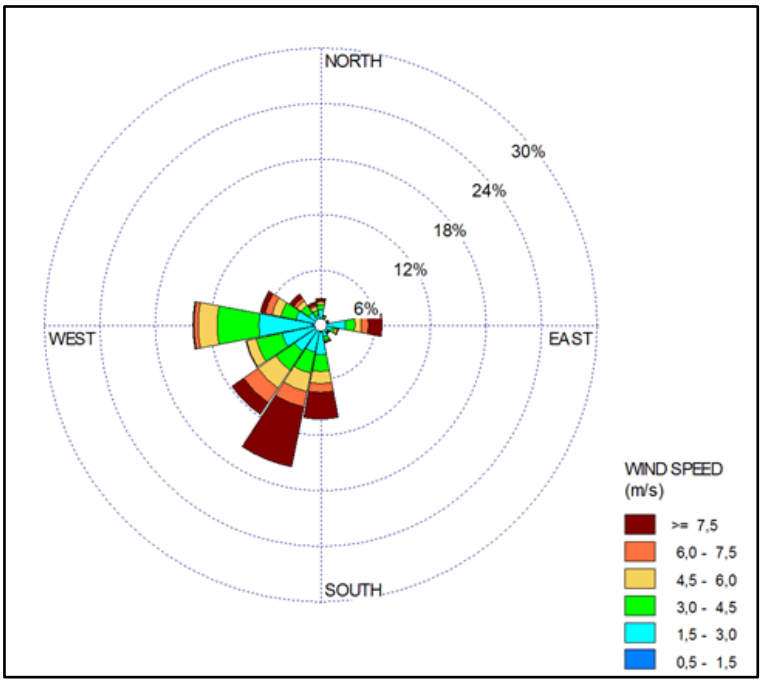

Figure 4.4: Wind rose for Alexander Bay using SAWS hourly wind speed and direction data from March 2009 to December 2014 (wind mast at a height of 10 meters).

Figure 4.4 shows a wind rose for a period of hourly wind speed and direction data where the wind mast was located at a height of 10 metres, which is the accepted height for climate observation. A south south-westerly wind dominates and occurs 22% of the time, a westerly wind is also very common at this height and occurred 19% of the time. The southerly wind (which dominates in Figure 4.3) occurs less than 12% of the time.

Wind speeds equal to, or faster than 7.5 m/s occur 16.2% of the time during the period where the wind mast was at a height of 33 metres and 14.1% of the time with the mast at a height of 10 metres. Calms (wind speeds below 0.5 m/s) occurred 7.64% of the time for the period where the wind mast was located at a height of 33 metres, and 8.37% of the time when the mast was at a height of 10 metres.

To conclude, wind speeds and especially wind direction observations have been impacted by the change of the height of the wind mast. This should be borne in mind when interpreting the wind speed and direction data observed at the Alexander Bay weather station during this 20-year period.

The following sections describe the stability conditions, mixing heights, temperature, and relative humidity over the study region. These variables were modelled for a period of one year and plotted as summer, winter and yearly averages for each point.

UNIVERSITEIT VAN PRETORIA
UNIVERSITY OF PRETORIA
YUNIBESITHI YA PRETORIA

4.1.2 Stability conditions

Data from point 39 (location of the proposed site) on the grid was used to plot the frequency distribution of Monin-Obukhov Lengths (Figure 4.5) within the ranges presented in Table 4.1.

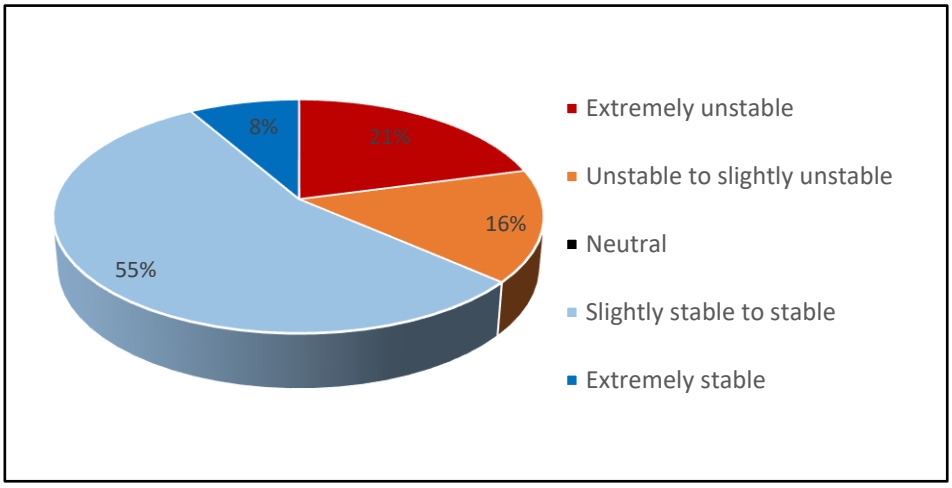

Figure 4.5: Distribution of the occurrence of Monin-Obukhov Lengths.

Figure 4.5 shows that more than half of the one year period at the proposed site can be classified as slightly stable to stable. Extremely unstable conditions were present 21% of the time, whereas unstable to slightly unstable conditions were present 15.5% of the time. Extremely stable conditions were present for about 8% of the time. A striking feature of the region is the fact that it is stably stratified (blue) for a significant period of time throughout the year.

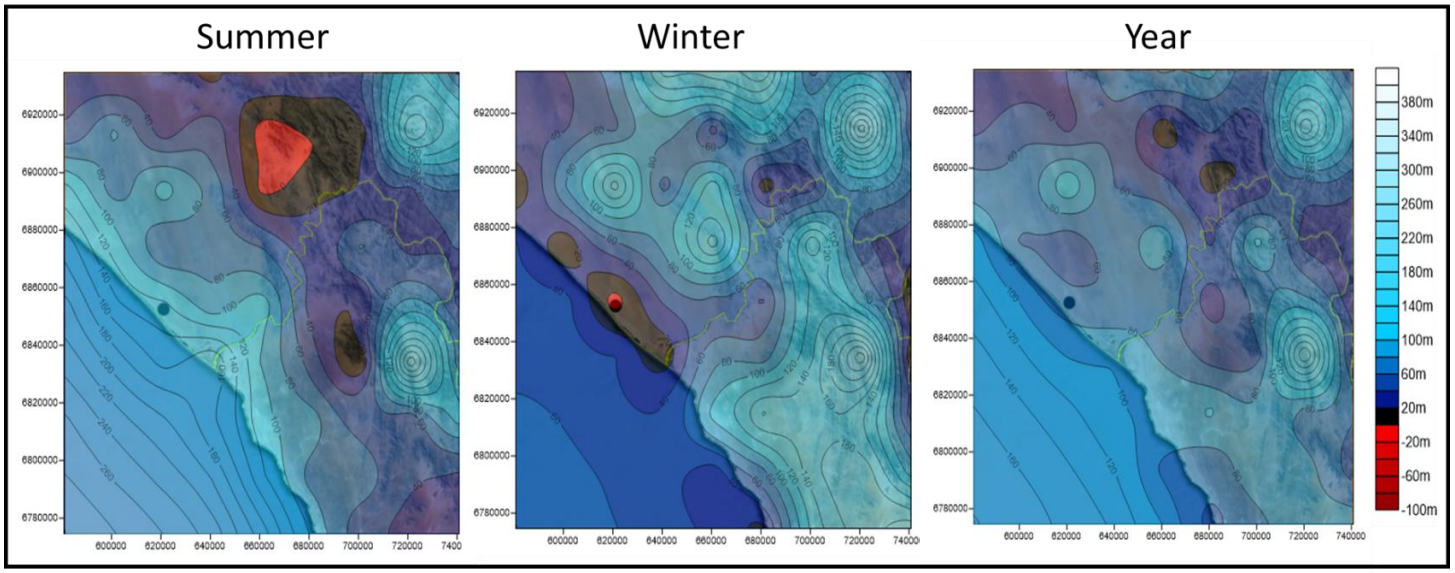

Figure 4.6: Monin-Obukhov Lengths for summer, winter and the entire year, over the study region.

In Figure 4.6, the bright red areas indicate regions of extreme instability, while the dark areas on the images indicate conditions of extreme stability. The Monin-Obukhov Lengths during the

UNIVERSITEIT VAN PRETORIA
UNIVERSITY OF PRETORIA
YUNIBESITHI YA PRETORIA

summer (January, February, March) vary from conditions of extreme instability to stable conditions. These values range between -10 metres and 279 metres throughout the grid. During winter (June, July, August), Monin-Obukhov Lengths vary from -8 metres to 257 metres, 99% of the region experiences stable conditions during winter.

The Monin-Obukhov Lengths for the period vary between a minimum of 6.5 metres and a maximum height value of 225 metres. The entire region experiences predominantly stable conditions for the 12-month period.

4.1.3 Mixing height

. As noted in Figure 4.7, the maximum mixing heights occur during summer over land. Mixing heights during summer vary between 143 metres and 610 metres, with an average of 306 metres during this period. Maximum mixing height is found over land during summer, while the minimum is located at the coastline. During winter, mixing heights varied between 120 metres and 374 metres, and the average mixing heights for all points was calculated as 248 metres. These mixing heights are larger over the ocean; the lower mixing height values are located over land. The most striking difference between the summer and winter plots is the location of the mixing heights maxima and minima. During winter, the mixing height maxima is located over the ocean, while in the summer months, the maxima is located over land.

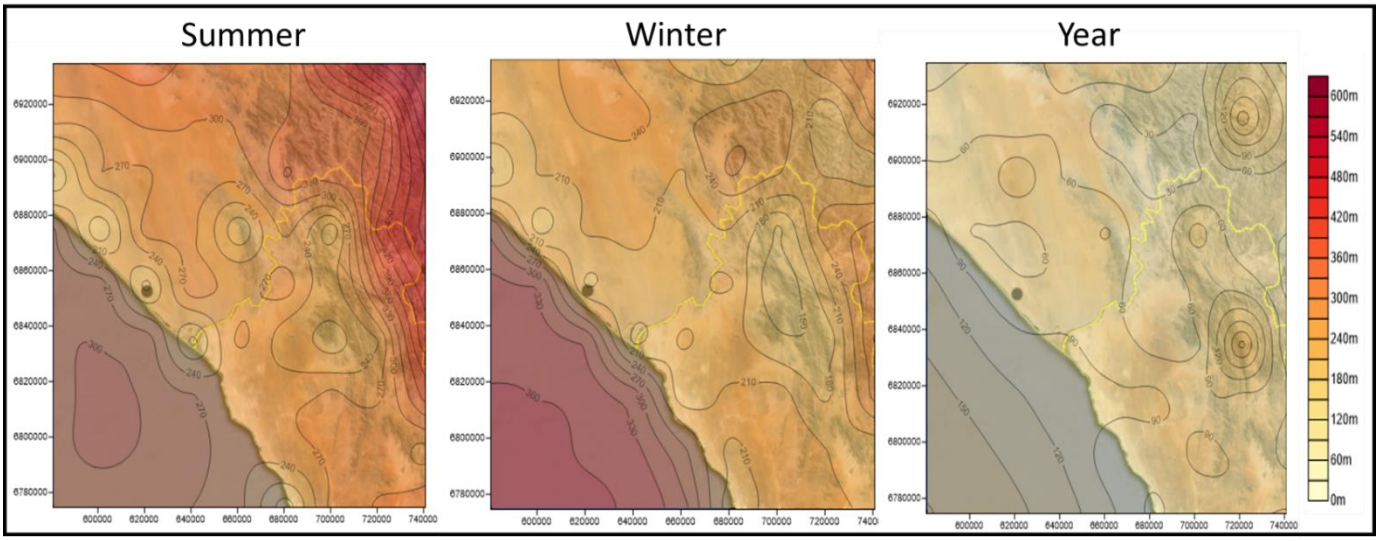

Figure 4.7: Mixing heights for summer, winter and the entire year, over the study region.

Annual mixing heights vary between a minimum of 6.5 metres and a maximum of 225 metres. Maximum average mixing heights occur over land and the ocean, while minimum average mixing heights for this period are predominately found over land. The average mixing height for all 81 points calculated for the year is 81 metres.

UNIVERSITEIT VAN PRETORIA
UNIVERSITY OF PRETORIA
YUNIBESITHI YA PRETORIA

4.1.4 Temperature

As shown in Figure 4.8, average monthly and daily temperatures at the coast do not vary a great deal, and it is rarely very hot or very cold. Temperatures start to rise from about 08:00 and reach a maximum between 13:00 and 15:00 in the afternoon; after 15:00, the temperatures start to drop and reach a minimum in the early morning hours. Maximum temperatures are experienced during January and February whereas minimum temperatures are experienced during July and August.

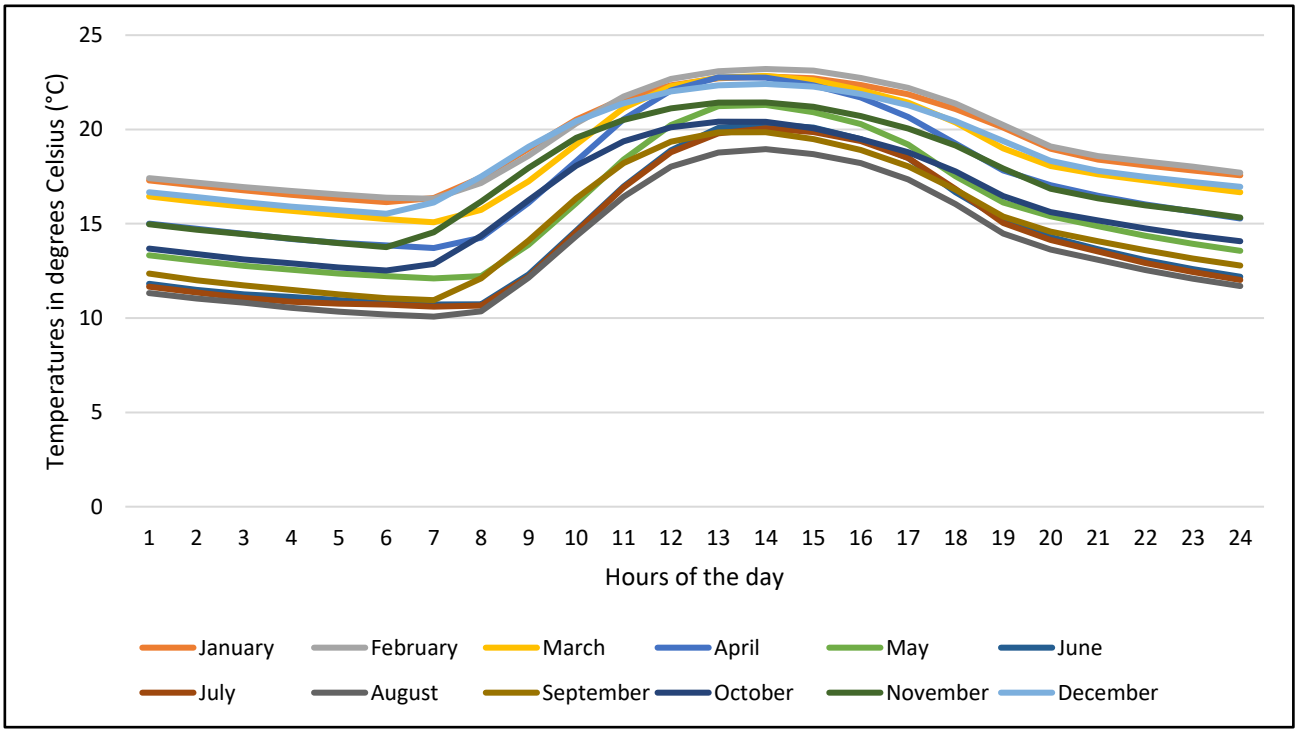

Figure 4.8: Daily temperature profile at Alexander Bay during the 20-year period.

As noted in Figure 4.9 below, summer, maximum temperatures are found over land. Temperatures in summer vary between 18°C and 26°C, with an average of 21°C for the 3-month period. During winter, temperatures between 9°C and 17°C were present and an average of these temperatures was calculated as 15°C. Temperatures in the winter are low throughout the grid and reach a minimum over land towards the north of the study region. The region of lower average temperatures for the summer and winter months coincides.

UNIVERSITEIT VAN PRETORIA
UNIVERSITY OF PRETORIA
YUNIBESITHI YA PRETORIA

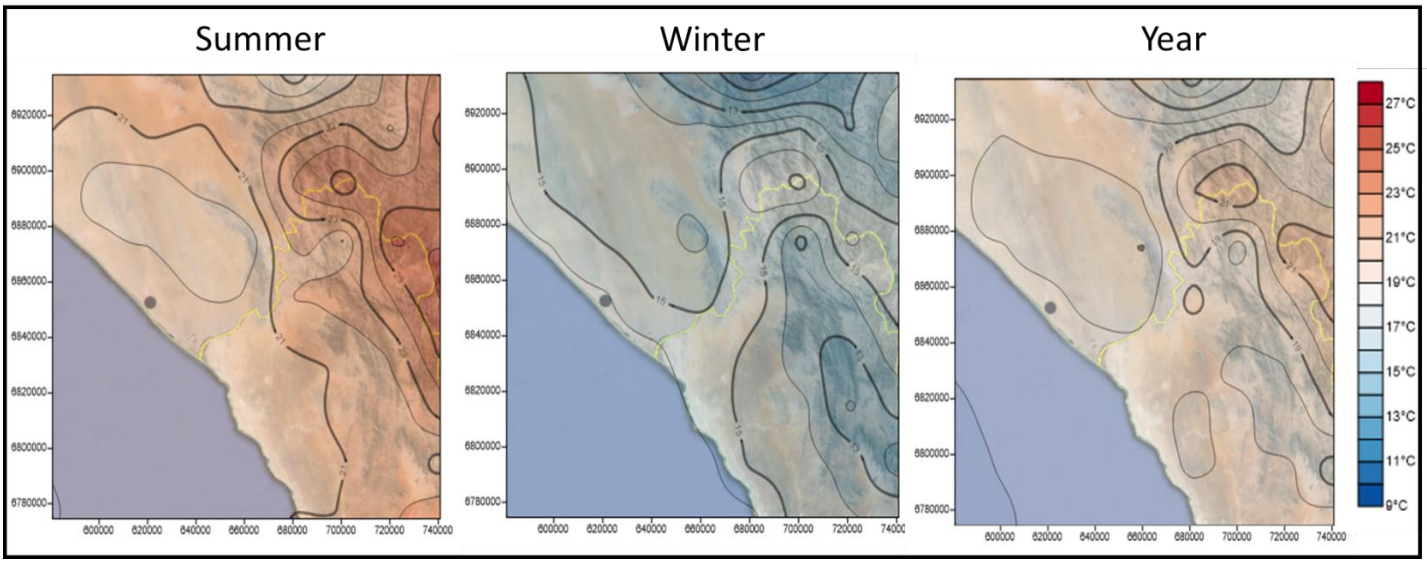

Figure 4.9: Temperatures for summer, winter and the entire year, over the study region.

Temperatures for the entire one-year period vary between a minimum temperature of 15°C and a maximum of 22°C. Maximum temperatures occur over land while minimum temperatures are also located over land, predominately in the northerly region of the grid. An average temperature over the entire grid for the whole year is 18°C.

Modelled meteorological data for the proposed site (from TAPM) was used to plot the frequency distribution of temperatures (Figure 4.10). This graph contains hourly data for the year 2014.

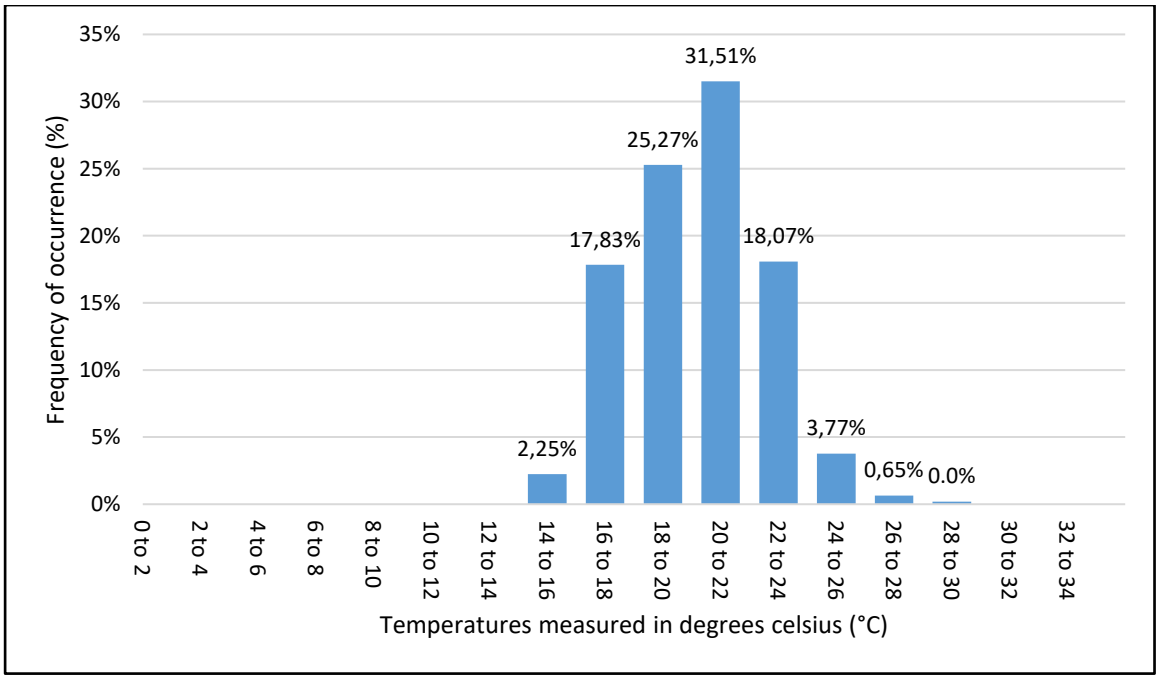

Figure 4.10: Temperature distribution for 2014 at the proposed site based on modelled meteorological data.

UNIVERSITEIT VAN PRETORIA
UNIVERSITY OF PRETORIA
YUNIBESITHI YA PRETORIA

According to the temperature distribution (Figure 4.10), most of the hours in the year (31%) had temperatures between 20°C and 22°C, and 25% of hours had temperatures ranging from 18°C to 20°C. Temperatures ranging from 16°C to 18°C and from 22°C to 24°C were the third most common during this period.

4.1.5 Relative humidity

Figure 4.11 shows that relative humidity is high over the ocean and close to the coast and drops significantly as one moves inland; this pattern is true for both the summer and winter months and for the period. During summer, relative humidity varies between 48% and 91%, with an average of 77% for the 3-month period. During winter, the relative humidity varies between 51% and 81%, and the average value for relative humidity values over all points was calculated as 72%. During winter, a larger region has lower relative humidity values. During summer, higher relative humidity values are present over most of the points.

Annual relative humidity varies between a minimum of 48% and a maximum of 86%. An average relative humidity value over the entire grid for the whole year is 73%.

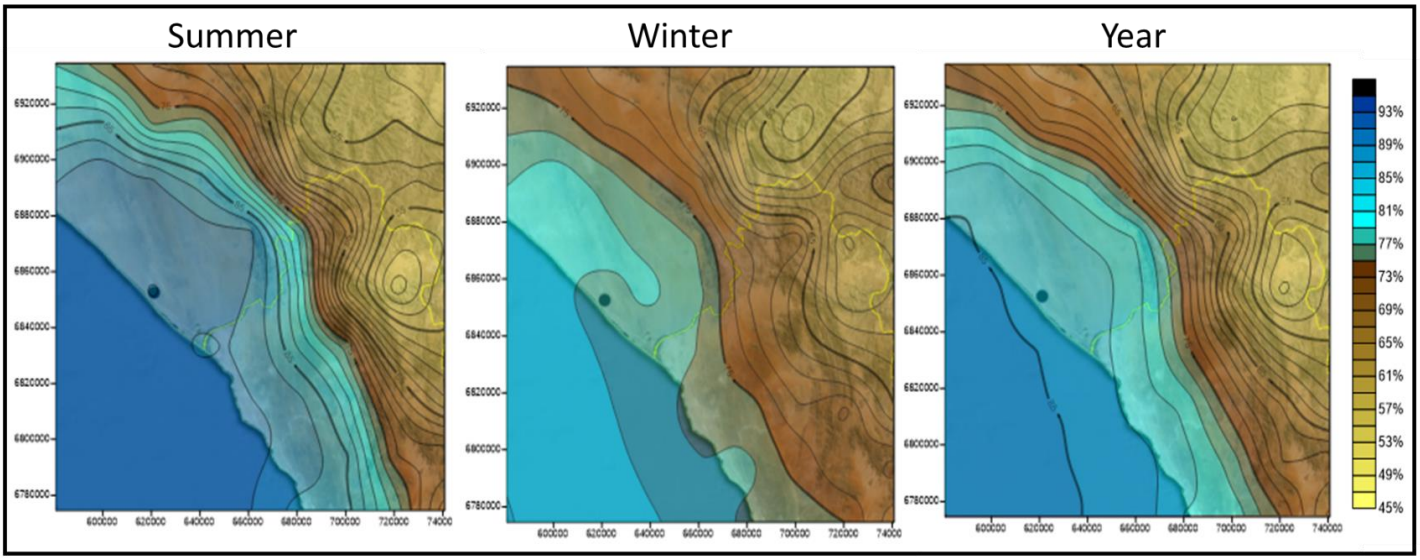

Figure 4.11: Relative humidity for summer, winter and the entire year, over the study region.

Hourly data from the Alexander Bay weather station was used to plot the frequency distribution of relative humidity in certain ranges for different times of the day for a 20-year period. Figures 4.12 show the frequency distribution of relative humidity at 00:00, 06:00, 12:00 and 18:00.

UNIVERSITEIT VAN PRETORIA
UNIVERSITY OF PRETORIA
YUNIBESITHI YA PRETORIA

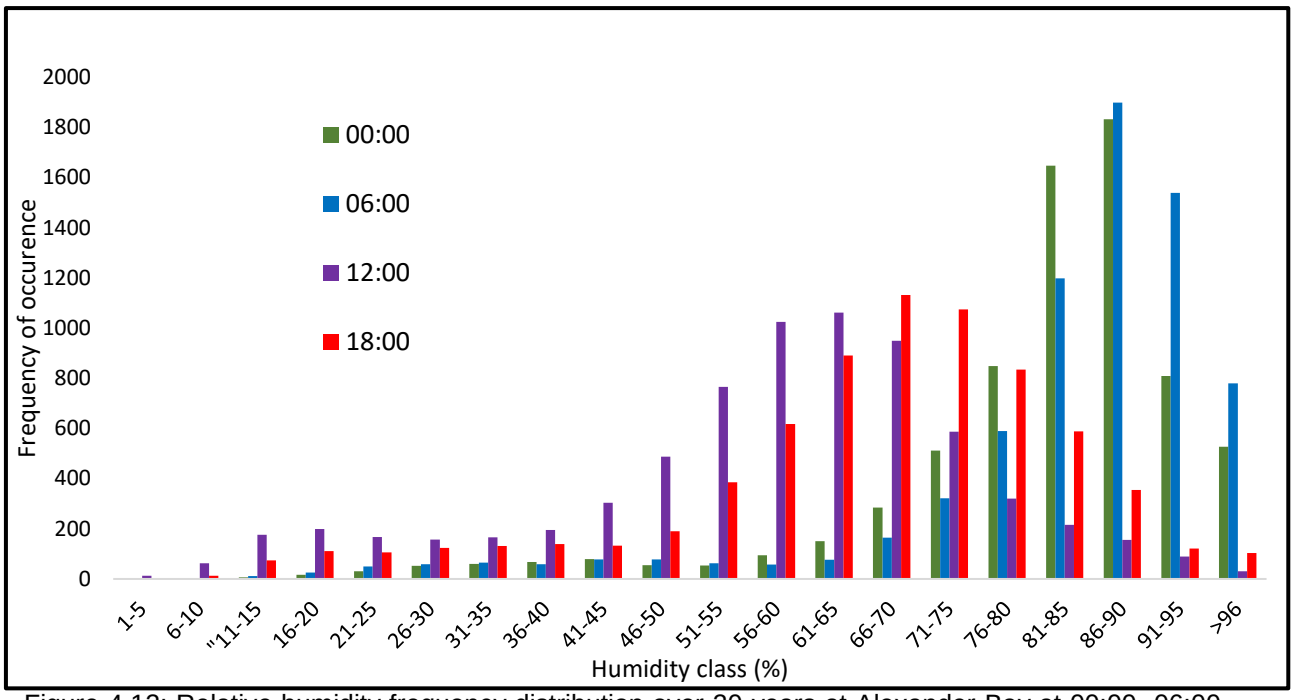

Figure 4.12: Relative humidity frequency distribution over 20 years at Alexander Bay at 00:00, 06:00, 12:00 and 18:00.

At 00:00, most hours in the 20-year period had relative humidity values of between 86% and 90%, similarly at 06:00 the majority of hours had relative humidity values in the same range. At 12:00, most of the cases in the 20-year period had relative humidity values of between 56% and 65% while 18:00 showed most hours had relative humidity values ranging between 66% and 75% at 18:00.

The above figure show that relative humidity values are higher during 00:00 and 06:00. At midday (12:00), as the temperature of the air rises, relative humidity values drop. As the sun sets and the air cools down during the night, relative humidity values increase and reach humidity values as noted.

UNIVERSITEIT VAN PRETORIA
UNIVERSITY OF PRETORIA
YUNIBESITHI YA PRETORIA

4.2 Air Dispersion Potential

Air Dispersion Potential (ADP) was calculated and plotted on the 81-point grid located over the study region. A combination of modelled wind speed, mixing height, and Monin-Obukhov Length data is used to describe the ADP for the region for different periods.

In this section, average ADP values for the year, summer, summer day/night, winter, winter day/night were calculated and plotted in Figures 4.13, 4.14, 4,15, 4.17 and 4.18, respectively. Figure 4.16 exhibits the components used to calculate ADP for summer during the day and night. Figures containing ADP components for the year, summer, winter, winter day/night can be found in Appendix A.

Annual average ADP for the study region is presented in Figure 4.13. Annual averages of ADP vary between 36 and 51 throughout the grid. Larger ADP values are found inland, while ADP values are smaller close to the coast. Over the ocean, average ADP values of between 40 and 44 are present.

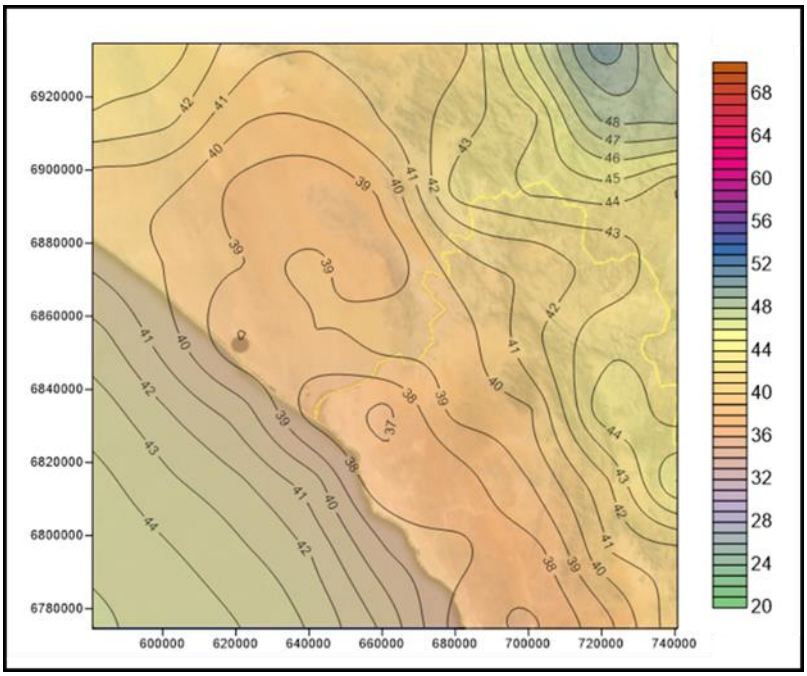

Figure 4.13: Annual average ADP for the study region.

Average ADP values during summer (Figure 4.14) vary from 34 to 54. The potential for air dispersion is better over land than over the ocean. ADP values drop approaching the coast. The unfavourable conditions near the coast can be attributed to lower mixing heights, lower wind speeds, and stable conditions.

UNIVERSITEIT VAN PRETORIA
UNIVERSITY OF PRETORIA
YUNIBESITHI YA PRETORIA

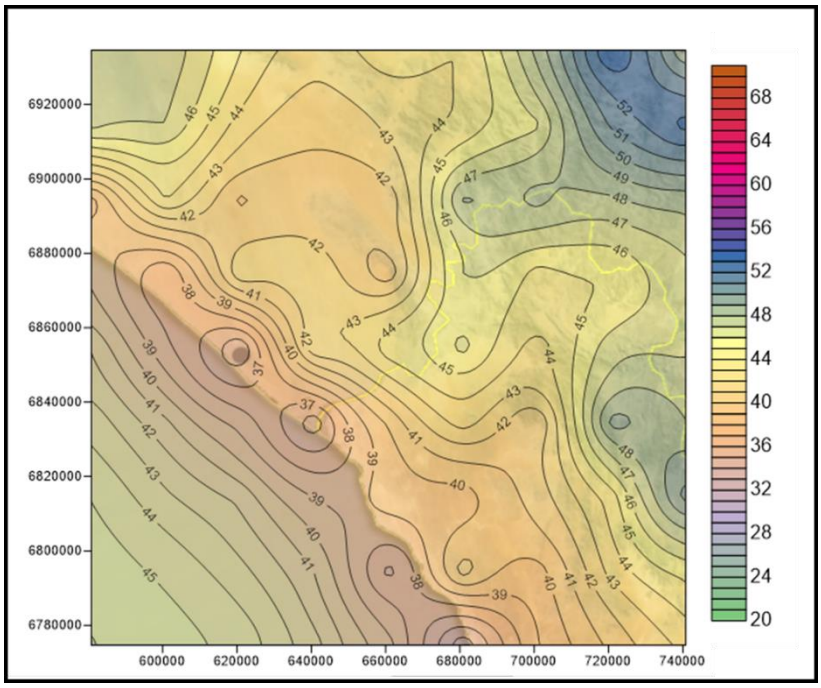

Figure 4.14: Average summer ADP for the study region.

When comparing the ADP values for summer during the day and the night (Figure 4.15), it is clear that conditions for air dispersion are much more favourable during the day because of larger mixing heights and greater instability during daytime. At night, as the earth cools, mixing heights become smaller and stable conditions prevail.

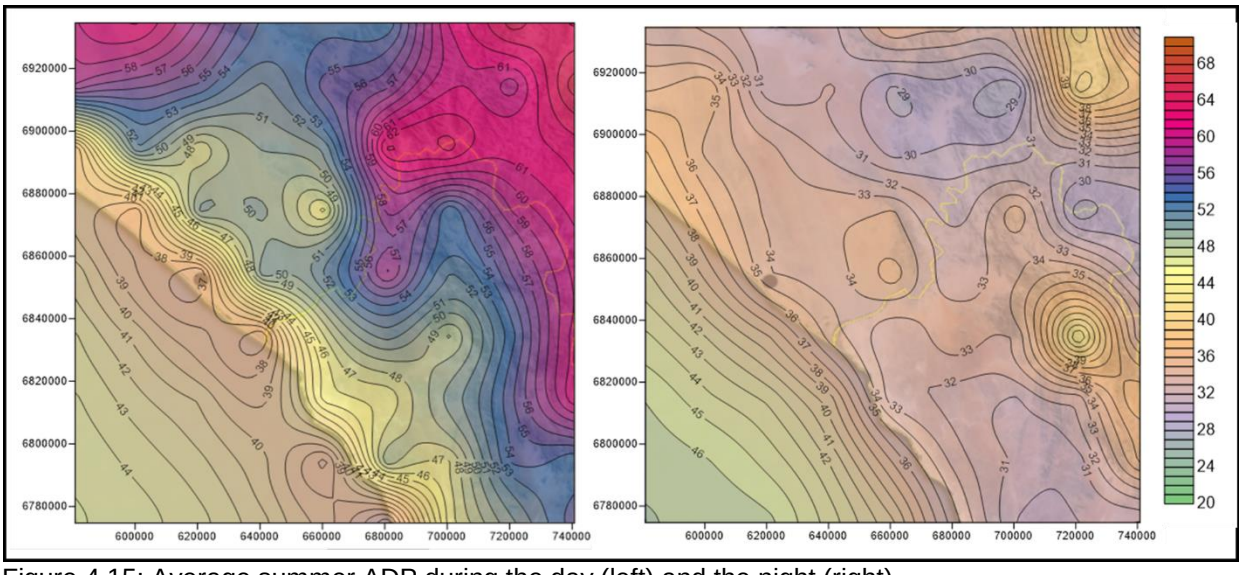

Figure 4.15: Average summer ADP during the day (left) and the night (right).

Both summer day and night ADP values show a similar pattern: the conditions are favourable over land, deteriorate towards the coast, and pick up again over the ocean. The preferred site

UNIVERSITEIT VAN PRETORIA
UNIVERSITY OF PRETORIA
YUNIBESITHI YA PRETORIA

is located very near the coast and, consequently, in an area of lower ADP during summer days and nights.

It is useful to analyse the contribution of the ADP parameters to the average ADP. Figure 4.16 presents the components of ADP (wind speed, mixing height, and Monin-Obukhov Length) for summer during the day and the night.

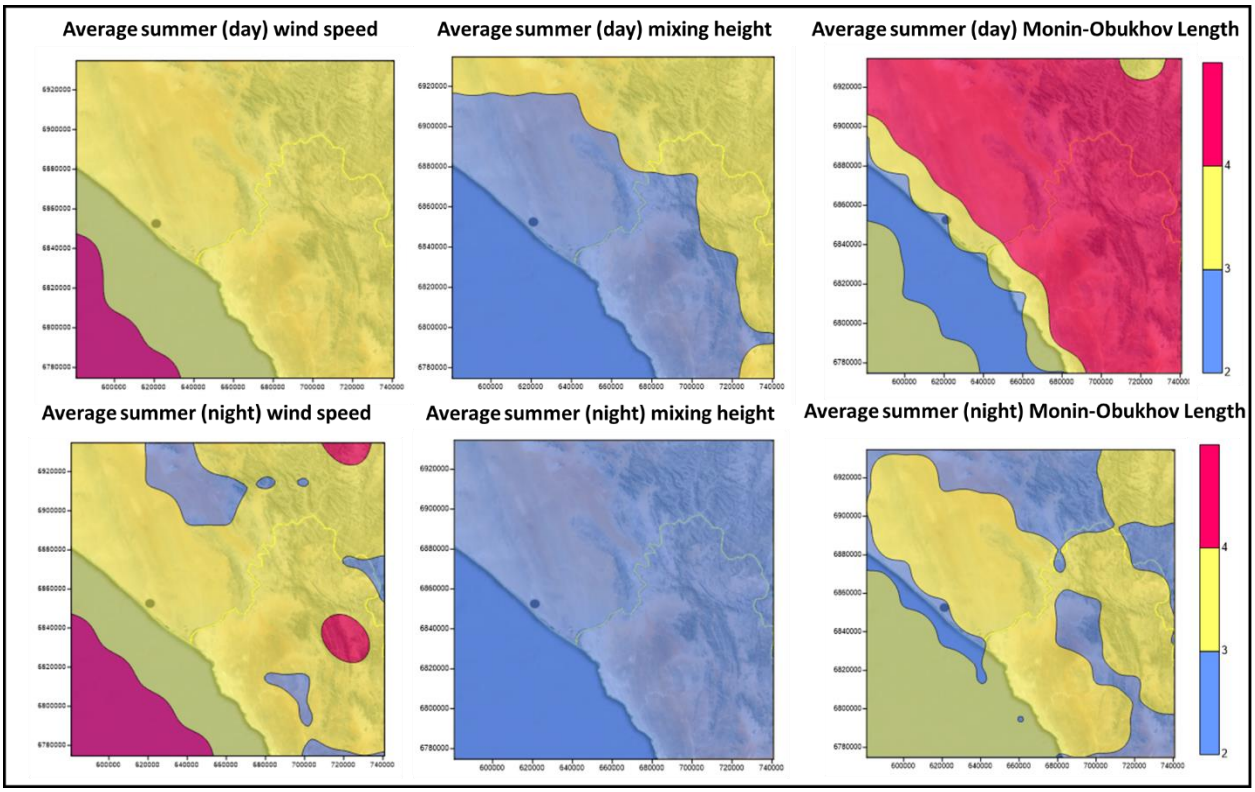

Figure 4.16: The components of ADP (wind speed, mixing height and Monin-Obukhov Length) for summer day and night.

Relatively favourable ADP values during the day in the summer are driven by favourable Monin-Obukhov Lengths over land, favourable wind speed over the ocean, and moderately favourable wind speeds over land. The moderately favourable mixing height conditions over land also contribute to the high ADP values in Figure 4.15.

Relatively unfavourable ADP values during the night in the summer can be attributed to the unfavourable contribution of mixing height throughout the entire region. Wind speed and Monin-Obukhov Length contributes moderately to ADP throughout most of the region, with a small area of favourable contribution from Monin-Obukhov Lengths over the ocean.

ADP values during winter (Figure 4.17) vary from 33 to 49. The potential for air dispersion is more favourable over the ocean than over the land, and becomes less favourable

UNIVERSITEIT VAN PRETORIA
UNIVERSITY OF PRETORIA
YUNIBESITHI YA PRETORIA

when moving towards the coastline. Warmer ocean temperatures will cause larger mixing heights and conditions of instability.

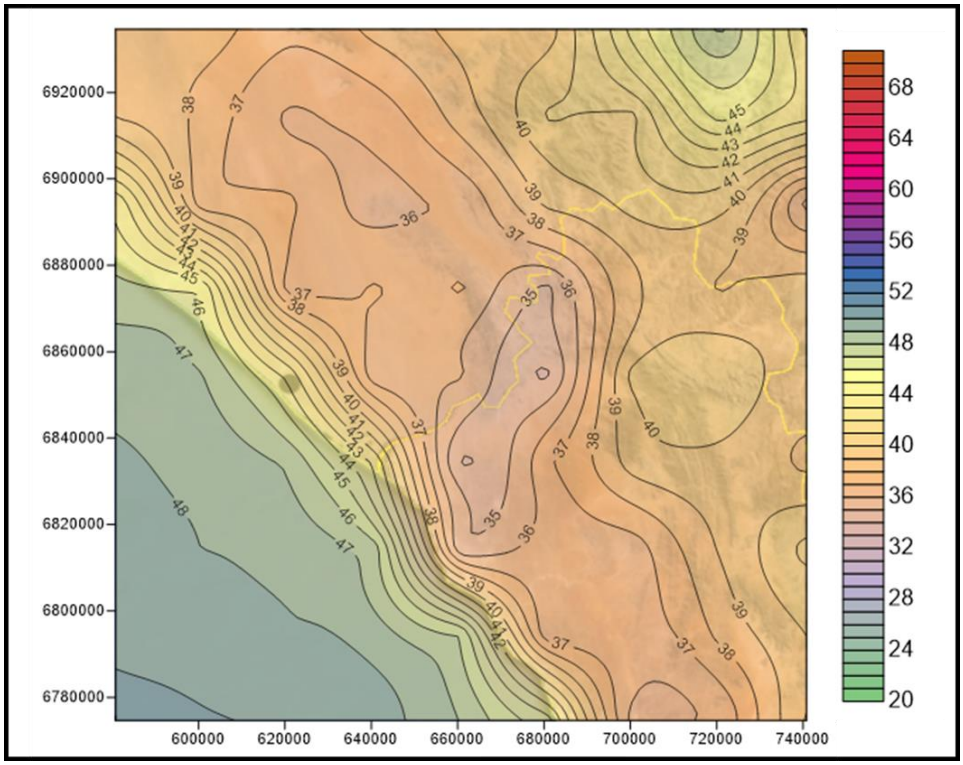

Figure 4.17: Average winter ADP for the study region.

Comparing the ADP values for winter during the day and the night (Figure 4.18), it is clear that conditions for air dispersion are more favourable during the day. Average daytime ADP during the winter even reaches values of up to 57 over land due to larger mixing heights and greater instability during daytime.

At night during the winter, very unfavourable conditions for air dispersion are present across most of the land, due to smaller mixing heights and stable conditions. During the winter day, ADP conditions, which are moderate over land, deteriorate towards the coast, but pick up again over the ocean. When studying the ADP conditions during the winter night, the situation differs. Most of the land experiences very unfavourable conditions, while further into the ocean, some favourable conditions occur. The preferred site is located very near the coast; this means that it will be in an area of average to unfavourable ADP during winter days and nights.

UNIVERSITEIT VAN PRETORIA
UNIVERSITY OF PRETORIA
YUNIBESITHI YA PRETORIA

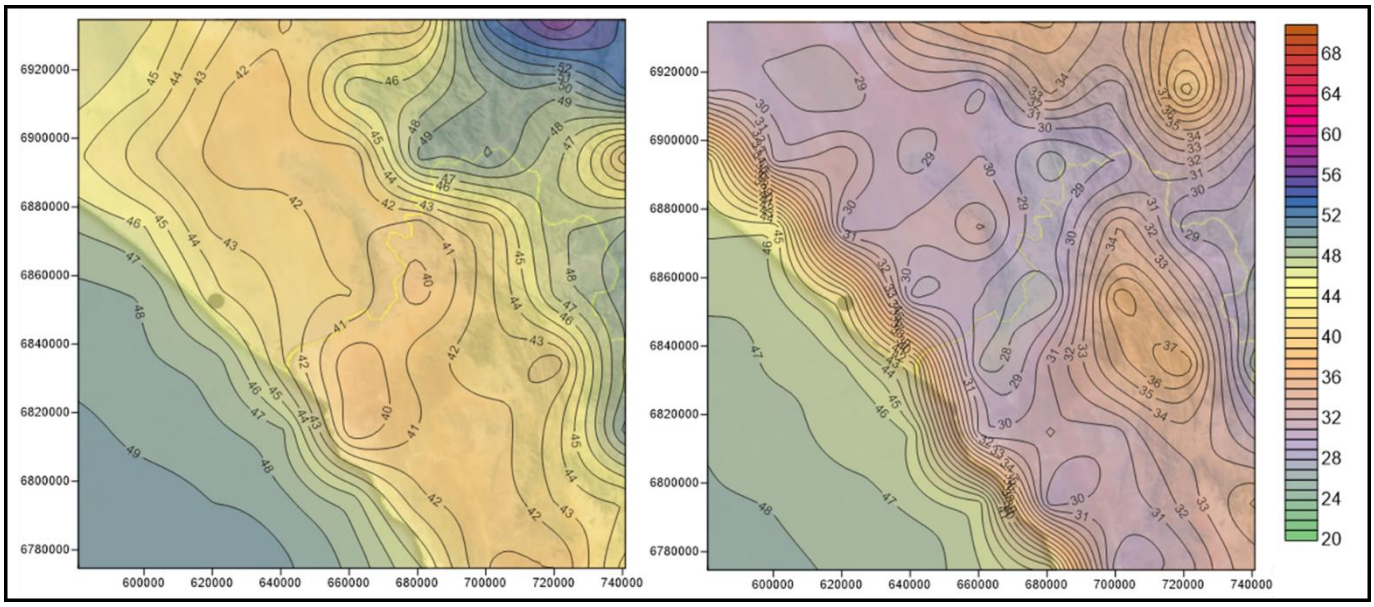

Figure 4.18: Average winter ADP during the day (left) and the night (right).

Figure A.4 in Appendix A displays the components of ADP (wind speed, mixing height, and Monin-Obukhov Length) for winter during the day and the night. Relatively favourable ADP values for winter day (Figure 4.18) over land are caused by the moderately favourable contribution of wind speed. In both instances, the unfavourable ADP values over land can be attributed to unfavourable conditions caused by Monin-Obukhov Length and mixing height.

Annual average ADP is moderate, with values only reaching 51. The highest ADP values are found in summer during the day and the lowest values in winter during the night. Overall, the biggest contributor to favourable dispersion of air pollution in the region is stability quantified by Monin-Obukhov Length. Wind speed mostly contributes moderately to ADP, while mixing height is predominantly unfavourable.

UNIVERSITEIT VAN PRETORIA
UNIVERSITY OF PRETORIA
YUNIBESITHI YA PRETORIA

4.3 Sea breeze, coastal fog and the Thermal Internal Boundary Layer

4.3.1 Sea breeze occurrence

The following tables show the occurrence of wind blowing from the land (Table 4.2) and from the ocean (Table 4.3), using SAWS wind direction data for the Alexander Bay weather station.

Table 4.1: Frequency of occurrence of wind from the land for the 20-year period at Alexander Bay.

Direction blowing from land	Direction in degrees	Frequency of occurrence in a 20-year period	Percentage of occurrence in a 20- year period
Between N and E	360° to 90°	30857	17.6%
Between NNE and ENE	20° to 70°	6122	3.5%
NE	40° to 50°	1343	0.8%

Table 4.2: Frequency of occurrence of wind from the ocean for the 20-year period at Alexander Bay.

Direction blowing from sea	Direction in degrees	Frequency of occurrence of wind in a 20-year period	Percentage of occurrence in a 20-year period
Between S and W	180° to 270°	92802	52.9%
Between SSW and WSW	200° to 250°	55229	31.5%
SW	220° to 230°	17404	9.9%

Wind from the ocean (south-westerly quadrant) was present for 52.9% of the time in a 20-year period, while wind from the land (north-easterly quadrant) only occurred for 17.6% of the time. It can be concluded that at Alexander Bay, sea breezes occur much more frequently than land breezes.

The occurrence of sea breezes at the site is calculated using modelled meteorological data. Hourly data from all points over the period of a year was used. A sea breeze occurs when the difference between land and sea temperatures is 3°C or more, mostly during the day (08:00 to 16:00) and when the wind is blowing from the ocean (180° to 270°).

UNIVERSITEIT VAN PRETORIA
UNIVERSITY OF PRETORIA
YUNIBESITHI YA PRETORIA

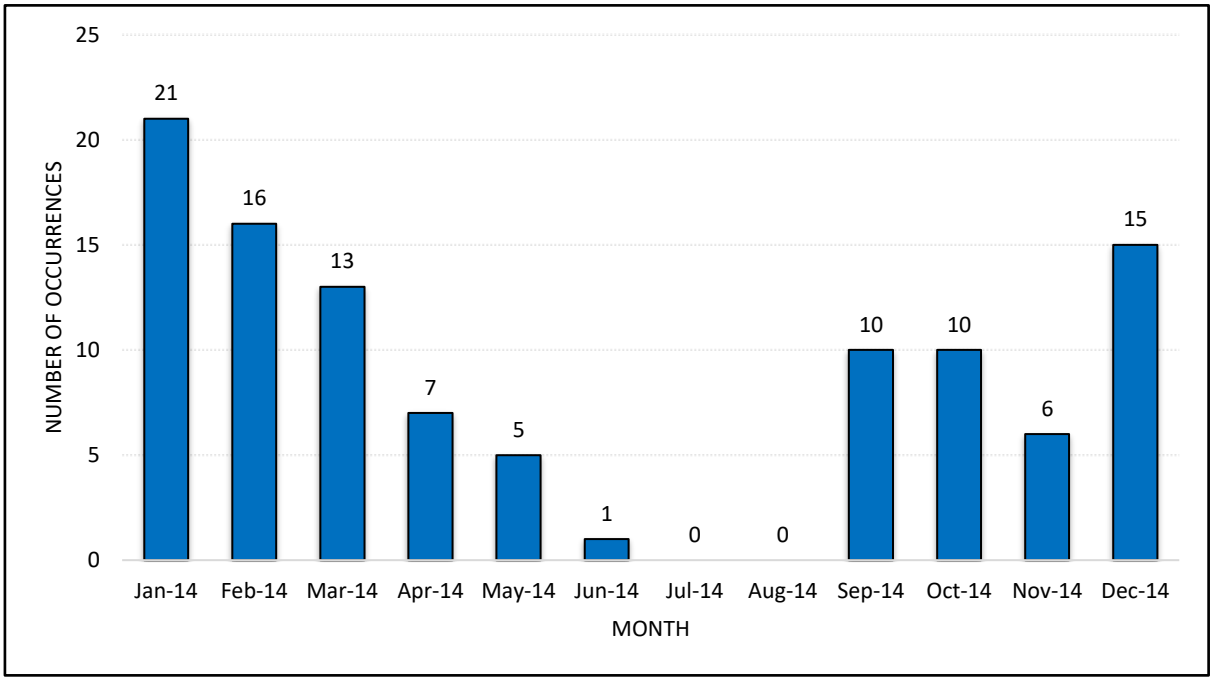

Figure 4.19: Monthly distribution of sea breeze occurrences for the study site.

Figure 4.19 shows that sea breeze occurrence in the summer dominates. Conditions for the occurrence of sea breezes are very favourable in the summer months, occurring a total of 52 times. Occurrence in the winter months, however, is much less, with a total of only 1 out of the annual total of 104 occurrences.

4.3.2 Coastal fog occurrence

Figure 4.20 characterizes the distribution of fog at the proposed site throughout 2014. January, March and November all experienced a high number of 18 foggy days (according to the classification used), while the lowest number of foggy days occurred during June and July.

UNIVERSITEIT VAN PRETORIA
UNIVERSITY OF PRETORIA
YUNIBESITHI YA PRETORIA

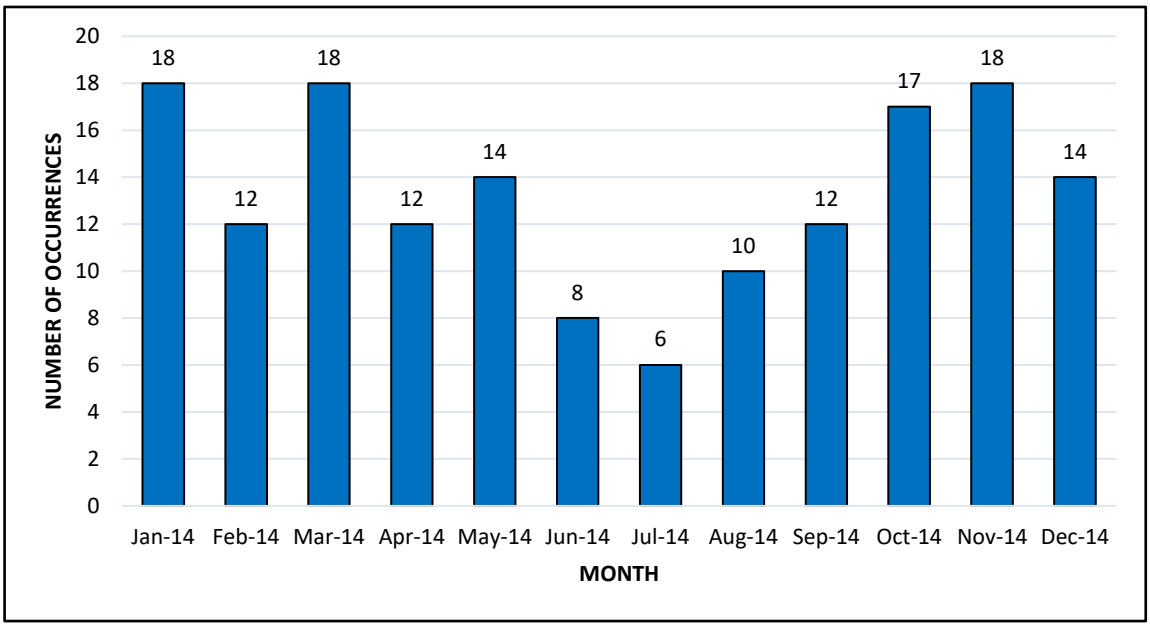

Figure 4.20: Monthly distribution of fog days for the study site.

Figure 4.21 illustrates the reason for the low occurrence of foggy days in July. Humidity values vary significantly throughout the month, with high humidity values (over 80%) only occurring a few times during this period. The difference between temperatures and dew point temperatures is greater than in summer months; this means that the air is drier. These factors contribute to the unfavourable conditions for fog formation.

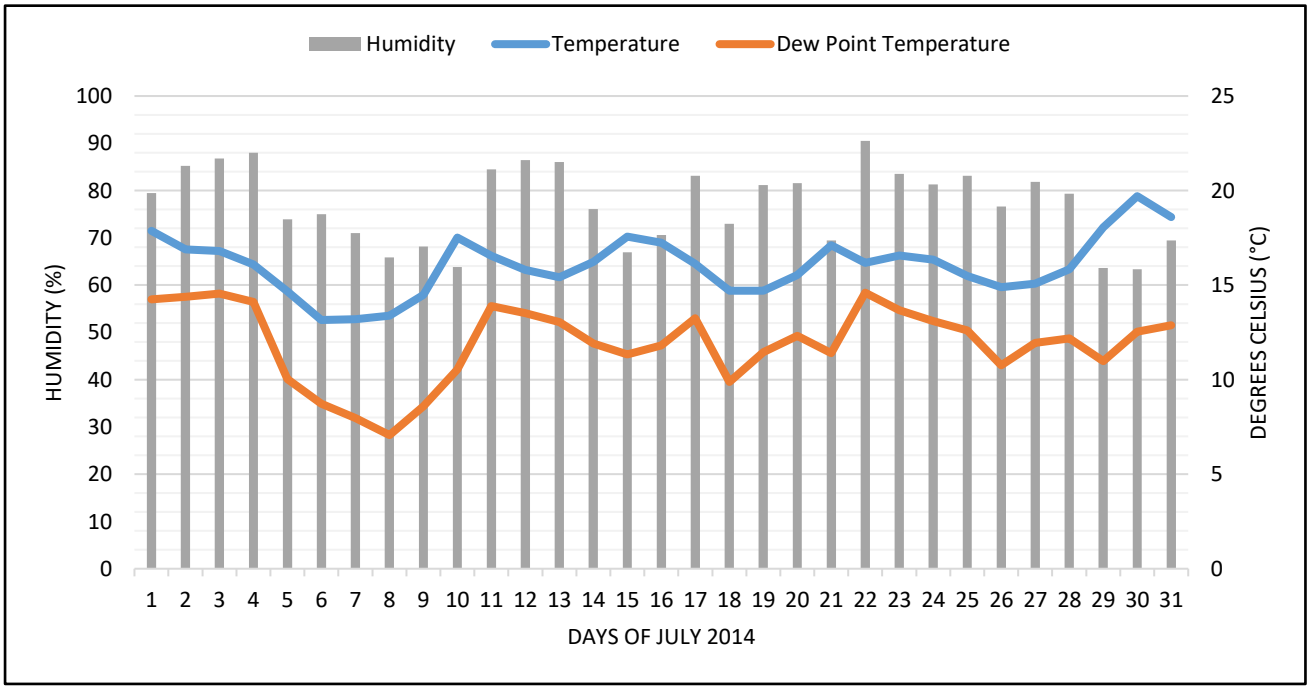

Figure 4.21: Average daily humidity, temperature and dew point temperature distribution throughout July 2014 at the proposed site.

UNIVERSITEIT VAN PRETORIA
UNIVERSITY OF PRETORIA
YUNIBESITHI YA PRETORIA

Figure 4.22 illustrates the reasons for the relatively high occurrence of foggy days in January. Humidity values are high (over 80%) throughout the entire month and do not vary as much as in winter. The high humidity values, together with the small differences between air and dew point temperatures, combine to produce favourable conditions for fog formation.

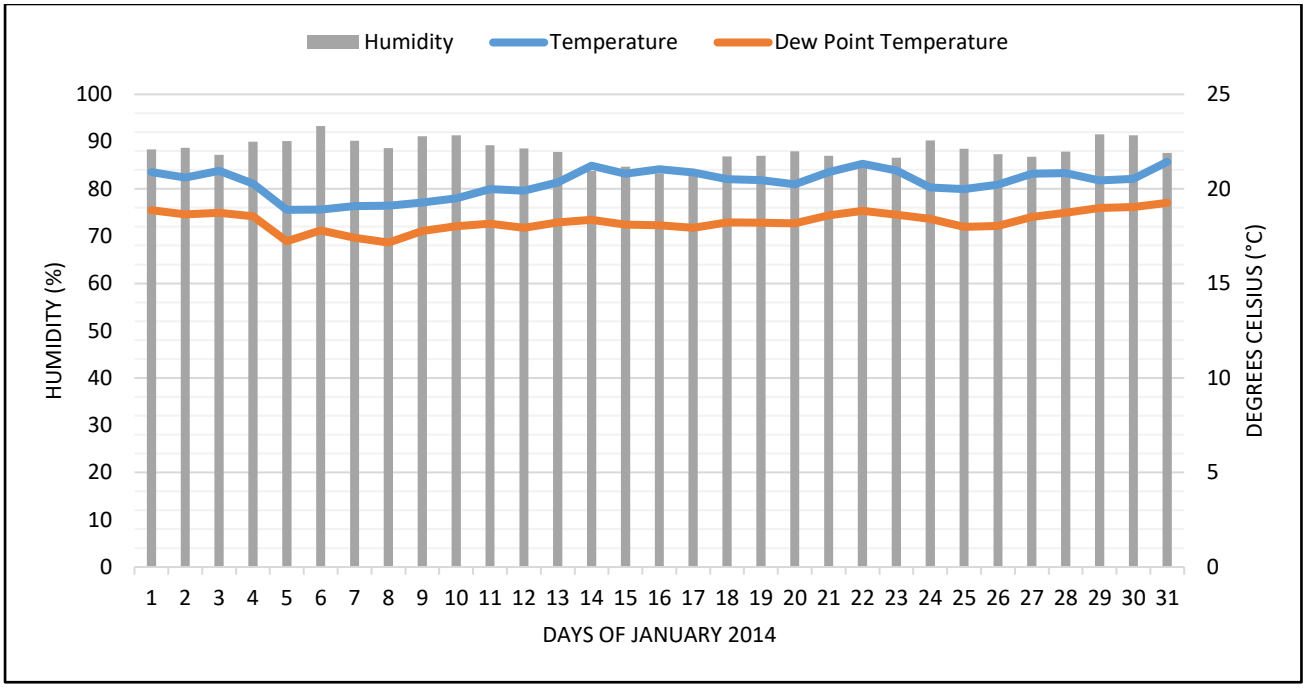

Figure 4.22: Average daily humidity, temperature and dew point temperature distribution throughout January 2014 at the proposed site.

Figure 4.23 identifies the hours during the day when fog occurs the most. According to the data, 265 hours are classified as foggy between 03:00 and 06:00 in the morning at the proposed site, while no hours were classified as foggy from 12:00 to 15:00 in the afternoon. It can be concluded that fog will be most common between 21:00 and 09:00.

UNIVERSITEIT VAN PRETORIA
UNIVERSITY OF PRETORIA
YUNIBESITHI YA PRETORIA

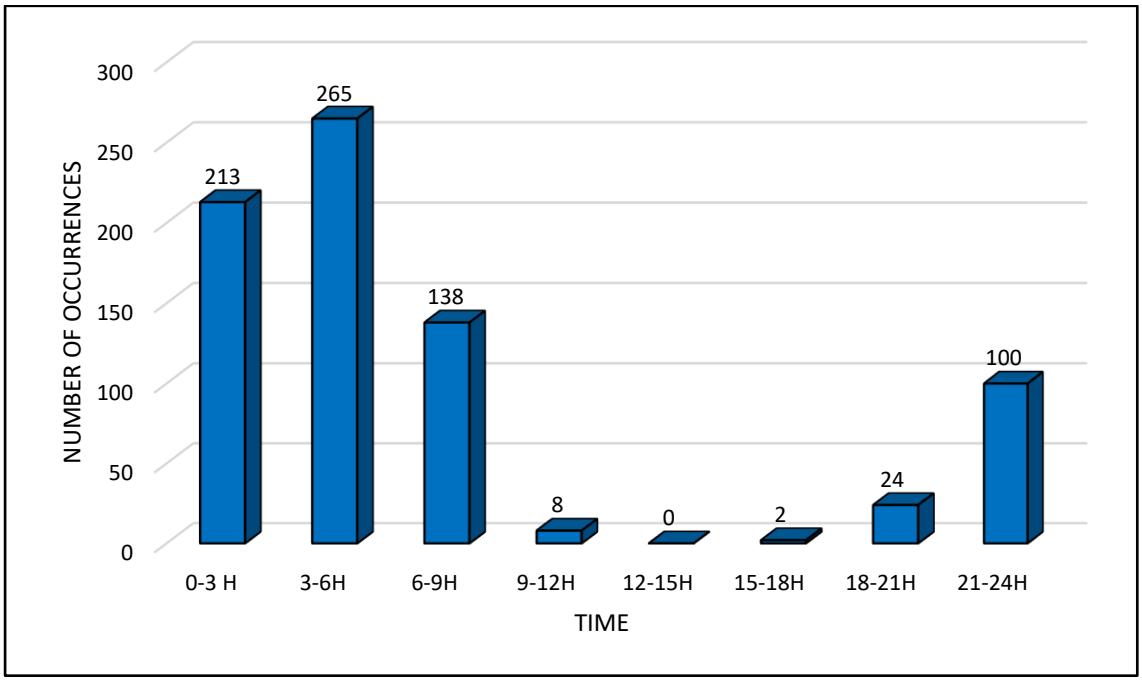

Figure 4.23: Hourly distribution of fog occurrence throughout a 24-hour period.

According to the meteorological data and the classification used to identify fog days, the amount of fog days in 2014 was 159. This number is high compared to the fog data for Alexander Bay from 1954 to 1986 when fog occurred between a minimum of 49 days and a maximum of 145 days annually for the period (Olivier, 2002).

As noted in Figure 4.23, conditions for fog occurrence are very favourable between 03:00 and 06:00 in the study region (located only a few kilometres from Alexander Bay). It must be borne in mind that fog observations were only made by SAWS at one specific time in the day, usually at 08:00, and is then classified as being foggy or not. If fog occurred at any other time during the day, it will not appear in this data and the day was not classified as being 'foggy'.

4.3.3 The Internal Boundary Layer

The formula for the IBL height (Equation 3.6) requires the calculation of the equilibrium height using Equation 3.8. The methodology is applied for summer (15 January 2016) and winter (15 July 2016). The time-space variation of the IBL height is calculated for early morning (09:00), midday (13:00), and late afternoon (17:00).

Figure 4.24 illustrates the observed and approximated kinematic heat flux for summer and winter. An approximation of modelled and observed heat flux values was calculated, using a polynomial of second degree $h(x) = ax^2 + bx + c$. As noted in Figure 4.27, the polynomial

UNIVERSITEIT VAN PRETORIA
UNIVERSITY OF PRETORIA
YUNIBESITHI YA PRETORIA

approximated kinematic heat flux values are close to the observed values, with correlation coefficients of 0.994 for the summer and 0.986 for the winter. This allows for the use of an analytical approach, instead of numerically solving the integral under the observed data.

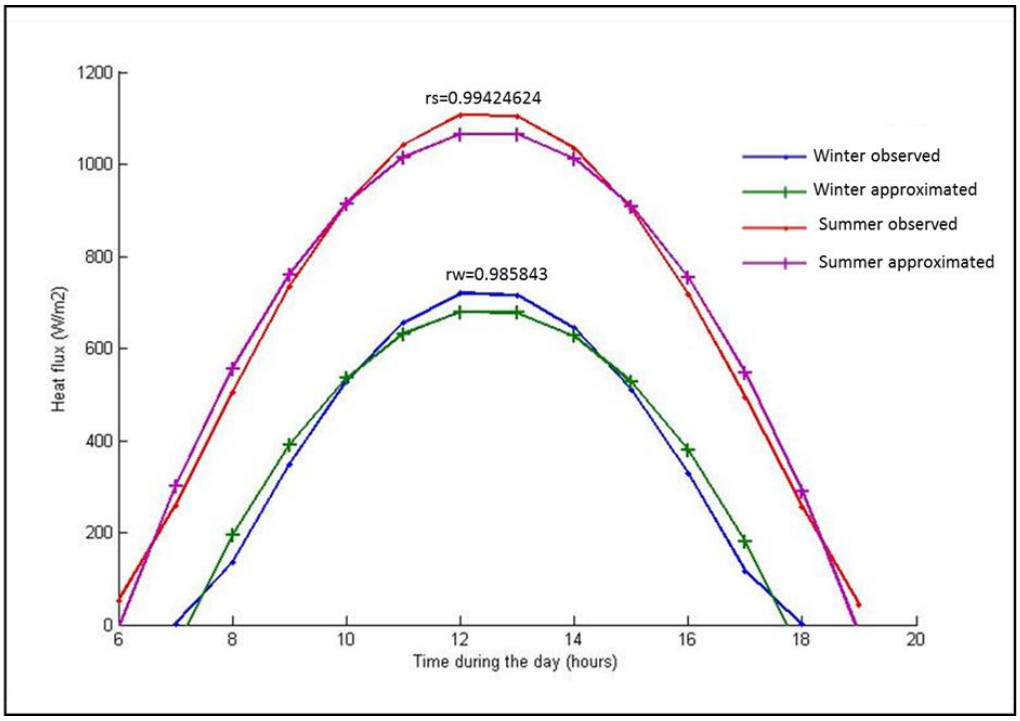

Figure 4.24: Observed and approximated heat flux values for both a winter and a summer case.

Table 4.4 presents the corresponding values for the polynomial coefficients for winter and summer.

Table 4.3: Polynomial coefficients for winter and summer.

	a	b	c
Winter	-24.573	612.756	-3135.343
Summer	-25.655	640.430	-2925.289

Instead of numerically solving the integral under the observed data, the coefficients from Table 4.4 are used to calculate analytically the equilibrium TIBL height, using the solution of the form:

$$\int_{x_{initial}}^{x_{final}} x^n \, dt = \frac{1}{n+1} x^{n+1} \qquad (4.1)$$

UNIVERSITEIT VAN PRETORIA
UNIVERSITY OF PRETORIA
YUNIBESITHI YA PRETORIA

Figure 4.25 illustrates TIBL height as a function of the distance from the shoreline (x) and the time during daytime (t). The approximation formula (Equation 3.6) was used to produce the TIBL height results, as shown in Figure 4.28.

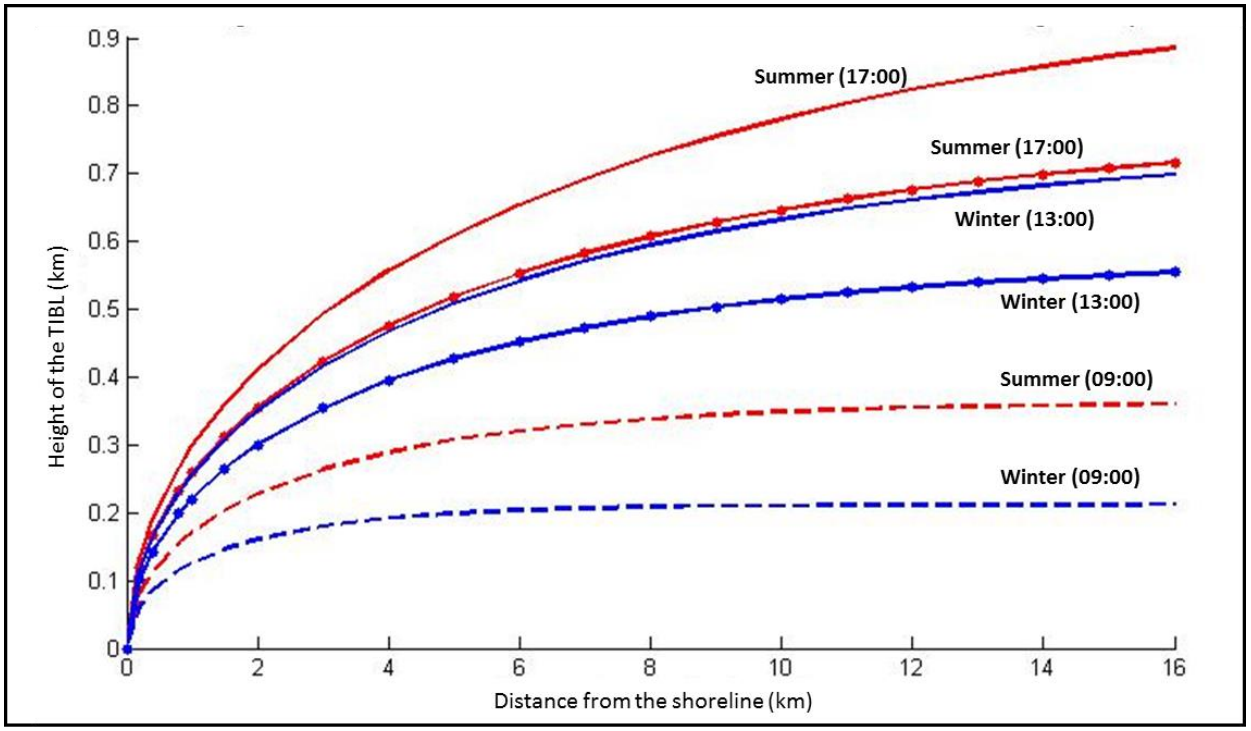

Figure 4.25: TIBL height as a function of the distance from the shoreline and the time during the day.

TIBL heights are dependent on kinematic heat fluxes. The TIBL will develop faster, grow higher and take longer to reach equilibrium height in the summer than a TIBL in the winter. In addition, a TIBL in the morning (09:00) has a lower equilibrium height and will, therefore, reach it faster. A TIBL that forms later in the day (17:00) has a higher equilibrium height and will take a greater distance from the shoreline to reach this height.

The methodology for the calculation of the IBL height was realized on MATLAB platform (Appendix B) and can be used for forecasting the time-space variation of the TIBL height. By means of output from a contemporary weather forecast model such as TAPM (used in this dissertation) or any other appropriate model, information regarding the height of the TIBL can assist in reducing cases of fumigation of pollutants.

UNIVERSITEIT VAN PRETORIA
UNIVERSITY OF PRETORIA
YUNIBESITHI YA PRETORIA

CHAPTER 5: CONCLUSION

5.1 Air-pollution climatology

An analysis of the air-pollution climate of the region includes wind climate, stability conditions, mixing heights, temperature, and relative humidity. These parameters all have an influence on pollution distribution from the CCGT power station in the region.

A knowledge of the annual, summer and winter distributions of the above-mentioned parameters can be helpful in the decision-making processes in the planning, designing, construction, and operation of the CCGT power station. For example, the maximum and minimum temperatures can be useful when deciding on building materials and equipment designed to operate in the conditions at the proposed site. Wind speed and humidity values are important when choosing appropriate building materials, as high wind speed and humidity values will have an influence on corrosion.

Wind speed, wind direction, mixing heights, and stability conditions play vital roles in assessing the air-pollution climate of a region. Low mixing heights, stable conditions, and low wind speeds will lead to conditions of low pollutants dispersion and high levels of harmful pollutants, while the opposite is true for higher wind speeds, high mixing heights, and unstable conditions.

5.2 Air Dispersion Potential

Applying the formula for ADP calculation together with the output of an appropriate weather forecasting model, can lead to the development of an ADP forecasting tool. Using the forecasted values for the needed parameters and the methodology described in Chapter 3 to calculate the ADP over a region can be of value in forecasting short- and long-term air-dispersion conditions over this, and any other region.

Knowledge of the ADP of the region for a specific period could influence the operation of the CCGT power station. The power station operator will have the option to plan high-emission activities for a period when the ADP of the region is predicted to be high and to slow down production when ADP is low. An ADP prediction tool, when used in conjunction with operational activities at the CCGT power station, could lower the effect of pollutants on the neighbouring population in Oranjemund.

UNIVERSITEIT VAN PRETORIA
UNIVERSITY OF PRETORIA
YUNIBESITHI YA PRETORIA

5.3 Sea breeze, coastal fog and the Thermal Internal Boundary Layer

The proximity of the proposed site to the ocean guarantees the occurrence of sea breezes, foggy days, and the formation of the TIBL. These meteorological conditions will have an effect on the way in which air-pollution disperses in the region and could influence the operation of the CCGT power station, the durability of building materials and the cost of maintenance.

The sea breeze circulation is an undesirable phenomenon in the case of the proposed CCGT power station. The re-circulation of emissions from the station will lead to high levels of pollutants concentrations at the site. According to the meteorological data, sea breeze conditions will occur on average 104 times annually at the site. These conditions are most prevalent during the summer, with a total of 50% of sea breeze occurrences in December, January, and February.

Coastal fog at the site of the CCGT power station will reduce visibility and cause dangerous working conditions. The occurrence of fog will also contribute to the corrosion of equipment and material. Coastal fog at the site will occur approximately 150 days annually. According to the data, fog conditions are most likely to occur at the site between 03:00 and 06:00 in the morning.

TIBL height is influenced by the season and by the time of day. The formula for calculating TIBL height can be used to forecast the height of the TIBL at different times during the day. The formation of the TIBL causes the fumigation of pollutants from emission sources and, consequently, high ground-level concentrations of pollutants. A tool to predict TIBL height based on heat flux is crucial in the daily operation of any industry emitting harmful pollutants.

All parameters needed for the forecasting of sea breeze conditions, coastal fog occurrence, and TIBL height can be relatively easily obtained using a weather forecasting model. Using the relevant meteorological parameters and the MATLAB scripts provided in Appendix B, all the above-mentioned meteorological phenomena can be predicted on a daily basis.

The prediction of these phenomena can assist in the reduction of unwanted processes by deciding and altering the operational hours of the CCGT power station based on the predicted results. For example, dangerous work could be done at times when conditions for fog development are unfavourable and high emissions be produced when the TIBL height is below stack height or when the development of a sea breeze circulation is less likely. Theoretical and modelling results can be utilized in order to assess the background

UNIVERSITEIT VAN PRETORIA
UNIVERSITY OF PRETORIA
YUNIBESITHI YA PRETORIA

meteorological and air-quality conditions needed for planning and design in many fields of human activities. Most of the tools in this dissertation can be incorporated into the daily operation at the CCGT power station.

Corrosion is one of the main concerns when considering the proposed location and the power station itself. There are a few corrosion-causing factors in this region. Rain, fog, and humidity in the atmosphere have adverse effects on some pollutants. NOx and SOx (both by-products of the CCGT power station production process) react with precipitation to form acids or acidic depositions. These newly formed substances can corrode metal. Salt crystal nuclei may cause damage to structures by abrasion and sea-salt aerosols can cause corrosion of structures. Fog, which occurs frequently at the site and may be transported up to 15 km inland by the south-westerly winds, is a weather hazard that reduces visibility and can contribute to weathering and mineral breakdown. Hydrogen Sulphide eruptions at the coast release Hydrogen gas into the atmosphere. Not only is this gas toxic, but it is also corrosive.

The annual ADP, as calculated in this paper, is moderate at best. ADP values are higher (more favourable) over land than at the coast. Very unfavourable ADP is experienced at night-time (18:00 to 06:00). Mixing heights are very small and unfavourable for most cases (see Appendix A) in this region. A striking feature of the region is that it is stably stratified for a significant period annually; this means that vertical motions are inhibited and that fanning of pollutants will prevail.

To conclude, the proposed location for the Kudu CCGT power station was seemingly chosen based only on technological and economic factors. The proposed location is in close proximity to the Kudu gas field and the ocean. The study region experiences complex meteorological conditions, due to the huge differences in ocean and land surfaces. Sea breezes and the TIBL are two of the undesirable phenomena that form, due to the above-mentioned discontinuity. A sea breeze can be experienced up to 15 km from the coast and the TIBL can extend up to 10 km inland before an equilibrium is reached

The coastal location of the CCGT power station as chosen at present will present many challenges for pollutant dispersion and structural upkeep. Placing the power station approximately 40 km inland could lessen or totally eliminate the effects of the unfavourable mesoscale meteorological phenomena (sea breeze and TIBL) and, consequently, also the processes of re-circulation and fumigation of pollutants. The site will experience less frequent conditions of fog and the effect of corrosive particles/chemicals released by the ocean will not be as significant. More favourable conditions for ADP are present inland than at the coast and the location will experience better overall conditions for pollutant dispersion.

UNIVERSITEIT VAN PRETORIA
UNIVERSITY OF PRETORIA
YUNIBESITHI YA PRETORIA

REFERENCES

Ackerman, S. 1995. “Sea and Land Breezes” University of Wisconsin. [Online] Available at: Cimss.ssec.wisc.edu/wxwise/seabrz.html [Accessed Jul. 2015].

Ahrens, C. 1994. Meteorology today. Minneapolis/St. Paul: West Pub.

American Meteorological Society (AMS) Glossary. 2012. Fog - AMS Glossary. [online] Available at: http://glossary.ametsoc.org/wiki/Fog [Accessed Nov. 2016].

Austin, J., Brimblecombe, P. and Sturges, W. 2002. Air-pollution science for the 21st century. Amsterdam: Elsevier.

Batchvarova, E. and Gryning, S.E. 1990. ‘Applied model for the growth of the daytime mixed layer’, Boundary-Layer Meteorol. 56, 261-274.

Batchvarova, E. and Gryning, S.E. 1994. ‘Applied model for the height of the daytime mixed layer and entrainment zone’, Boundary-Layer Meteorol. 71, 311-323.

Benson, J. 2005. “Boundary-layer response to a change in surface roughness.” 15 August 2005. Master of Science. Department of Meteorology. University of Reading, Berkshire. United Kingdom.

Brown, J., Colling, A., Park, D., Phillips, J., Rothery, D. and Wright J. 1989. Seawater: Its composition, properties and behaviour. Pergamon Press, Oxford

Cimorelli, A. J., Perry, S.G., Venkatram, A., Weil, J. C., Paine, R. J., Wilson, R. B., Lee, R. F., Peters, W. D., Brode, R. W. and Paumier, J. O. 2004. AERMOD: Description of Model Formulation, EPA-454/R-03-004. U.S. Environmental Protection Agency, Research Triangle Park, NC.

Council for Scientific and Industrial Research (CSIR). 2005a. Environmental Impact Assessment. “Proposed Kudu CCGT Power Plant at Uubvlei, near Oranjemund, Republic of Namibia.” Volume 1: Final Environmental Impact Report CSIR Report ENV-S-C 2005-057. Stellenbosch. 335 pp, including Executive Summary and Appendices. Prepared for Namibia Power Corporation (Pty) Ltd.

Council for Scientific and Industrial Research (CSIR). 2005b. Environmental Impact Assessment. “Proposed Kudu CCGT Power Plant at Uubvlei, near Oranjemund, Republic of Namibia.” Volume 2: Specialist Studies Report CSIR Report ENV-S-C 2005-057. 306 pp. Stellenbosch. Prepared for Namibia Power Corporation (Pty) Ltd.

Davis, J. 2000. Corrosion. Materials Park, OH: ASM International.

Department of Environmental Affairs (DEAT). 2004a. National environmental Management: Air Quality Act (No. 39 of 2004). National ambient air quality standards. Government Gazette No. 1210. 24 December 2009.

Department of Environmental Affairs (DEAT). 2004b. National Environmental Management: Air Quality Act (No. 39 of 2004). National Dust Control Regulations. Government Gazette No. 36974. 1 November 2013.

Department of Environmental Affairs (DEAT). 2012. National Ambient Air Quality Standard for Particulate Matter with aerodynamic diameter less than 2.5 micron meters (PM2.5). Government Gazette No. 35463. 29 June 2012.

Nasa.gov. 2016. Hydrogen Sulphide Eruptions Along the Coast of Namibia: Natural Hazards. [Online] Available at: http://earthobservatory.nasa.gov/NaturalHazards/view.php?id=13155 [Accessed May 2015].

Elliott, W. 1958. The growth of the atmospheric internal boundary layer. Transactions, American Geophysical Union, 39(6), p.1048.

The Environmental Protection Agency (EPA), 1991. Hydrogen Sulphide Corrosion: Its Consequences, Detection and Control. Office of Water. United States.

Faiz, A. 1990. Automotive air-pollution. Washington, DC (1818 H St. NW, Washington 20433): Infrastructure and Urban Development Dept., World Bank.

Foken, T. 2006. 50 Years of the Monin-Obukov Similarity Theory. Boundary-Layer Meteorol, Vol 119 (3), pp. 431-447.

UNIVERSITEIT VAN PRETORIA
UNIVERSITY OF PRETORIA
YUNIBESITHI YA PRETORIA

Garratt, J. 1990. The internal boundary layer - A review. Boundary-Layer Meteorol, 50(1-4), pp.171- 203.
Godish, T. 1997. Air quality. Boca Raton, Fla.: CRC/Lewis Publishers.
Google Earth Pro. 2016a. "TAPM Grid" Lat -28.424604 and Lon 16.246414. September 4, 2013 [Accessed May 2015].
Google Earth Pro. 2015b. "Namibia" Lat -27.596441 and Lon 15.898947. April 10, 2013 [Accessed Jan. 2016].
Goudie, A. and Viles, H. A. 2015. Landscapes and landforms of Namibia. Dordrecht: Springer.
Gryning, S.E. 2005. 'The height of the atmospheric boundary layer during unstable conditions. Roskilde: Risø National Laboratory. (Denmark. Forskningscenter Risoe. Risoe-R; No. 1536(EN)).
Heidom, KC. 1998. "Sea and Land breezes" [Online] Available at: http://www.islandnet.com/~see/weather/elements/seabrz.htm [Accessed Jan. 2016].
Holzworth, G. 1967. "Mixing Dephts, Wind Speeds and Air-Pollution Potential for Selected Locations in the United States", J.Appl.Meteorol., 6, 1039-1044.
Hsu, S. 1988. Coastal meteorology. San Diego: Academic Press.
Hurley, P., Physick, W., Luhar, A., 2005a. TAPM – a practical approach to prognostic meteorological and air pollution modelling. Environ. Model. Softw. 20, 737–752.
Hurley, P., Edwards, M., Physick, W., Luhar, A., 2005b. TAPM V3 – model description and verification. Clean Air 39 (4), 32–36.
International Finance Corporation (IFC). 2007. Environmental, Health and Safety General Guidelines. 30 April 2007.
Kanevce, G. and Kanevce, L. 2006. "Dispersion modelling for regulatory applications." Thermal Science 10 (2), 141-154.
KuduPower. 2014. "Namibia's flagship power generation project". Kudu Power Project. 19 September 2014. [Online] Available at: http://www.nampower.com.na/public/docs/kudu/Kudu%20Power%20Project%20-%20Update%20Presentation%20-%20September%202014.pdf [Accessed Dec. 2014].
Luhar, A.K. 1995. 'Studies of fumigation processes inn atmospheric thermal internal boundary layers', XTwelth Australian Fluid Mechanics Conference, The University of Sydney, Australia.
Lawrence, M. 2005. The Relationship between Relative Humidity and the Dew Point Temperature in Moist Air: A Simple Conversion and Applications. Bull. Amer. Meteor. Soc., 86(2), pp. 225-233.
Lazaridis, M. 2010. First principles of Meteorology and Air-Pollution. Dordrecht: Springer
Lewis, E. and Schwartz, S. 2004. Sea salt aerosol production: Mechanisms, Methods, Measurements, and Models. Washington, DC: American Geophysical Union.
Liu, D. and Lipták, B. 2000. Air-pollution. Boca Raton: Lewis Publishers.
Maun, M. 2009. The biology of coastal sand dunes. Oxford: Oxford University Press (p117-132).
MetEd. 2016. MetEd.ucar.edu. "Forecasting Sea Breezes" [Online] Available at: http://www.meted.ucar.edu/mesoprim/seabreez/s3p0.htm [Accessed Jun. 2016].
Miller, S.T.K., Keim, B.D., Talbot, R.W. and Mao, H. 2003. 'Sea breeze: structure, forecasting, and impacts.', Reviews of Geophysics, 41, 3, 1-1 – 1-31.
Misra, P. 1980. Dispersion from tall stacks into a shore line environment. Atmospheric Environment (1967), 14(4), pp.397-400.
Namcor 2014. "Kudu-Gas to power project" [Online] Available at: http://www.namcor.com.na/kudu [Accessed Nov. 2014].
Namibia Statistics Agency (NSA). 2011. Population and Housing Census Regional Profile, Karas Region. March 2014. [Online] Available at: http://www.nsa.org.na/files/downloads/e2a_Karas%20Region.pdf [Accessed Jan. 2015].
NamPower. 2015. "NamPower - Power Stations." [Online] Available at: http://www.nampower.com.na/Page.aspx?p=183 [Accessed Feb. 2015].
Obukhov, A. 1971. Turbulence in an atmosphere with a non-uniform temperature. Boundary-Layer Meteorol, 2(1), pp.7-29.

UNIVERSITEIT VAN PRETORIA
UNIVERSITY OF PRETORIA
YUNIBESITHI YA PRETORIA

Olivier, J. 2002. Fog-water harvesting along the West Coast of South Africa: a feasibility study. Water SA, 28(4).

Pallet, J. 2009. Southern African Institute for Environmental assessment (SAIEA). "Kudu gas power station near Oranjemund, Namibia." Prepared for the Council for Scientific and Industrial Research. [Online] Available at: http://www.saiea.com/case_studies09/11%20KuduPowerStation.pdf [Accessed Dec. 2016].

Robertson, A., Jarvis, A., Mendelsohn, J. & Swart, R. 2012. Namibia's Coast: Ocean Riches and Desert Treasures. Directorate of Environmental Affairs, Ministry of Environment and Tourism, Namibia.

Rouault, M. 2015. Origin, development and demise of a Benguela Nino in the tropical Atlantic in 2010 and 2011.

Sandburg, C. 1916. Just About Everything You Wanted to Know about Fog. [Online] Available at: http://starryskies.com/articles/2007/10/fog.html [Accessed Jul. 2016].

Savelyev, S. A. and Taylor, P. A. 2005. 'Internal boundary layers: I. Height formulae for neutral and diabatic flows', Boundary-Layer Meteorol, 115, 1-25.

Siemens. 2015. "Combined Cycle - Siemens." [Online] Available at: http://www.energy.siemens.com/hq/en/industries-utilities/power/processes/combined-cycle.htm [Accessed Jan. 2015].

The Southern African Institute for Environmental Assessment (SAIEA). 2006. "Kudu gas to power project: Integrated impact and mitigation report." May 2006. [Online] Available at: http://www.nampower.com.na/public/docs/kudu/eia/Kudu_SAIEA%20Integrated%20ImpactMitigation%20Report_May%202006.pdf [Accessed Dec. 2014].

Skrotzki, B. 1956. Electric generation: Steam stations. New York: McGraw-Hill.

Statistic South Africa (Statssa). 2011. Richtersveld Local Municipality, Census 2011.

Stokie, J. M. 2011. "The mathematics of atmospheric dispersion modelling." Siam Review, Vol 53 (2), 349-372.

Stull, R. 1988. An Introduction to Boundary Layer Meteorology. 1st ed. Dordrecht: Springer Netherlands.

Stunder, M., Sethuraman, S. 1985. 'A Comparative Evaluation of the Coastal Internal Boundary-Layer, Height Equations', Boundary-Layer Meteorol. 32, 177-204.

Thomas, R. G. 2008b. "An air quality baseline assessment for the Vaal Triangle Airshed in South Africa." November 2008. Master of Science. University of Pretoria, Pretoria. South Africa.

Van Zyl, P.G., Beukes, J.P., Du Toit, G., Mabaso, D., Hendriks, J., Vakkari, V., et al. 2014. Assesment of atmospheric trace metals in the western Bushveld Igneous Complex, South Africa. S AFr J Sci. 2014; 110(3/4), Art. #2013-0280, 11 pages.

Venkatram, A. 1986. An examination of methods to estimate the height of the coastal Internal Boundary Layer. Boundary-Layer Meteorol, 36 (1-2), pp.149-156.

Walmsley, J. L. 1989. 'Internal Boundary-Layer Height Formulae – A Comparison with Atmospheric Data', Boundary-Layer Meteorol. 47, 251–262.

Wilkes, C. 2007. "Power Plant Layout Planning – Gas Turbine Inlet Air Quality Considerations." GE Energy.

World Health Organization (WHO). 2005. WHO Air quality guidelines for particulate matter, ozone, nitrogen dioxide and Sulphur dioxide. Summary of risk assessment.

UNIVERSITEIT VAN PRETORIA
UNIVERSITY OF PRETORIA
YUNIBESITHI YA PRETORIA

Appendix A – Air Dispersion Potential Component Plots

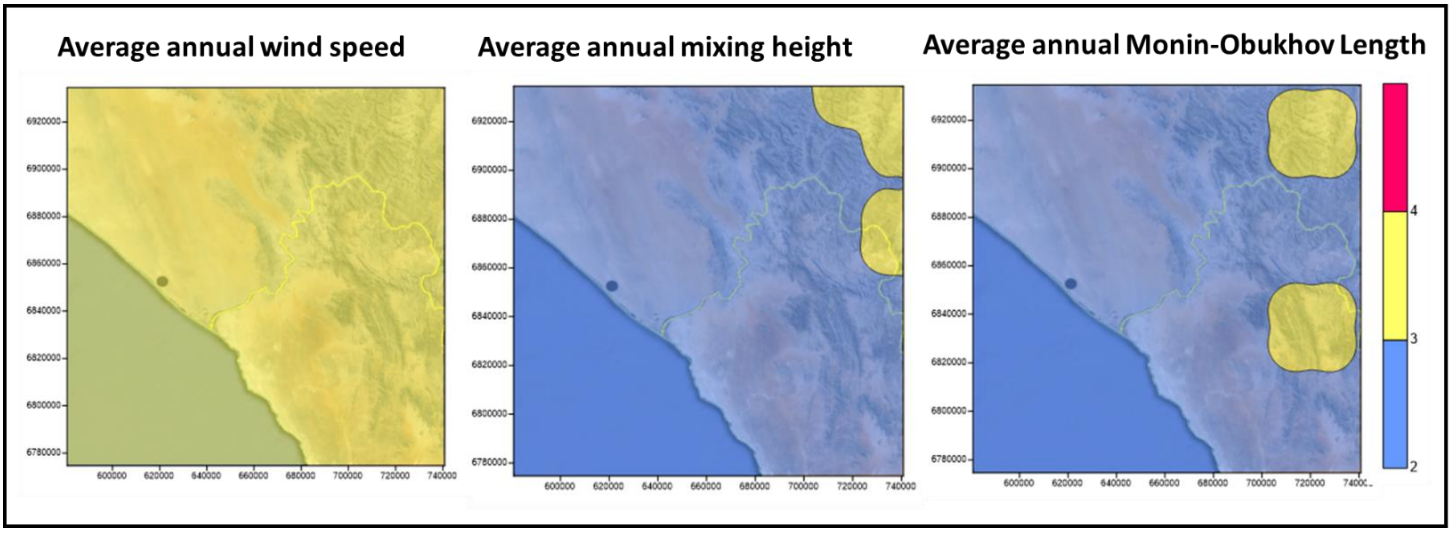

Figure A.1: The components of annual ADP (wind speed, mixing height and Monin-Obukhov Length) over the study region where blue indicates an unfavourable contribution to average ADP, yellow indicates a moderate contribution, and pink a favourable one.

.

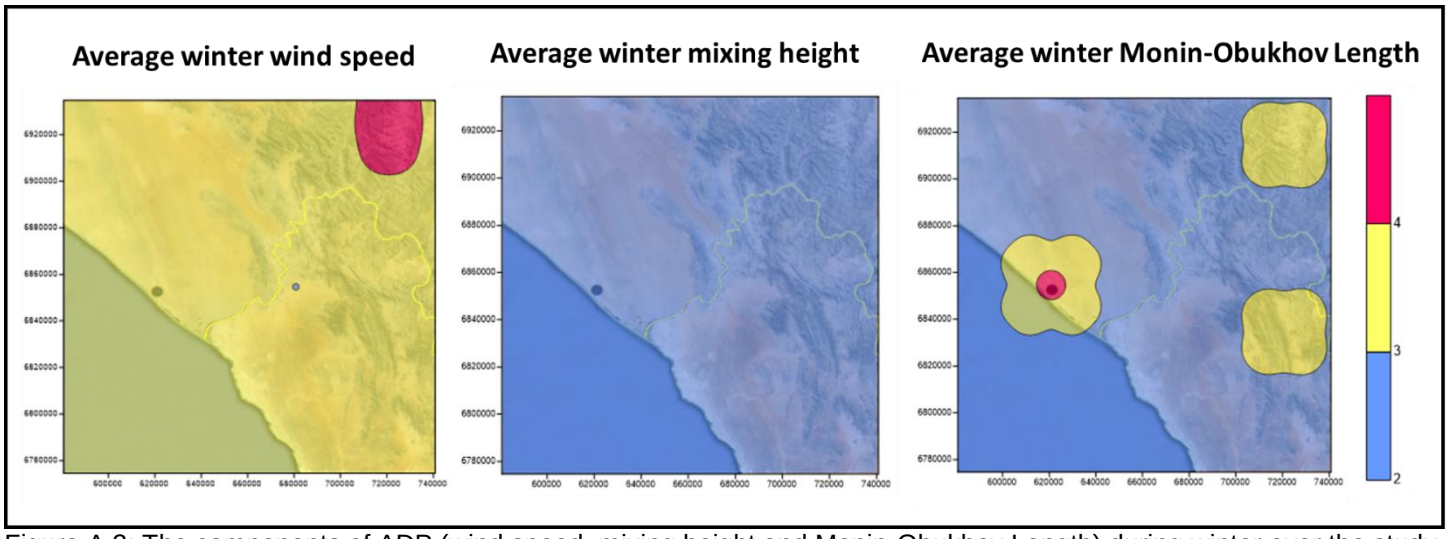

Figure A.2: The components of ADP (wind speed, mixing height and Monin-Obukhov Length) during winter over the study region where blue indicates an unfavourable contribution to average ADP, yellow indicates a moderate contribution, and pink a favourable one.

UNIVERSITEIT VAN PRETORIA
UNIVERSITY OF PRETORIA
YUNIBESITHI YA PRETORIA

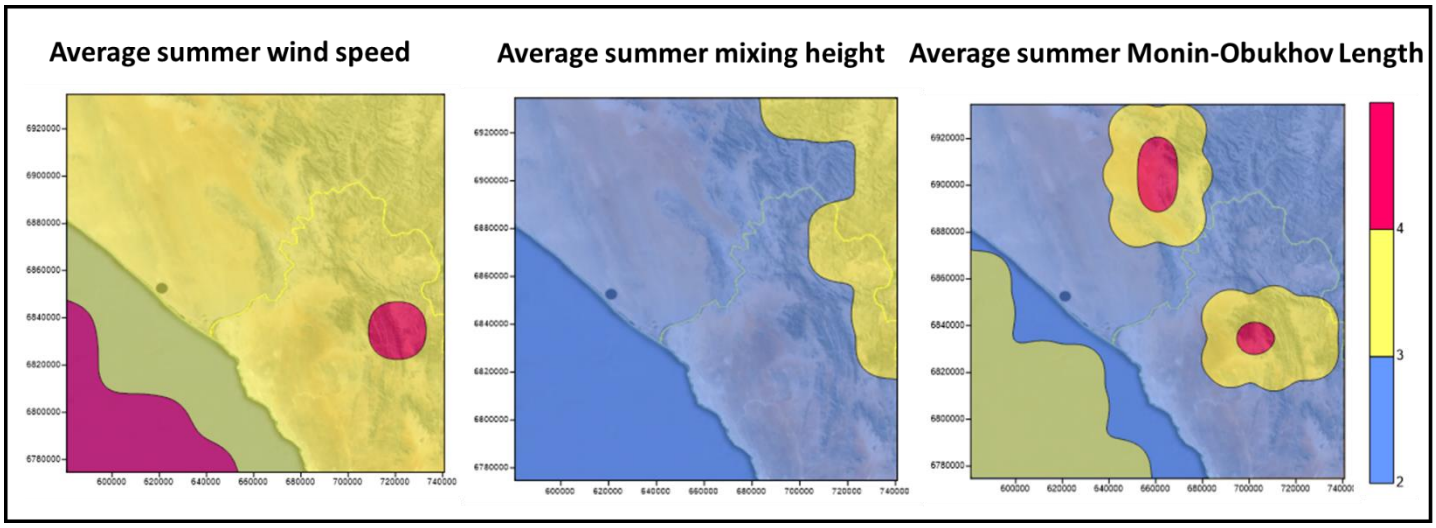

Figure A.3: The components of ADP (wind speed, mixing height and Monin-Obukhov Length) during summer over the study region where blue indicates an unfavourable contribution to average ADP, yellow indicates a moderate contribution, and pink a favourable one.

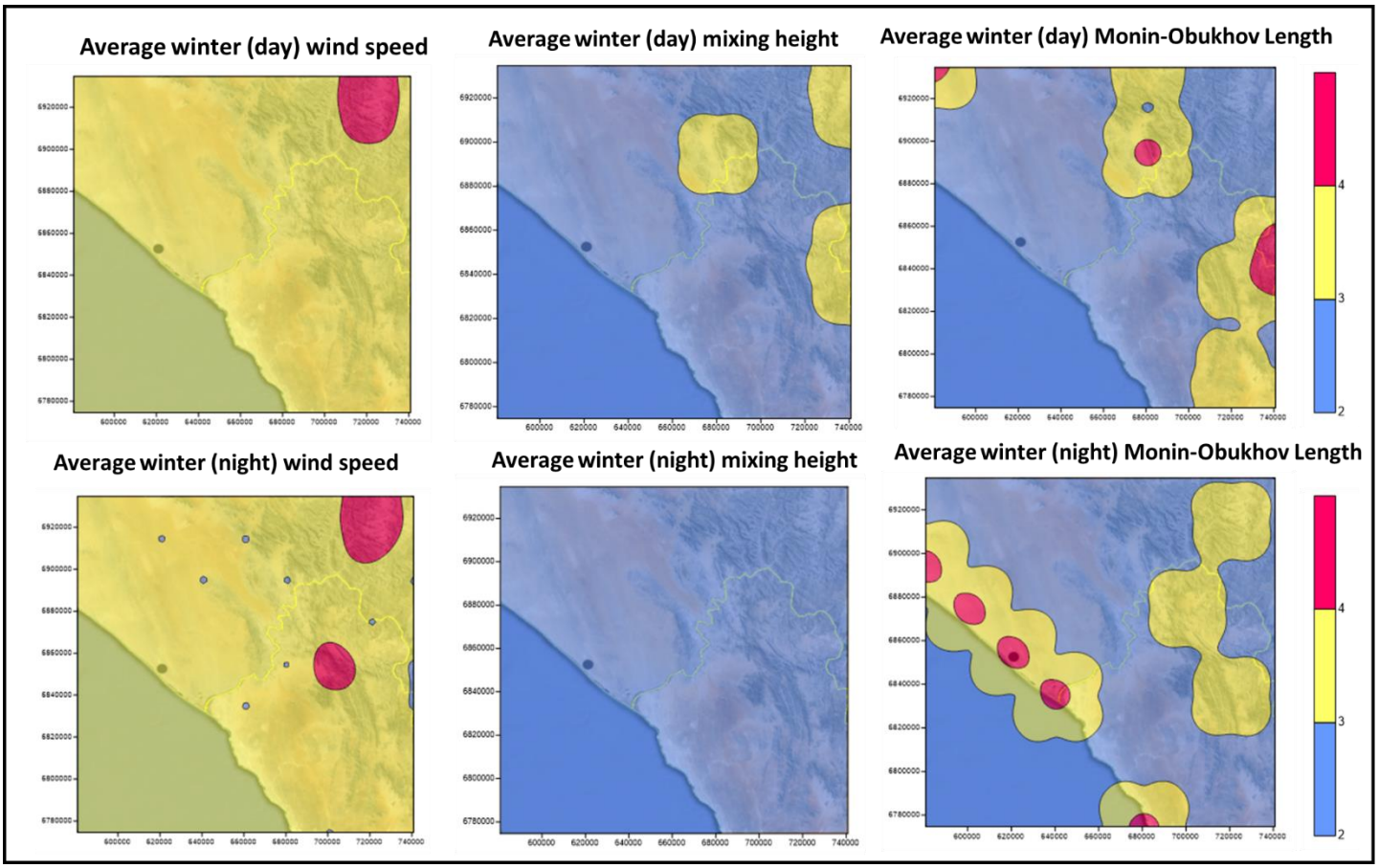

Figure A.4: The components of ADP (wind speed, mixing height and Monin-Obukhov Length) for winter during the day and night where blue indicates an unfavourable contribution to average ADP, yellow indicates a moderate contribution, and pink a favourable one.

UNIVERSITEIT VAN PRETORIA
UNIVERSITY OF PRETORIA
YUNIBESITHI YA PRETORIA

Appendix B – MATLAB Scripts

Script for the calculation of sea breeze occurrence

```
% ------------------------------------------------------------------------------------------------------------
% Program for calculating the occurrence of hours during the day (between 08:00
%and 16:00) where land and ocean temperatures differ with more than 3.00 degrees
%Celsius and wind is blowing from the ocean (between 180° and 270°)
% ------------------------------------------------------------------------------------------------------------
% The output from a weather forecast model used for a particular study should
%supply relevant parameters for points over the ocean and land.
% ------------------------------------------------------------------------------------------------------------
% The input file(s) for Namibia study are as follow for 81 points: di (8760,5,81)
% Here: i,1- M-Month, i,2 D-Day, i,3 H-Hour, i,4 T-Temperature, 5 WD-Wind direction
% ------------------------------------------------------------------------------------------------------------
% Importing data
% ------------------------------------------------------------------------------------------------------------
   clear all;
   di= xlsread ('Allpoints2variables.xlsx','1','A2:J709561');
% ------------------------------------------------------------------------------------------------------------
% Determining the size of the data array (number of rows and columns)
% ------------------------------------------------------------------------------------------------------------
   rc = size(di);
% ------------------------------------------------------------------------------------------------------------
% Using the above input file one creates the temperature differences
% between land (TL average temperature over all land points) and ocean (TO
% average temperature over all ocean point) DT = Tl - TO
% ------------------------------------------------------------------------------------------------------------
      md = [31 29 31 30 31 30 31 31 30 31 30 31];
      lmh = [0 744 1416 2160 2880 3624 4344 5088 5832 6552 7296 8016];
      for i = 1:8760;
         m = di(i,1);
         d = di(i,2);
         h = di(i,3);
         for k = 1:81;
         dp (k) = 0.0;
         dpw (k) = 0.0;
         end
         for k = 1:81;
         n = (k-1)*8760 + lmh(m) + (d-1)*24 + h;
         dp (k) = di(n,4);
         dpw (k) = di(n,5);
      end
      lo = [1 1 1 1 1 1 1 1 1 1 1 1 1 1 1 1 1 1 1 1 1 1 1 1 2 1 1 1 1 1 1 1 2 2 1 1
1 1 1 1 1 2 2 2 1 1 1 1 1 1 2 2 2 2 1 1 1 1 1 2 2 2 2 1 1 1 1 2 2 2 2 2 1 1 1 1 2 2 2 2 2 1 1 1 1];
% ------------------------------------------------------------------------------------------------------------
% Calculating DT
```

UNIVERSITEIT VAN PRETORIA
UNIVERSITY OF PRETORIA
YUNIBESITHI YA PRETORIA

```
% ------------------------------------------------------------------------------------------------------
tl = 0.0;
       To = 0.0;
       wd = 0.0;
       for k = 1:81;
          if (lo (k) == 1)
          tl = tl + dp(k);
          end
       if (lo(k) == 2)
          to = to + dp(k);
       end
       wd = wd + dpw(k);
       end
       tl = tl/61;
       to = to/20;
       dt = tl - to;
       wd = wd/81;
       di (i,6) = dt;
       di (i,7) = wd;
       end
% ------------------------------------------------------------------------------------------------------
% The array: DI (8760,7) contains 1-M; 2-D; 3-H; 4-T; 5-WD; 6-DT; 7-WD (average)
% ------------------------------------------------------------------------------------------------------
% Using DI data to calculate days with breeze monthly, seasonal (winter
% season and summer season) and annual breeze days.
% ------------------------------------------------------------------------------------------------------
% Defining days with favorable breeze conditions. The results will be
% kept in: DB (365,3) which contains 1-M, 2-D, 3-no of days.
% ------------------------------------------------------------------------------------------------------
for i = 1:366;
       db (i,1) = 0.0;
       db (i,2) = 0.0;
       db (i,3) = 0.0;
       db (i,4) = 0.0;
       db (i,5) = 0.0;
   end
%  ------------------------------------------------------------------------------------------------------
% Finding breeze days on the basis of DT average between the hours 8:00
% and 16:00 which satisfy the condition DT > BC (where BC is the
% threshold for breeze condition).
% BC value is defined at the beginning of the script. Below defines the beginning of
%months starting with 1 January and end 31 of December
% ------------------------------------------------------------------------------------------------------
tc = 3.00;
   lm = [0 31 59 90 120 151 181 212 243 273 304 334];
      hb = 8.0;
```

UNIVERSITEIT VAN PRETORIA
UNIVERSITY OF PRETORIA
YUNIBESITHI YA PRETORIA

```
    he = 16.0;
    hdi = he-hb;
  for i = 1:8760;
    m = di(i,1);
    d = di(i,2);
    h = di(i,3);
    dt = di(i,6);
    wd = di(i,7);
    k = lm(m) + d;
    if (h >= hb && h <= he)
      db (k,1) = m;
      db (k,2) = d;
      db (k,3) = db(k,3) + dt/hdi;
      db (k,4) = db(k,4) + wd/hdi;
    end
  end
    for k = 1:365;
      if (db(k,3) >=tc && db(k,4) >= 180 && db(k,4) <= 270)
        db (k,5) = 1;
      end
    end
    an = 0.0;
    for i = 1:365;
      an = an + db(i,5);
    end
% ------------------------------------------------------------------------------------------------------
%       Calculating monthly, seasonal, annual breeze days
% ------------------------------------------------------------------------------------------------------
    for i = 1:12;
    msa (i) = 0.0;
    msa (i,2) = 0.0;
    end
    for k = 1:365;
      m = db(k,1);
      d = db(k,2);
      q = lm(m) + d;
      msa (m,1) = m;
      msa (m,2) = msa(m,2) + db(q,5);
    end
      ws = msa(6,2) + msa(7,2) + msa(8,2);
      ss = msa(12,2) + msa(1,2) + msa(2,2):
% ------------------------------------------------------------------------------------------------------
%                                   END OF PROGRAM
% ------------------------------------------------------------------------------------------------------
```

UNIVERSITEIT VAN PRETORIA
UNIVERSITY OF PRETORIA
YUNIBESITHI YA PRETORIA

Script for the calculation of fog day occurrence

```
% ------------------------------------------------------------------------------------------------------------
% It calculates the fog conditions based on the observed temperature T, relative
%humidity RH and calculated dew point temperature TD. Using the criteria that when
% the difference DT = T - DPT is small the fog conditions are highly probable (T = TD
% is the absolute criteria for fog).
% ------------------------------------------------------------------------------------------------------------
% The input file(s) for Namibia study is for the Kudu point is: di (8760,6)
% Here: 1-Month, 2-Day, 3-Hour, 4-Temp, 5-Relative Humidity, 6-Dew Point Temp
% ------------------------------------------------------------------------------------------------------------
% Importing data
% ------------------------------------------------------------------------------------------------------------
         clear all;
        di = xlsread ('Point39fog.xlsx');
% ------------------------------------------------------------------------------------------------------------
% Determining the size of the data array (number of rows and columns)
% ------------------------------------------------------------------------------------------------------------
        rc = size (di);
% ------------------------------------------------------------------------------------------------------------
% Using the above input file one creates the temperature differences
% between observed temperature and calculated dew point temperature DT = T - TP
% The days for conditions are calculated by if DT < DPC., where DPC = 1.
% ------------------------------------------------------------------------------------------------------------
% The formula for: TD = 243.04 * (ln (RH/100) + ((17.625 * T) / (243.04 + T))) /
%(17.625 - ln (RH/100) - ((17.625 * T) / (243.04 + T)))
% The di (8760, 1-M, 2-D, 3-H, 4-T, 5-RH, 6-TD, 7-DT = T - TD, 8-NO)
% ------------------------------------------------------------------------------------------------------------
      dpc = 1;
      for i = 1:8760;
      di (i,6) = 0;
      di (i,7) = 0;
      di (i,8) = 0.0;
      end
% ------------------------------------------------------------------------------------------------------------
      for i = 1:8760;
         m = di (i,1);
         d = di (i,2);
         h = di (i,3);
         t = di (i,4);
         rh = di (i,5);
         td1 = (243.04 * (log(rh/100)) + ((17.625*t) / (243.04+t));
         td2 = (17.625 - log(rh/100)) - ((17.625*t) / (243.04+t));
         td = td1/td2;
         di (i,6) = td;
         dt = t - td;
         if (dt <= dpc)
```

UNIVERSITEIT VAN PRETORIA
UNIVERSITY OF PRETORIA
YUNIBESITHI YA PRETORIA

```
            di (i,8) = 1;
         end
         if (dt > dpc)
            di (i,8) = 0;
         end
         di (i,7) = dt;
      end
% ------------------------------------------------------------------------------------------------------------
% Calculating the daily values of fog conditions results are stored in: df (365, 1-m, 2-
% d, 3-no of Fog1, 4-no Fog2, 5-no Fog3, 6-no Fog4, 7-no of Fog 5, 8-Fog yes or no)
% ------------------------------------------------------------------------------------------------------------
      lmh = [0 744 1416 2160 2880 3624 4344 5088 5832 6552 7296 8016];
      lm = [0 31 59 90 120 151 181 212 243 273 304 334];
         for i = 1:365;
            for k = 1:4;
               df (i,k) = 0;
            end
         end
% ------------------------------------------------------------------------------------------------------------
% Array df (365, 1-M, 2-D, 3-Fog hourly sum, 4-Fog day? 1-Yes/0-No;)
% ------------------------------------------------------------------------------------------------------------
   for i = 1:8760;
      m = di (i,1);
      d = di (i,2);
      h = di (i,3);
      k = lm (m) + d;
      df (k,1) = m;
      df (k,2) = d;
      if (di (i,8) == 1)
         df (k,3) = df (k,3) + 1;
      end
   end
      for i = 1:365;
         if (df (i,3) >= 1)
            df (i,4) = 1;
         end
      end
% ------------------------------------------------------------------------------------------------------------
% Calculation of monthly winter (ws), summer (ss), annual (an) values of fog.
% ------------------------------------------------------------------------------------------------------------
 for i = 1:12;
      msf (i,1) = 0.0;
      msf (i,2) = 0.0;
 end
       for k = 1:365;
         m = df (k,1);
```

UNIVERSITEIT VAN PRETORIA
UNIVERSITY OF PRETORIA
YUNIBESITHI YA PRETORIA

```
        d = df (k,2);
        q = lm (m) + d;
        msf (m,1) = m;
        msf (m,2) = msf (m,2) + df (q,4);
      end
       ws = msf (6,2) + msf (7,2) + msf (8,2);
       ss = msf (12,2) + msf (1,2) + msf (2,2);
        an = 0;
      for i = 1:365;
        an = an + df (i,4);
      end
% ------------------------------------------------------------------------------------------------------
% Calculation of time of fog: Array dft (365, 1-M, 2-D, 3-0 to 3h, 4-3 to 6h, 5-6 to 9h,
% 6-9 to 12h, 7-12 to 15h, 8-15 to 18h, 9-18 to 21h, 10-21 to 24h)
% ------------------------------------------------------------------------------------------------------
   for i = 1:365;
      for k = 1:10;
      dft (i,k) = 0;
      end
   end
      for i = 1:8760;
     m = di (i,1);
     d = di (i,2);
     h = di (i,3);
     k = lm (m) + d;
     dft (k,1) = m;
     dft (k,2) = d;
     he = 3;
     hb = 0;
     dh = 3;
     for n = 1:8;
        if (h > hb && h <= he)
           dft (k, n+2) = dft (k, n+2) + di (i,8);
        end
        hb = hb + dh;
        he = he + dh;
     end
      end
% ------------------------------------------------------------------------------------------------------
% Calculation of Fog for 0-9h and 9-18h: Array dfnd (365, 1-M, 2-D, 3-0 to 9h, 4-9 to
% 18h)
% ------------------------------------------------------------------------------------------------------
      for i = 1:365;
        for k = 1:4;
           dfnd (i,k) = 0;
        end
```

UNIVERSITEIT VAN PRETORIA
UNIVERSITY OF PRETORIA
YUNIBESITHI YA PRETORIA

```
    end
% ------------------------------------------------------------------------------------------------------
    for i = 1:365;
        dfnd (i,1) = dft(i,1);
        dfnd (i,2) = dft(i,2);
        dfnd (i,3) = dft (i,3) + dft (i,4) + dft (i,5);
        dfnd (i,4) = dft (i,6) + dft (i,7) + dft (i,8);
    end
% ------------------------------------------------------------------------------------------------------
% Calculation of monthly night day values: Array dfh (12, 1M, 2 No during, 3 Number
% during day)
% ------------------------------------------------------------------------------------------------------
        for i = 1:12;
            dfh (i,1) = 0;
            dfh (i,2) = 0;
            dfh (i,3) = 0;
        end
% ------------------------------------------------------------------------------------------------------
        ann = 0;
        and = 0;
    for i = 1:365;
        ann = ann + dfnd (i,3);
        and = and + dfnd (i,4);
    end
     for k = 1:365;
        m = dfnd (k,1);
        d = dfnd (k,2);
        q = lm (m) + d;
        dfh (m,1) = m;
        dfh (m,2) = dfh (m,2) + dfnd (q,3);
        dfh (m,3) = dfh (m,3) + dfnd (q,4);
    end
       wsh = dfh (6,2) + dfh (7,2) + dfh (8,2);
       ssh = dfh (12,2) + dfh (1,2) + dfh(2,2);
       ann = 0;
       and = 0;
    for i = 1:365;
        ann = ann + dfnd (i,3);
        and = and + dfnd (i,4);
    end
% ------------------------------------------------------------------------------------------------------
%                                        END OF PROGRAM
% ------------------------------------------------------------------------------------------------------
```

UNIVERSITEIT VAN PRETORIA
UNIVERSITY OF PRETORIA
YUNIBESITHI YA PRETORIA

Script for the calculation of the Equilibrium IBL Height

```
% ------------------------------------------------------------------------------------------------------
% The script calculates the equilibrium internal boundary height (HE) using
% the kinematic heat flux as modeled by appropriate weather/air-pollution
% model (TAPM).
% ------------------------------------------------------------------------------------------------------
% Data for January 15 (summer) and July 15 (winter) will be processed; the
% array TS contains the time intervals for summer and TW for winter day
% time. The array QS and QW contain the corresponding kinematic heat fluxes
% for summer and winter.
% ------------------------------------------------------------------------------------------------------
ts = [6 7 8 9 10 11 12 13 14 15 16 17 18 19];
qs = [51.5 259.8 504.9 732.9 913.8 1041.9 1106.9 1104.7 1034.5 901.6 716.3 494.6
256.2 43.7];
tw = [7 8 9 10 11 12 13 14 15 16 17 18];
qw = [2.2 135.3 347.1 527.4 655.6 719.2 714.9 643.4 510.2 327.7 116.2 0.5];
% ------------------------------------------------------------------------------------------------------
% Approximation of the modeled heat fluxes by polynomial of second degree
% n = 2
% y (t) = a*t^2 + b*t + c is performed
% ------------------------------------------------------------------------------------------------------
% Summer approximation of QS:
   n = 2;
   p = polyfit (ts, qs, n);
   for i = 1:14;
   aps (i) = -25.6554945054944 * ts(i)^2+640.430659340658 * ts(i)-2925.289;
   if (aps (i) < 0)
      aps (i) = 0;
   end
   end
    rs = corrcoef (qs, aps);
%The answers for summer a = -25.6554945054944 ; b = 640.430659340658 ;
% c = - 2925.289
% The correlation coefficient between observed data and polynomial
% approximation is rs = [0.994996534512449;]
% ------------------------------------------------------------------------------------------------------
% Winter approximation of QW
   n = 2;
  p1 = polyfit (tw, qw, n);
  for i = 1:12;
     apw (i) = -24.5737 * tw(i)^2+612.756 * tw(i)-3135.34328;
     if (apw (i) < 0)
        apw (i) = 0;
     end
  end
   rw = corrcoef (qw, apw);
```

UNIVERSITEIT VAN PRETORIA
UNIVERSITY OF PRETORIA
YUNIBESITHI YA PRETORIA

```
% ------------------------------------------------------------------------------------------------------------
% The answer for winter a = -24.5737 ; b = 612.756  ; c = -3135.34328
% The correlation coefficient between observed data and polynomial
% approximation is rw = 0.993599953831055
%                   plot (ts, qs, ts, aps, tw, qw, tw, apw);
% ------------------------------------------------------------------------------------------------------------
% Calculation of the equilibrium height for summer and winter
% ------------------------------------------------------------------------------------------------------------
% The general formula is:
%
%           h_e^2 (x)=h_e^2 (0)+2/(Y(1−2F)) ∫_0^te Q_e (t)dt
%
% Which can be written as:
%
%           he^ 2+ ho^2 + const*
%           The integral nconst = 7.
%
% ------------------------------------------------------------------------------------------------------------
% The analytical solution of the definite integral of a*t^2+b*t+c
% The solution is 1/3 * t^3+1/2 * b * t^2+c * t in boundaries between 0 and tf
% ------------------------------------------------------------------------------------------------------------
   as = -25.655;
   bs = 640.4307;
   cs = -2925.289;
   aw = -24.5737;
   bw = 612.756;
   cw = -3135.34328;
   ti = [9 13 17];
   for i = 1:3;
      ds (i) = as*(7^3)/3 + (bs*7^2)/2 + cs *7;
      ins( i) = sqrt ((as*ti(i)^3)/3 + (bs*ti(i)^2)/2 + cs*ti(i) - ds(i)) *11;
      dw (i) = (aw*7^3)/3 + (bw*7^2)/2 + cw *7;
      inw (i) = sqrt ((aw*ti(i)^3)/3 + (bw*ti(i)^2)/2 + cw*ti(i) - dw(i)) *11;
   end
% ------------------------------------------------------------------------------------------------------------
% The results for the equilibrium height at 9:00 13:00 and 17:00 are
%  hes = [364 779 1015]; hew = [212 578 757];
% These values are to be used in the calculation of the IBL distribution h = h(t, x)
% ------------------------------------------------------------------------------------------------------------
%                                   END OF SCRIPT
% ------------------------------------------------------------------------------------------------------------
```

UNIVERSITEIT VAN PRETORIA
UNIVERSITY OF PRETORIA
YUNIBESITHI YA PRETORIA

Script for the calculation of TIBL height

```
% ------------------------------------------------------------------------------------------------------
% The script evaluates the Thermal Internal Boundary Layer (TIBL) height as a
%function of the distance from the shore line (x) and the time during day time (t).
% ------------------------------------------------------------------------------------------------------
% The approximation formula can be found in Chapter 3 of the dissertation entitled
%"Assessment of the Baseline Meteorological and Air Quality Conditions over
%Uubvlei, Oranjemund, Namibia" UP, 2016
% ------------------------------------------------------------------------------------------------------
% The general formula for h is:
%
%          h^2 (x,t) = h^2 (0)+(h_e(t)^2 - h^2 (0))(1-e^(-x/L(t)) )
%
% h (0) - Initial height, x - Distance from the shore, L – Equilibrium distance, t - Time
% ------------------------------------------------------------------------------------------------------
% Distances for the calculation (21)
% beta=11
% ------------------------------------------------------------------------------------------------------
   x = [ 0 0.2 0.4 0.8 1 1.5 2 3 4 5 6 7 8 9 10 11 12 13 14 15 16];
   hes = [0.364 0.779 1.015];
   hew = [0.212 0.578 0.757];
   for i = 1:3;
   ls (l) = 11 * hes (i);
   lw (i) = 11 * hew (i);
   end
% ------------------------------------------------------------------------------------------------------
   for k = 1:3;
      hest = hes (k);
      lst = ls (k);
      hewt = hew (k);
      lwt = lw (k);
   for i = 1:21;
      hst (k,i) = hest^2 * (1-exp(-x(i)/lst));
      hs (k,i) = sqrt (hst(k,i));
      hwt (k,i) = hewt^2 * (1-exp(-x(i)/lwt));
      hw (k,i) = sqrt (hwt(k,i));
      xp (i) = x(i);
   end
   end
   figure
% ------------------------------------------------------------------------------------------------------
         Plot (x, hs, x, hw);
% ------------------------------------------------------------------------------------------------------
%                                    END OF PROGRAM
% ------------------------------------------------------------------------------------------------------
```